AD_____

AWARD NUMBER: W81XWH-04-1-0920

TITLE: Preclinical Evaluation of Serine/Threonine Kinase Inhibitors Against Prostate Cancer Metastases

PRINCIPAL INVESTIGATOR: Theresa A. Guise, M.D.

CONTRACTING ORGANIZATION: University of Virginia
Charlottesville, VA 22904

REPORT DATE: November 2008

TYPE OF REPORT: Final

PREPARED FOR: U.S. Army Medical Research and Materiel Command
Fort Detrick, Maryland 21702-5012

# REPORT DOCUMENTATION PAGE

*Form Approved*
*OMB No. 0704-0188*



| 1. REPORT DATE | 2. REPORT TYPE | 3. DATES COVERED |
|---|---|---|
| 1 November 2008 | Final | 15 Oct 2004 – 14 Oct 2008 |

**4. TITLE AND SUBTITLE**

Preclinical Evaluation of Serine/Threonine Kinase Inhibitors Against Prostate Cancer Metastases

**5a. CONTRACT NUMBER**

**5b. GRANT NUMBER**
W81XWH-04-1-0920

**5c. PROGRAM ELEMENT NUMBER**

**6. AUTHOR(S)**

Theresa A. Guise, M.D.

E-Mail: tag4n@virginia.edu

**5d. PROJECT NUMBER**

**5e. TASK NUMBER**

**5f. WORK UNIT NUMBER**

**7. PERFORMING ORGANIZATION NAME(S) AND ADDRESS(ES)**

University of Virginia
Charlottesville, VA 22904

**8. PERFORMING ORGANIZATION REPORT NUMBER**

**9. SPONSORING / MONITORING AGENCY NAME(S) AND ADDRESS(ES)**
U.S. Army Medical Research and Materiel Command
Fort Detrick, Maryland 21702-5012

**10. SPONSOR/MONITOR'S ACRONYM(S)**

**11. SPONSOR/MONITOR'S REPORT NUMBER(S)**

**12. DISTRIBUTION / AVAILABILITY STATEMENT**
Approved for Public Release; Distribution Unlimited

**13. SUPPLEMENTARY NOTES**

**14. ABSTRACT**
This proposal studied the role of TGFβ signaling in prostate cancer. To summarize, it is a useful target for treatment of prostate cancer bone metastases, provided that the tumor cells are responsive to the factor and show components of osteolytic lesions. TGFβ inhibitors are not beneficial when the bone metastases phenotype is predominantly osteoblastic. Smad-independent pathways downstream of the TGFβ receptors, such as p38 MAP kinase, do not appear to be appropriate targets for pharmacological treatment of prostate cancer bone metastases. There is no advantage to combined treatment targeting TGFβ receptors and p38 MAP kinase. PMEPA1 may be an important target of TGFβ in prostate cancer cells and responsible for potentiating responsiveness of tumor cells in bone to the local actions of bone-released TGFβ. Its regulation and isoform-specific effects are complex and will be the subject of future grant proposals. TGFβ inhibition increases bone mass systemically thru effects to stimulate differentiation of osteoblasts and inhibiting osteoclasts. The effects on osteoblasts may be via stat3 induction of Wnt ligand production.

**15. SUBJECT TERMS**
Prostate cancer, Bone metastases, TGFbeta

| 16. SECURITY CLASSIFICATION OF: | | | 17. LIMITATION OF ABSTRACT | 18. NUMBER OF PAGES | 19a. NAME OF RESPONSIBLE PERSON |
|---|---|---|---|---|---|
| a. REPORT | b. ABSTRACT | c. THIS PAGE | | | 19b. TELEPHONE NUMBER *(include area code)* |
| U | U | U | UU | 71 | USAMRMC |

**Table of Contents** **Page**

## GENERAL INTRODUCTION

Prostate cancer has a propensity to grow in the skeleton and cause significant morbidity. Once housed in bone, prostate cancer is incurable. Bone is a rich storehouse of growth factors, which stimulate signaling in metastatic cancer cells. Bone-derived TGFβ increases tumor secretion of factors that activate bone remodeling, fueling a vicious cycle (**Figure 1**), which drives the growth and survival of prostate bone metastases. In prostate cancer cells, TGFβ signals through two receptor subunits and, further downstream, p38 MAP kinase. Hypothesis: *TGFβ mediates prostate cancer metastases to bone via p38 MAP kinase pathway. TGFβ and/or p38MAP kinase signaling inhibitors will reduce the development and progression of prostate cancer bone metastases to bone.* Two orally active inhibitors of these serine/threonine kinases will be tested in an animal model of prostate cancer bone metastases. We propose three Specific Aims. **Aim 1**: To test a TGFβRI kinase inhibitor and a p38 MAPK inhibitor against three human prostate cancer models of skeletal metastasis in mice. **Aim 2**: To determine the molecular targets of these inhibitors in prostate cancer cells *in vitro* and test their impact on tumor growth and bone metastases *in vivo*. **Aim 3**: To test the efficacy of combined TGFβRI and p38 MAP kinase inhibitors against three prostate cancer models *in vivo*.

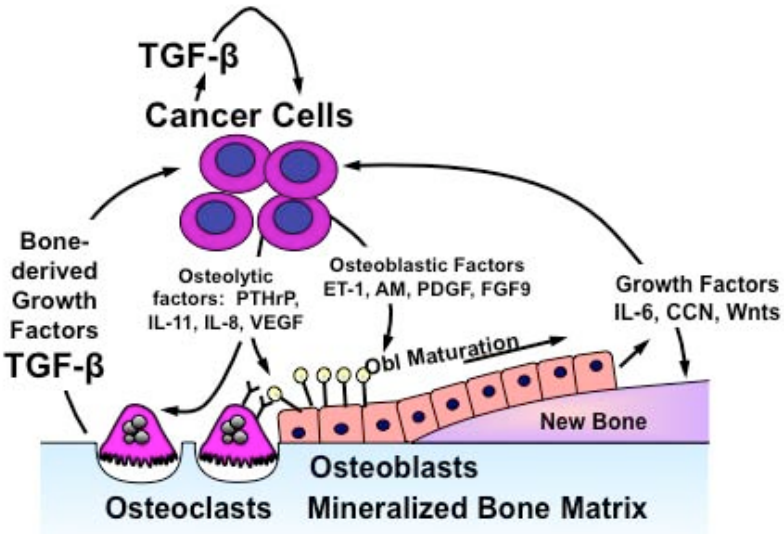


**Figure 1**: **The Vicious Cycle** between cancer and bone. Cancer cells secrete factors that stimulate osteoblasts to proliferate, differentiate and secrete growth factors that are deposited into bone matrix and enrich the tumor microenvironment. Tumor cells also secrete osteolytic factors; many via osteoblast production of RANK ligand (lollipops), which binds to RANK (Ys) on osteoclasts. Growth factors released from bone matrix by osteoclastic bone resorption further enrich the local mileau. TGFß may act at multiple sites of the vicious cycle.

**Summary of basic progress after three years and year 4 no cost extension:**

- TGFβRI kinase inhibitor *effective* against osteolytic bone metastases
- TGFβRI kinase inhibitor *ineffective* and possibly deleterious against osteoblastic bone metastases.
- p38 MAPK inhibitor *ineffective* in several models of bone metastases and accelerates PC3 bone metastases. Additional experiments with this class of inhibitor and the combined treatments proposed in Aim 3 have consequently been abandoned.
- Inhibition of TGFβ signaling without effect on growth of tumors at soft tissue sites
- PMEPA1 identified as major target gene of TGFβ and role of PMEPA1 as regulator of TGFβ signaling found.
- Completion of histological analyses of animal models with bone metastases +/- treatments
- Test of PMEPA1 function by knockdown in prostate cancer cells in vitro and in vivo in a mouse model of bone metastasis

**Tasks Completed**: Included as an Appendix at the end of this report is a reproduction of the original Statement of Work, with the addition of a status summary for each of the 23 originally-proposed Tasks

## BODY OF REPORT

**Original Background.** The skeleton is a major site of metastasis by advanced prostate cancer. In a recent year 220,900 cases of prostate cancer were diagnosed in the United States, where it is now the most commonly diagnosed cancer and the second most common cause of cancer mortality in men, with 28,900 deaths (Crawford, 2003). One fourth of diagnosed patients will die from the disease, the majority of them with metastases to the skeleton. Once cancer becomes housed in bone, it is incurable. The average survival from time of diagnosis of skeletal metastases in prostate cancer patients is 40 months. When prostate tumor cells metastasize to the skeleton, the most common response is osteoblastic: characterized by net formation of disorganized new bone, which results in fractures, severe and intractable bone pain, and nerve compression. Metastasis to bone thus causes prolonged, serious morbidity for many prostate cancer patients. Treatment to prevent or halt the progression of bone metastases (Reddi et al, 2003; O'Keefe and Guise, 2003). would increase survival and improve quality of life for men with prostate cancer

***Transforming growth factor-β in cancer is a two-edged sword***. TGFβ is a growth inhibitor and a tumor suppressor at early stages of the oncogenic cascade. However, advanced cancers often lose the growth inhibition by TGFβ but continue to respond to the factor. The net effect is that TGFβ is a metastasis enhancer for advanced cancers. Since bone is a major source of active TGFβ, the factor plays a crucial role in the vicious cycle of bone metastases. Blockade of the TGFβ pathway effectively decreases metastases in several animal models (Yin et al, 1996; Muraoka et al, 2002; Yang et al, 2002).

***Transforming growth factor-β in bone*** is released from mineralized matrix in active form by osteoclastic resorption (Dallas et al, 2002), which is very prominent in prostate cancer metastases. TGFβ acts on tumor cells to increase the secretion of factors that inappropriately stimulate bone cells (Chirgwin & Guise, 2003a,b). The interactions between bone and cancer constitute a vicious cycle, which enhances skeletal metastases (Mundy, 2002). Extensive data show that TGFβ is a major bone-derived factor responsible for driving the vicious cycle of cancer metastases in bone. TGFβ increases tumor secretion of factors such as endothelin-1, IL-6, IL-11, PTHrP, and VEGF. These factors stimulate both osteoblastic synthesis of disorganized new bone and osteolytic destruction of the skeleton adjacent to tumor cells. The cellular and molecular components of the vicious cycle between tumor and bone offer opportunities for therapeutic intervention to decrease skeletal metastases (Coleman, 2002; Guise & Chirgwin, 2003a). TGFβ in particular is an important target for intervention against prostate cancer skeletal metastases.

***Therapy to block TGFβ signaling in bone metastases.*** Previous work has demonstrated the effectiveness of TGF-β inhibition to decrease metastases, but these experiments have used protein-based treatment or ex vivo manipulations of the tumor cells (Yin et al, 1996; Muraoka et al, 2002; Yang et al, 2002). Orally active small-molecule inhibitors of the TGFβ pathway would be much more practical. This proposal will test two inhibitors of serine/threonine kinases. The first directly targets the TGFβ receptor kinase. The second targets p38 MAP kinase, which is a major downstream effector of TGFβ signaling in cancer cells. Both targets are serine/threonine kinases. Our preliminary data show that inhibition of TGFβ signaling is effective in an animal model of cancer bone metastases. The work proposed will test the two serine/theronoine kinases inhibitors in animal models of human prostate cancer in bone: one in which the response is osteolytic, two others in which it is osteoblastic. The experiments proposed will rapidly provide the preclinical data necessary for these two drugs to be placed in clinical trails for prostate cancer bone metastases.

**Hypotheses:** 1) TGFβ mediates prostate cancer metastases to bone via p38 MAP kinase. Specific serine/threonine kinase small-molecule inhibitors of the type I TGFβ receptor kinase and of p38 MAP kinase will reduce the development and progression of prostate cancer metastases to bone, due to either osteoblastic or osteolytic diseases. 2) Orally active inhibitors of these serine/threonine kinases will be effective in animal models of prostate cancer bone metastases to decrease metastases and tumor burden and to increase survival. 3) The two drugs may be more effective in combination than singly, if p38 MAP kinase also mediates TGFβ-independent metastatic functions. 4) Specific targets of TGFβ signaling in prostate cancer cells contribute directly to the bone phenotype of metastases. One such factor may be the type I membrane protein PMEPA1, which is regulated by TGFβ and expressed by prostate cancers. 5) Expression of PMEPA1 on the surface of cancer cells will

increase the development and progression of prostate cancer metastases to bone.

**Specific Aim 1:** To determine the effect of TGFβRI kinase or p38 MAPK blockade separately against 3 human prostate cancer models of skeletal metastasis in mice (hypotheses 1 & 2). Data provided below were also included in the previous annual progress reports.

*Summary of Results and Challenges Experienced*: We tested the TGFβRI kinase, SD-208, on the development and progression of bone metastases due to PC-3 and LuCAP23.1 prostate cancers. This aim has taken longer than originally planned because we had to determine long-term pharmacokinetics for drug delivery in the food. 50-100 mg/kg of SD-208 added to food result in drug levels effective in a mouse model of breast cancer metastases to bone. In the prostate cancer models SD-208 reduced osteolytic bone metastases due to PC-3, but increased osteoblastic bone metastases due to LuCAP23.1. There was no effect on the mixed tumor, C42B, which is unresponsive to TGFβ. The p38MAP kinase inhibitor, SD-282 increased bone metastases due to PC-3 prostate cancer and had no effect on LuCAP23.1 or C42B. Since SD-282 had no positive effects in 3 models, we will not pursue Aim 3, which was to combine SD-208 and SD-282 treatments. Further, the company from which we obtained SD-208, Scios, was purchased by Johnson & Johnson and the drug development program was closed. Therefore, we could no longer obtain SD-208 or SD-282. Since SD-282 had no effect on bone metastases due to C42B or LuCAP23.1 and had adverse effects on PC-3 bone metastases, we did not pursue other studies using SD-282.

This unanticipated loss of the source of SD-208 presented a significant challenge to complete the proposed aims of this experiment. However, since TGFβ inhibitors are in clinical trials for patients with all types of bone metastases, we had an obligation to obtain and test other TGFβ inhibitors. Thus, we established collaborations with Lilly (Dr. Jonathan Yingling) and Genzyme (Dr. John MacPherson). The current clinical trial is using the Lilly TGFβ receptor I kinase inhibitor; we have tested this in models of breast cancer and melanoma and found it to be effective. Future experiments testing this drug in prostate cancer bone metastases will be performed. We will also obtain the other TGFβ inhibitor, a neutralizing antibody, 1D11, and test this against prostate cancer bone metastases due to PC-3, LuCAP23.1 and C42B.

Acquisition of material transfer agreements with Lilly and Genzyme took significant time. Since SD-208 showed potential deleterious effects against osteoblastic bone metastases due to LuCAP23.1 in a small experiment (reported here), we pursued other avenues to obtain SD-208, during the time it took to establish collaborations with Lilly and Genzyme. We needed large quantities of SD-208 to perform a larger experiment to confirm the possible deleterious effects of TGFβ inhibition with SD-208 on LuCAP23.1 osteoblastic metastases. Therefore, we secured services from the chemical synthesis company, Epichem, and 120 grams of SD-208 were synthesized for use in vivo experiments. The cost of synthesis was upwards of and outside the budget of this DOD award so we secured other funds to supplement the DOD award. Once the drug was synthesized, we confirmed its biological activity in vitro and in vivo. The

entire process of SD-208 synthesis and testing biological activity took greater than one year. When we submitted the DOD award, we had an unlimited supply of SD-208, at no cost. Since SD-208 is no longer freely available from Scios, the time and money needed far exceeded what we originally anticipated. Thus, the timeline for the experiments in this aim was extended, requiring the no cost extension to complete. At the time of submission of this report, June 2009, we have just completed the large in vivo experiments testing SD-208 effects on LuCAP23.1 and C42B and are in the process of analyzing the data. In this report, we report detailed analysis of the smaller experiment for LuCAP23.1. There was insufficient tumor take in the C42B experiment to perform adequate statistical analysis, so this in vivo experiment was also repeated (C42B +/- SD-208), with larger n, and is under analysis. Finally, it should be noted that each in vivo experiment utilizing LuCAP23.1 or C42B takes approximately 6 months to achieve adequate tumor volume for adequate data analysis. SD-208 is given by daily oral gavage and requires significant technician time.

The possible deleterious effects of TGFβ inhibition on LuCAP23.1 osteoblastic tumors could be due to effects on the tumor or the host. LuCAP23.1 is a xenograft and cannot be studied in vitro, so we analyzed histology sections of bone metastases or RNA extracted from tumor tissue for evidence of TGFβ signaling. Although we found nuclear phosphoSmad2 staining in bone metastases, there were lower levels of RNA for TGFβ receptor 2 and 1 in LuCAP23.1 and C42B compared with osteolytic tumors PC-3 and MDA-MB-231. This was especially true for receptor 2. We therefore investigated the effects of TGFβ blockade on normal bone remodeling and are reported intial studies in a recently published manuscript (Mohammad et al., PLoSONE, 2009). These studies show that TGFβ inhibition has distinct effects to increase bone mass and mineralization by increasing osteoblast differentiation and activity as well as to inhibit osteoclast formation and activity. These studies, described in detail below, were undertaken in collaboration with Dr. Tamara Alliston (UCSF) and Dr. Robert Ritchie (Berkley). We have initiated studies to further dissect the molecular mechanisms by which TGFβ acts on osteoblasts and how this will affect osteoblastic prostate cancer bone metastases. For these studies, preliminary results reported here, we established a collaboration with Dr. Neil Bhowmick (Vanderbilt). Our new data show that osteoblasts exposed to TGFβ inhibition have increased production of canonical Wnt ligands, Wnt3a and Wnt8b, via STAT3. Such ligands may increase bone formation and affect prostate cancer growth to explain why TGFβ inhibition may affect osteoblastic tumors differently than osteolytic tumors.

**Specific Aim 2:** To determine the molecular targets of the inhibitors in prostate cancer cells in vitro by gene array analysis (hypothesis 4). The role of an already-identified target of TGFβ, PMEPA1, will be tested in the animal models by overexpressing it in 2 prostate cancer cell lines (hypothesis 5).

*Summary of Results:* Gene array targets of TGFβ on PC-3 prostate cancer were validated by quantitative real-time PCR and were described in the progress report for year one. We found that PMEPA1 is expressed in three different isoforms, which may have different subcellular localizations and biological

activities. We altered the design of this aim based on data acquired during the funding periond. Since PMEPA1 is already overexpressed in PC-3 cells, we constructed knockdown rather than overexpression clones. Stable knockdown cell lines have been made and characterized in vitro and in vivo. Knockdown of PMEPA1 in PC-3 prostate cancer cells caused a reduction in bone metastases in vivo. Characterization of the complex PMEPA1 promoter is complete.

**Specific Aim 3:** To test the efficacy of combined TβRI and p38 MAPK inhibitors against 3 prostate cancer models in vivo (hypothesis 3).

*Summary of Results:* Since the p38 MAPK inhibitor was entirely without benefit in Aim 1, combination trials with this drug would be a pointless waste of research animals and this Aim will not be pursued. This was indicated in last year's progress report. We utilized resources and directed efforts at characterization of the effects of TGFβ inhibition on normal bone remodeling, as described above in summary for Aim 1.

**RESULTS:**

***Aim 1: The p38MAP kinase inhibitor, SD-282, accelerated development of osteolytic lesions due to PC-3 prostate cancer (Figure 2).*** TGF-β activates the Smad signaling pathway but can also act through Smad-independent pathways including p38, a member of the mitogen-activated protein (MAP) kinase family, which is activated in response to inflammatory and environmental stresses. We tested an ATP-competitive inhibitor selective for p38α MAP kinase, the indole-5-carboxamide SD-282 in several animal models of bone metastases. SD-282 prevents bone loss and inhibits osteoclastogenesis in several experimental settings and decreases tumor growth in an animal model of multiple myeloma, where it decreases the phosphorylation of p38.

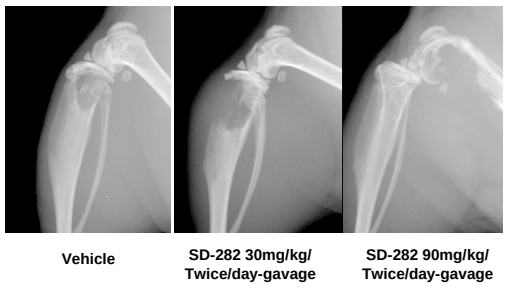


**Figure 2**: **p38MAPK inhibitor SD-282** and PC-3 bone metastases. Representative radio-graphs (4X magnification) of legs from mice with PC-3 prostate cancer cells 8wks post tumor inoculation. Larger osteolytic bone lesions in mice treated with SD-282 (right 2 panels) compared to vehicle (left panel).

We tested SD-282 on bone metastases caused by PC-3 prostate cancer and MDA-MB-231 breast cancer cells (both giving osteolytic lesions, but data only shown for PC-3 prostate cancer) and the osteoblastic prostate cancer xenograft LuCaP 23.1. Nude mice were treated with 30 or 90mg/kg/twice/day of SD-282 by gavage. Treatment was started after detection of lesions by x-ray. In MDA-MB-231 tumor-bearing mice, SD-282 increased osteolytic lesion area, as assessed by computerized image analysis of radiographs, at either 30mg/kg ($p=0.0056$) or 90mg ($p=0.0012$) doses. Histomorphometry showed that in SD-282-treated mice there was a tendency towards an increase in tumor burden in accompanied by a reduction in total bone

area. No change in osteoclast number at the tumor:bone interface was noted. In PC-3 tumor-bearing mice, SD-282 similarly increased osteolytic bone destruction, as assessed by computerized image analysis of radiographs, with either 30mg/kg (p=0.0152) or 90mg (p=0.0419) doses of the drug (**Figures 2-4**). However, in mice with LuCaP23.1 prostate xenografts SD-282 had no effect on bone lesions, as assessed by x-ray. (**Figures 5,6**) The results with the two osteolytic metastasis models are opposite to those predicted from the known effects of SD-282 on bone and on myeloma cells. They suggest that p38 MAP kinase may not be a useful drug target for treatment of bone metastases and that small molecule inhibitors of p38 MAPK may worsen osteolytic metastases by unknown and tumor-specific mechanisms.

TGFβRI kinase inhibitor reduced osteolytic bone metastases due to PC-3 prostate cancer. In contrast (and similar to results observed with osteolytic breast cancer model, MDA-MB-231 but not shown), the TGFβRI kinase inhibitor, SD-208, reduced osteolytic bone metastases and improved survival in mice bearing PC-3 prostate cancers (both treatment and prevention protocols (Figure 2, 3).

Conclusion: Taken together with data that a p38MAPK inhibitor was ineffective and even increased PC-3 and MDA-MB-231 bone metastases, it may be better to target the Smad pathway than total TGFβ signaling. The latter may be less effective, if downstream p38MAP kinase blockade adversely affects bone metastases.

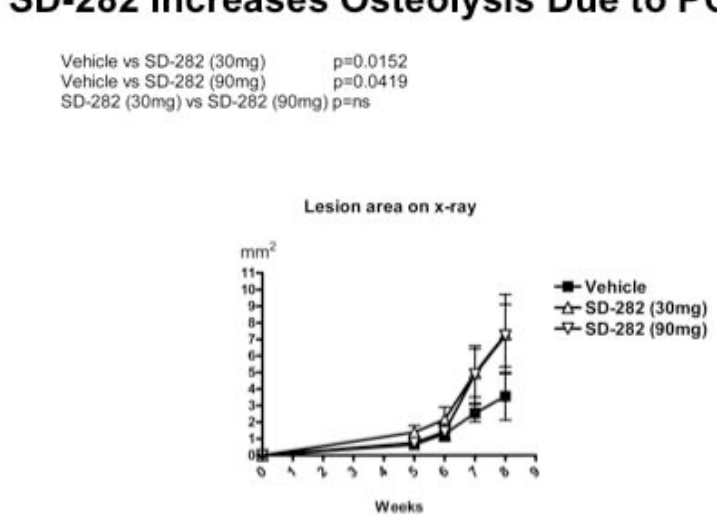


**Figure 3**: Osteolytic lesion area due to PC-3 prostate cancer is increased with the p38 MAP kinase inhibitor SD-282.

## SD-282 Accelerates Weight Loss Due to PC-3

Vehilce vs SD-282 30 mg p=ns
Vehilce vs SD-282 90 mg p<0.0001
SD-282 30 mg vs SD-282 90 mg p<0.003

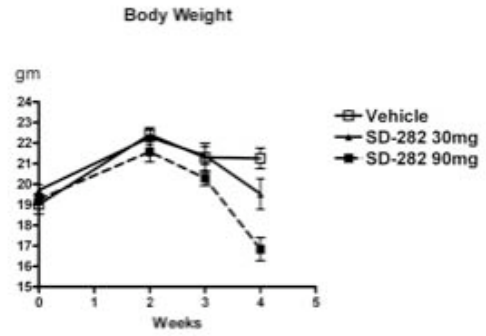


**Figure 4**: Weight loss due to PC-3 prostate cancer is increased with the p38 MAP kinase inhibitor SD-282.

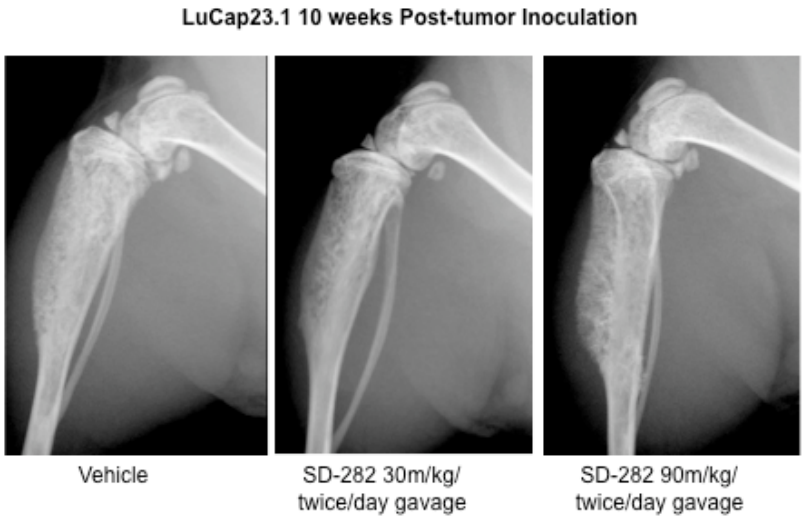


**Figure 5:** Representative radiographs (4X magnification) of the lower extremity from mice bearing LuCap23.1 prostate cancer xenograft 10 weeks post tumor inoculation intra-tibialy. No difference in osteoblastic bone lesion in vehicle treated mice (left panel) versus mice treated with SD-282 at 2 different doses (right 2 panels)

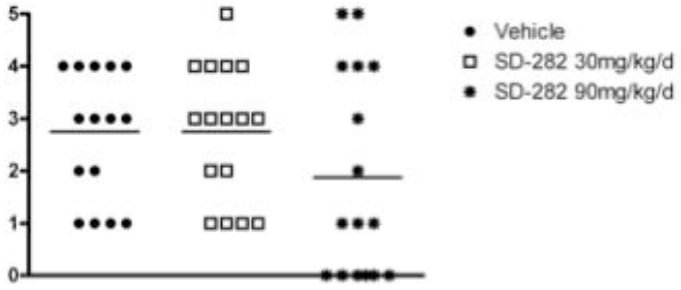


**Figure 6:** Radiographic assessment of LuCAP23.1 bearing mice treated with SD-282 shows no effect.

***Part 2: TGFβRI kinase inhibitor has no effect and possibly accelerates osteoblastic bone metastases due to prostate cancer LuCAP23.1, while having beneficial effects to reduce osteolysis due to PC-3 prostate cancer.*** TGFβ has been implicated in the pathogenesis of prostate cancer metastases to bone, so we tested SD-208 in a models of human prostate cancer, PC-3 osteolytic bone metastases and LuCAP23.1, which grows as osteoblastic lesions when directly injected into bone. LuCAP23.1 (obtained from our collaborator, Robert Vessella, University of Washington) is an androgen-sensitive, PSA-producing human tumor derived from an osteoblastic bone metastasis. It causes osteoblastic lesions in 10-12 weeks.

Male nude mice were inoculated into the left cardiac ventricle with PC-3 cells ($10^5$ cells, n=11-14/group) to cause osteolytic metastases. Immunostaining of tissue sections of PC-3 bone metastases showed that nuclear localization of phosphorylated Smad2 and, therefore, that TGF-β signaling is activated in PC-3 cells at sites of bone metastases. Mice were treated with SD-208 (50mg/kg/d po) or a vehicle and followed by x-ray. SD-208 did not decrease bone metastases incidence compared to vehicle (vehicle 10/11 vs SD-208 12/14). However SD-208 decreased progression of PC-3 bone metastases as measured by radiographic osteolytic area compared to vehicle-treated mice (6.7±3.3mm² vs 15.3±2.8mm², $P$<0.05) and increased mouse survival (57 to 69 days median survival, $P$<0.05) (**Figure 7, 8).**

To study osteoblastic metastases, we inoculated cells from the LuCap 23.1 human prostate cancer xenograft in the tibia of nude mice ($2x10^5$ cells, n=14-16/group). Similar to PC-3, immunostaining of phosphorylated Smad2 demonstrated that TGF-β signaling is active in LuCap cells at site of bone metastases. However a treatment with SD-208 (50mg/kg/d po) did not decrease metastases incidence, nor the skeletal tumor burden measured by histomorphometry compared to vehicle-treated mice. New bone formation induced by LuCAP23.1 tumor in tibia was not increased by SD-208 while bone mineral density measured in vertebra free of tumor cells was increased by SD-208 (270% increase of BV/TV, *P*<0.01) (**Figures 9-11**). Serum PSA was not statistically different between the treatment and control groups, however, since the tumors did not take at the expected rate, the experimental power was less than originally planned (**Figure 12**).

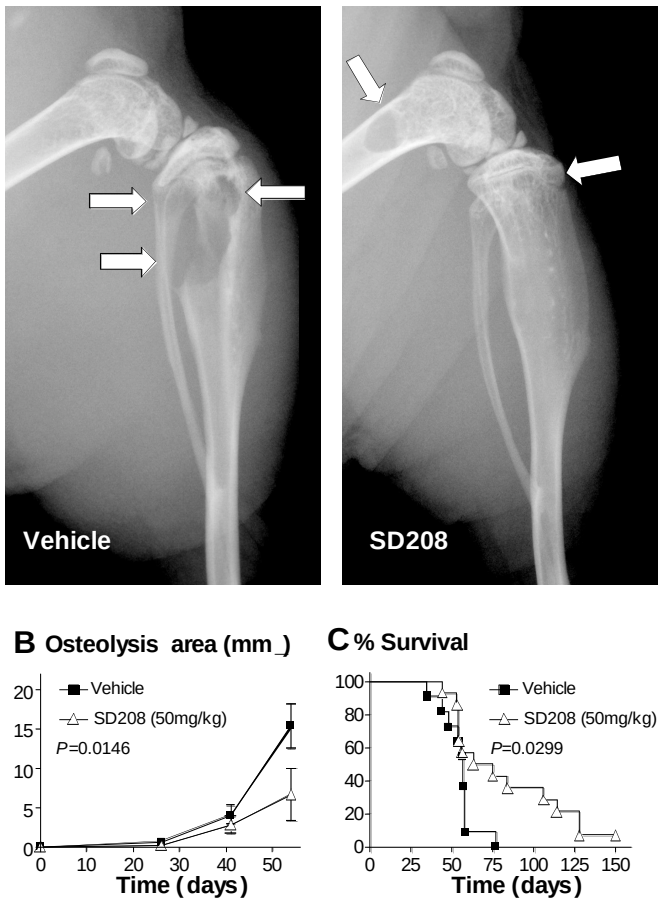


**Figure 7. SD-208 prevents PC-3 bone metastases**. Mice inoculated i.c. with $10^5$ cells PC-3 cells & given 50mg/kg SD-208 (n=14) or vehicle (n=11) 2d prior to inoculation. **A**. X-rays (4X mag) of distal femur & proximal tibia. Arrows point to osteolytic lesions. **B**. Osteolytic lesion area. Ave ± SE, by 2-way ANOVA. **C.** Kaplan-Meier survival curves.

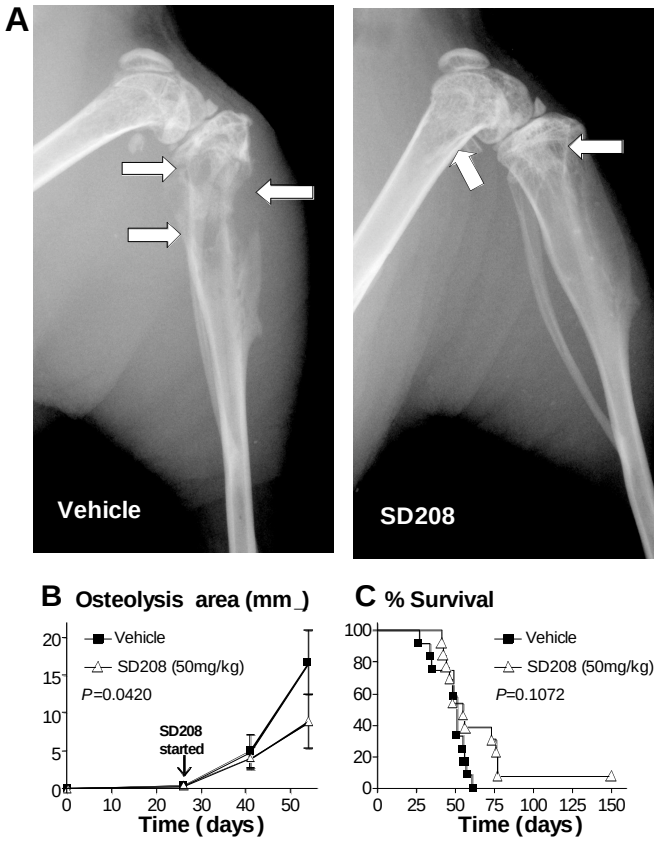


**Figure 8: Treatment of established PC-3 bone metastases with SD-208**. As in Figure 18, except mice given 50mg/kg SD-208 (n=13) or vehicle (n=12) beginning at d28, when metastases seen on X-ray.

Our results show that although TGF-β signaling inhibition with SD-208 increases bone formation, it did not increase the osteoblastic reaction of bone metastases. This is despite early radiographic evidence that such metastases were accelerated. However SD-208 effectively inhibited osteolytic metastases due to PC-3 prostate cancer cells. Therefore TGF-β blockade should be an efficient therapeutic modality to treat a wide range of bone metastases that have a predominant osteolytic rather than osteoblastic phenotype. The data from this single experiment suggest no benefit or detrimental effects of TGF-β blockade n osteoblastic bone metastases, but tumor take rates were lower than expected. Therefore, to confirm these experiments, we just completed a larger study with similar experimental design. Preliminary qualitative data are consistent with the first study. We are currently processing the bones to perform quantitative bone histomorphometry. The laboratory is moving to Indiana University on July 15, 2009, and final analysis cannot be completed before the move. Once the new laboratory is equipped, we will complete final analysis.

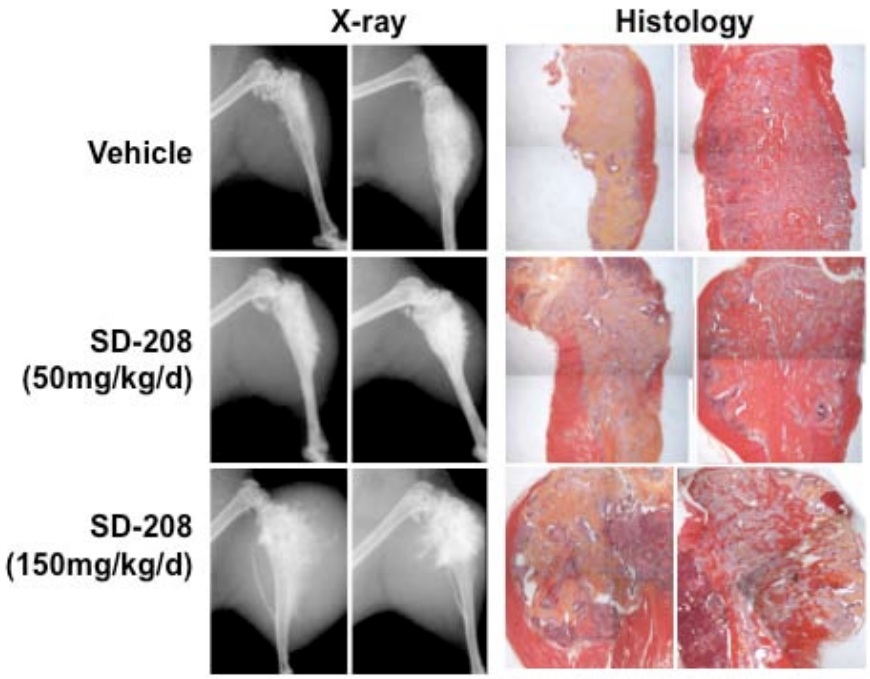


**Figure 9: TGF-β Inhibition with SD-208 has no effect on LuCaP 23.1.** 4-week old, male, athymic mice were inoculated into the tibias with LuCaP 23.1 human prostate cancer osteoblastic xenograft (n=14-15/group). Mice received SD-208 (50 or 150mg/kg/day, po) at 12 weeks post tumor inoculation when tumors were evident and continued for 26 weeks for the protocol.

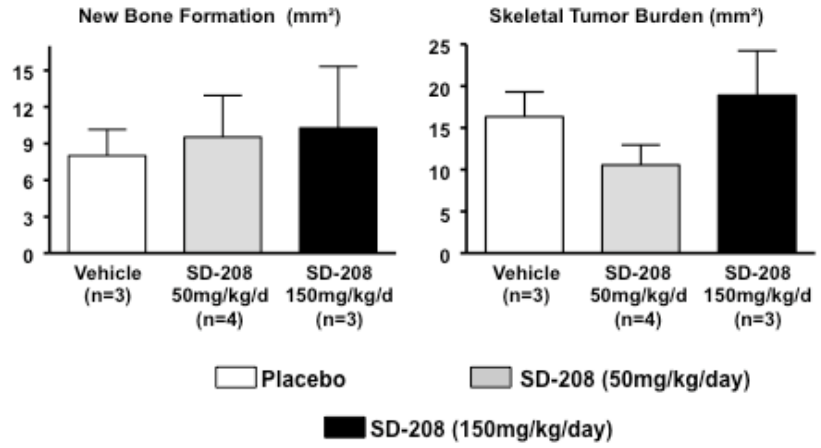


**Figure 10: TGF-β Inhibition with SD-208 Does not Increase Bone Formation and Tumor Growth in the LuCaP 23.1 Model.** 4-week old, male, athymic mice were inoculated into the tibias with cells from the LuCaP 23.1 human prostate cancer osteoblastic xenograft (n=14-15/group). Mice received SD-208 (50 or 150mg/kg/day, po) or vehicle starting 3 days prior to cancer cell inoculation and throughout the protocol. Hind limbs were removed from mice inoculated with LuCap23.1 at death, fixed in 10% formalin, decalcified in 14% EDTA and embedded in paraffin. Sections were stained with H&E to assess new bone formation (left panel) and skeletal tumor burden (right panel) using the MetaMorph imaging analysis system. Results are shown as the average ± SEM and groups were compared using a 1-way ANOVA test.

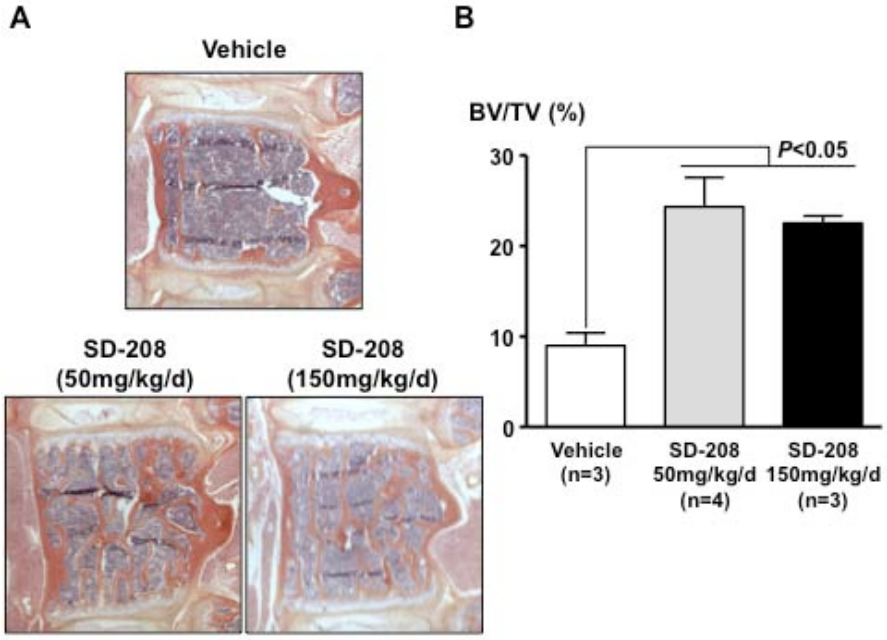


**Figure 11:** TGF-β Inhibition Increases Bone Mineral Density in Cancer-Free Vertebras in the LuCaP 23.1 Mouse Model. The thoraco-lumber vertebrae were removed from mice inoculated with LuCap23.1 at death, fixed in 10% formalin, decalcified in 14% EDTA and embedded in paraffin. Sections were stained with H&E to assess skeletal tumor burden and new bone formation using the MetaMorph imaging analysis system. A. Representative sections of vertebra. B. Quantification of trabecular bone volume (BV/TV) on tissue sections (Average ± SEM). Groups are compared using a 1-way ANOVA test and a Dunnett's multiple comparison post-test.

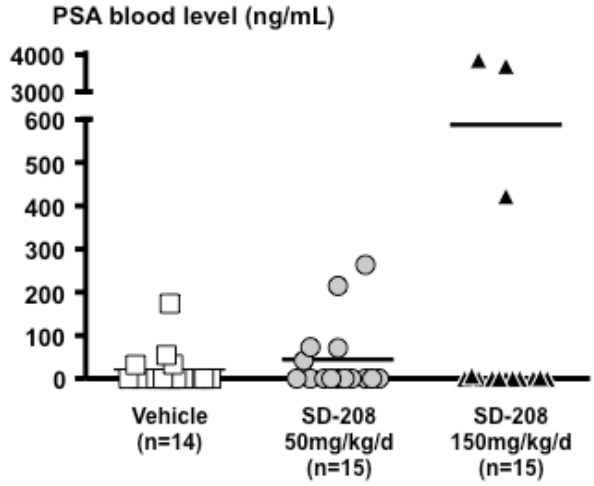


**Figure 12:** SD-208 Does not Increase PSA Blood Level in the LuCaP 23.1 Mouse Model. LuCaP 23.1 cells secrete the prostate specific antigen (PSA), which was measured in the plasma of mice using a human PSA ELISA kit according to the manufacturer's instructions (ANOGEN). Results are shown as a scattered plot and groups were compared using a 1-way ANOVA.

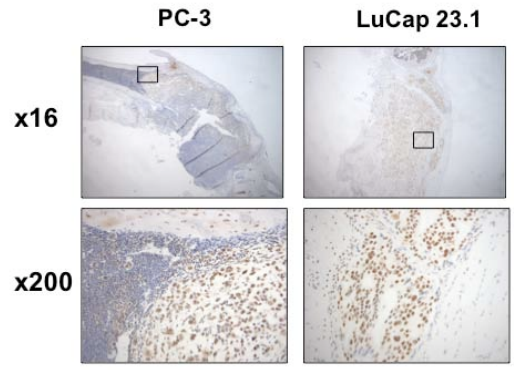


**Figure 13: Activated Smad Pathway in PC-3 and LuCap 23.1 Cells in Bone. Phosphorylated Smad2** is localized in the nucleus of PC-3 and LuCap23.1 prostate cancer cells in mouse bones. Bone tissue sections were stained using a rabbit polyclonal antibody against phosphorylated Smad2 Ser465/467 (dilution 1:500; Cell Signaling Technology) with a biotinylated goat anti-rabbit antibody (1:2000 dilution, Chemicon) and the Vectastain Elite ABC kit (Vector Laboratories)

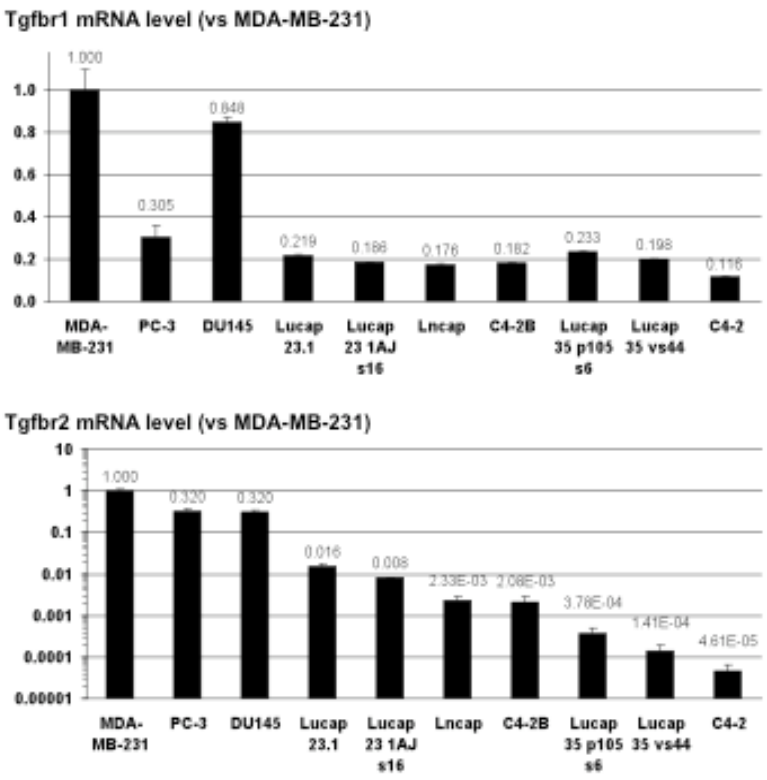


**Figure 14:** Expression of TGF-β receptor type I and II in cancer cells.
Lucap 23.1, Lucap 23 1AJ s16, Lucap 35 p105 s6 and Lucap 35 vs44 human prostate cancer cells were maintained in SCID mice. Tumor were harvested and fragments were conserved at -80°C in RNA later (Qiagen) until RNA extraction. MDA-MB-231 human breast cancer cells and PC-3, DU145, LnCap, C4-2 and C4-2B human prostate cancer cells were grown in DMEM or RPMI media supplemented with 10% heat inactivated FBS until the cell monolayer reach near confluency. Total RNA from cancer cells grown in vitro and in vivo was extracted using a GenElute™ Mammalian Total RNA kit (Sigma Aldrich) according to the manufacturer's instructions. RNA from each sample (500ng) was reverse transcribed using the enzyme Superscript II (Invitrogen) according to the manufacturer's instructions and anchored oligo(dT) (Thermo Scientific) for priming. The resulting cDNAs were then processed for real-time PCR using QuantiTect SYBR Green PCR Kit (Qiagen). Reactions were carried out in a MyiQ™ Single-Color Real-Time PCR Detection System (BioRad, Hercules, CA) for 45 cycles (95°C for 1min, 60°C for 30sec, 72°C for 30sec) after an initial 15-min incubation at 95°C. Sequences of the primers for Tgfbr1 (NM_004612) were as followed: sense 5'-GATGGGCTCTGCTTTGTCTC-3', antisense 5'-CAAGGCCAGGTGATGACTTT-3'', and for Tgfbr2 (NM_001024847 ) were as followed: sense 5'-TTTTCCACCTGTGACAACCA-3', antisense 5'-GGAGAAGCAGCATCTTCCAG-3'. Target gene expression was normalized against the housekeeping gene RPL32 (Ribosomal protein L32, NM_001007073 , sense 5'-CAGGGTTCGTAGAAGATTCAAGGG-3', antisense 5'-CTTGGAGGAAACATTGTGAGCGATC-3'). Considering the possible presence of mouse RNA in the Lucap tumors, the specificity of primers for human RNA was tested against mouse RNA. None of the pairs of primers used gave any amplification products using mouse RNA. Samples were analyzed in triplicates and 2 to 3 Lucap tumors were collected for each variants. Relative quantities of RNA were calculated against a standard curve prepared with diluted cDNA. Samples were analyzed in triplicates, and relative quantities are expressed as the average ± SEM against MDA-MB-231. Values indicate the relative average level of mRNA.

***TGFβ blockade increases bone mass due to effects on osteoblasts and osteoclasts.*** Since our original data suggested that TGFβRI kinase inhibition

may worsen osteoblastic metastases, we determined the effect of TGFβ inhibition on normal bone cell function. We have new data that SD-208 has direct effects to increase osteoblast activity. This host response to the drug could accelerate osteoblastic disease in prostate cancer.

The possible deleterious effects of TGFβ inhibition on LuCAP23.1 osteoblastic tumors could be due to effects on the tumor or the host. LuCAP23.1 is a xenograft and cannot be studied in vitro, so we analyzed histology sections of bone metastases or RNA extracted from tumor tissue for evidence of TGFβ signaling. Although we found nuclear phosphoSmad2 staining in bone metastases, there were lower levels of RNA for TGFβ receptor 2 and 1 in LuCAP23.1 and C42B compared with osteolytic tumors PC-3 and MDA-MB-231. This was especially true for receptor 2, and it is not clear what amount of TGFβ signaling is active in LuCAP23.1 (**Figure 12, 13**). We have initiated studies to determine TGFβ signaling in vivo, and these will be completed once we have moved to Indiana University. We therefore investigated the effects of TGFβ blockade on normal bone remodeling and are reported initial studies in a recently published manuscript (Mohammad et al., PLoSONE, 2009). These studies we performed with Dr. Tamara Alliston (UCSF) and Dr. Robert Ritchie (Berkley) show that TGFβ inhibition has distinct effects to increase bone mass and mineralization by increasing osteoblast differentiation and activity as well as to inhibit osteoclast formation and activity (described in greater detail below). We have initiated studies to further dissect the molecular mechanisms by which TGFβ acts on osteoblasts and how this will affect osteoblastic prostate cancer

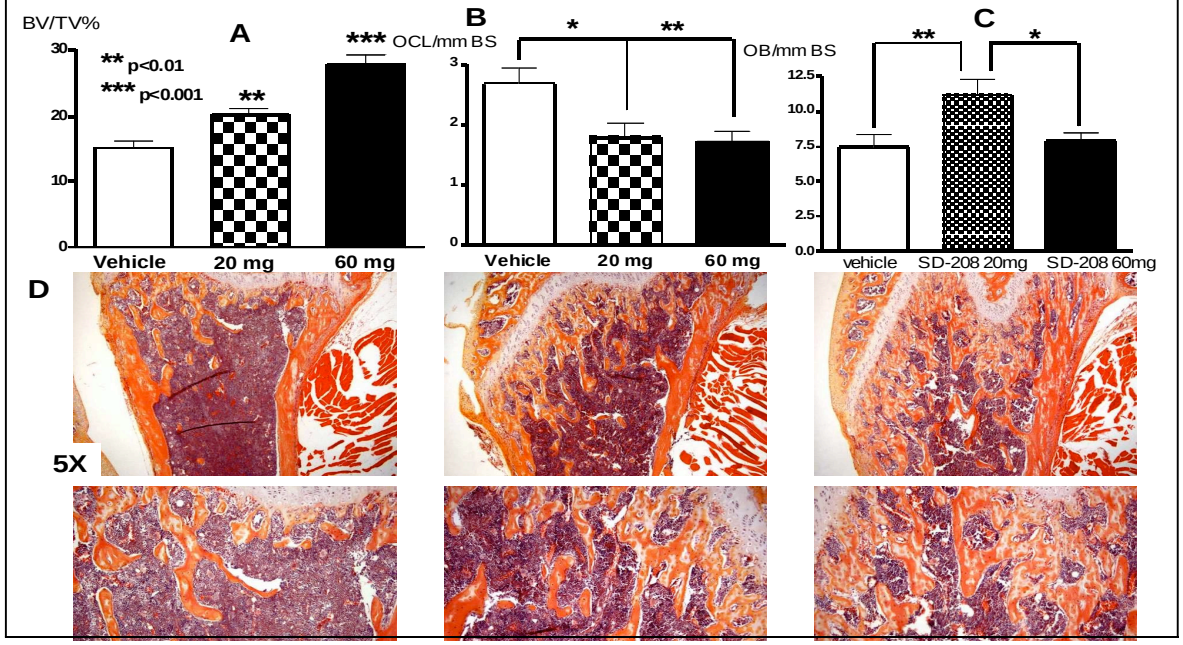


**Figure 15**: **(A) Histomorphometry**. SD-208 60 or 20mg/kg/d significantly increased trabecular bone volume (TBV). (**B**) **Osteoclast number** reduced by both doses**. (C)** 20mg/kg/d increased **osteoblast number** vs. vehicle. **(D)** Bone histology (H&E):Mid-sagital femur at 5x (upper) & 10x (lower).

bone metastases. For these studies, preliminary results reported here, we established a collaboration with Dr. Neil Bhowmick (Vanderbilt). Our new data show that osteoblasts exposed to TGFβ inhibition have increased production of canonical Wnt ligands, Wnt3a and Wnt8b, via STAT3. Such ligands may increase bone formation and affect prostate cancer growth to explain why TGFβ inhibition may affect osteoblastic tumors differently than osteolytic tumors. We have just submitted a new U01 proposal with Dr. Bhowmick to investigate the role of osteoblast-derived Wnt ligand production on tumor growth in vivo.

**TGF-β signaling blockade increases bone mass, osteoblast differentiation and bone formation , while decreasing osteoclast formation and resorption.** Pharmacologic approach with SD-208: We observed in mice with bone metastases that TGF-β blockade had effects to increase bone at sites unaffected by tumor, so we next determined the effects of pharmacological TGFβ receptor blockade on bone remodeling. Nude mice treated with SD-208 (20 or 60 mg/kg po qd) for 4 weeks had increased bone mineral density (by DXA), at the tibia, femur and total body sites. Bone histomorphometry revealed an increase in trabecular bone volume, increased osteoblast and reduced osteoclast numbers (**Figure 15**). Blockade of TGFβ signaling with SD-208 in a human osteoclast culture inhibited in vitro bone resorption, independent of the effect on osteoclast number. Further, TGFβ impaired osteoblast differentiation; this was blocked by SD-208 (**Figure 16**). Since T cells have been shown to impact bone remodeling more detailed studies were performed in immunocompetent mice (Mohammad et al, PLoSONE, 2009). To examine the role of TGF-β in the maintenance of the postnatal skeleton, we evaluated the effects of pharmacological inhibition of the TβRI kinase on bone mass, architecture and material properties. TβRI blockade increased bone mass and multiple aspects of bone quality, including trabecular bone architecture and macro-mechanical behavior of vertebral bone. This was associated with increased osteoblast differentiation and bone formation, and reduced osteoclast differentiation and bone resorption. Furthermore, there was increased expression of Runx2 and EphB4, which promote osteoblast differentiation, and ephrinB2, which antagonizes osteoclast differentiation. Through these anabolic and anti-catabolic effects, TβRI inhibitors coordinate changes in multiple bone parameters, including bone mass and mineralization that collectively increase bone fracture resistance.

**TGF-ß mediated Wnt regulation in osteoblasts**. Our collaborator, Neil Bhowmick, previously reported that TGF-ß down regulates STAT3 activity. Stat3 promoted Wnt3a transcriptional in prostate stromal cells (Li et al, 2008). Promoters of eight of the nine canonical Wnt isoforms (Wnt2, 2b, 3, 3a, 6, 7b, 8a, and 8b). contain similar Stat3 binding motifs in their promoters. We screened primary osteoblasts for expression of canonical Wnt isoforms in response to SD-208. PCR suggested Wnt3a and Wnt8b were the most abundant Wnt ligands expressed by primary mouse osteoblasts. Wnts were induced by SD-208 and inhibited by TGF-ß (**Figure 17)**. Stat3 expression is critical for Wnt3a expression and likely Wnt8b. Expression of the Stat3 antagonist, StatIP1, was reduced two-fold in primary osteoblasts treated with SD-208 (**Figure 18**). These data reveals a novel pathway downstream of TGF-ß signaling in osteoblasts that may regulate canonical Wnt expression and many other factors such as HGF, VGEF, and Hif1a. Blocking TGF-ß signaling may induce multiple canonical Wnt ligands in osteoblasts - a mechanism of osteoblastic growth that may also accelerate osteoblastic bone metastases.

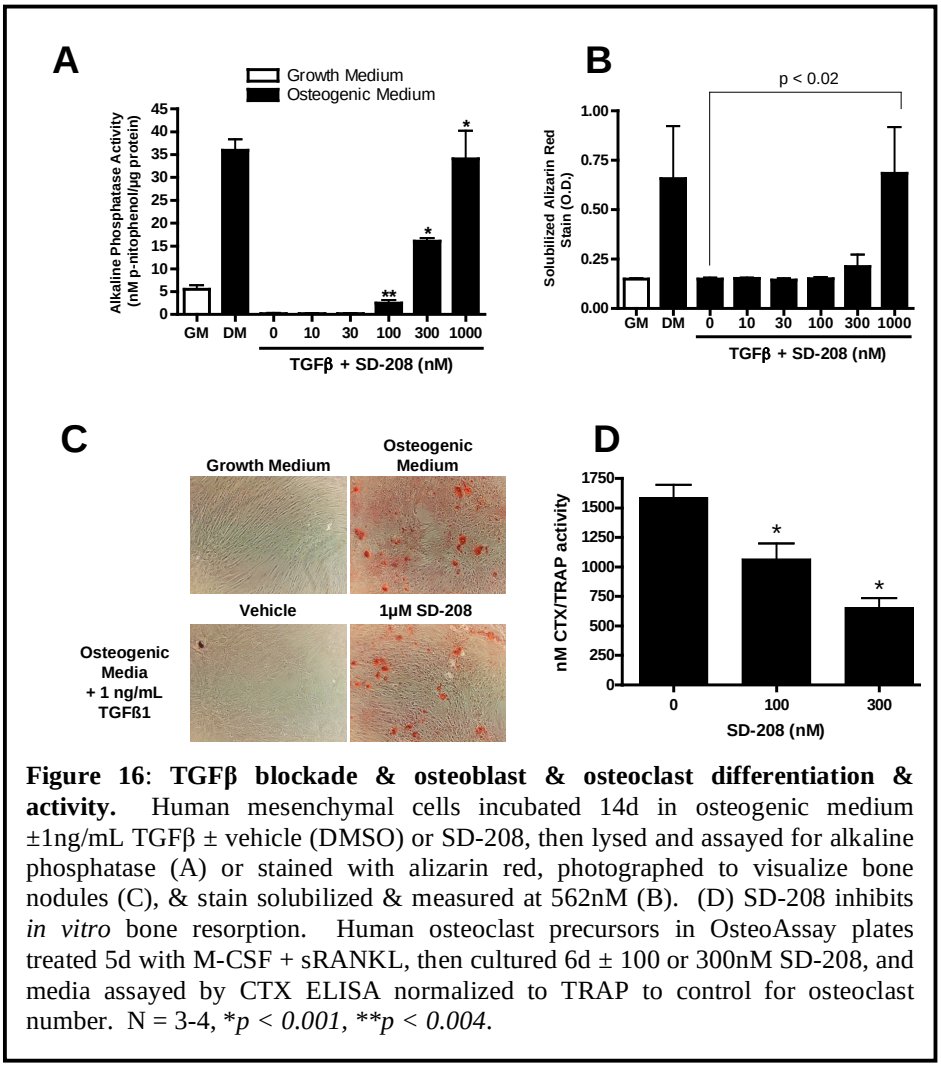


**Figure 16**: **TGFβ blockade & osteoblast & osteoclast differentiation & activity.** Human mesenchymal cells incubated 14d in osteogenic medium ±1ng/mL TGFβ ± vehicle (DMSO) or SD-208, then lysed and assayed for alkaline phosphatase (A) or stained with alizarin red, photographed to visualize bone nodules (C), & stain solubilized & measured at 562nM (B). (D) SD-208 inhibits *in vitro* bone resorption. Human osteoclast precursors in OsteoAssay plates treated 5d with M-CSF + sRANKL, then cultured 6d ± 100 or 300nM SD-208, and media assayed by CTX ELISA normalized to TRAP to control for osteoclast number. N = 3-4, *$p < 0.001$, **$p < 0.004$.

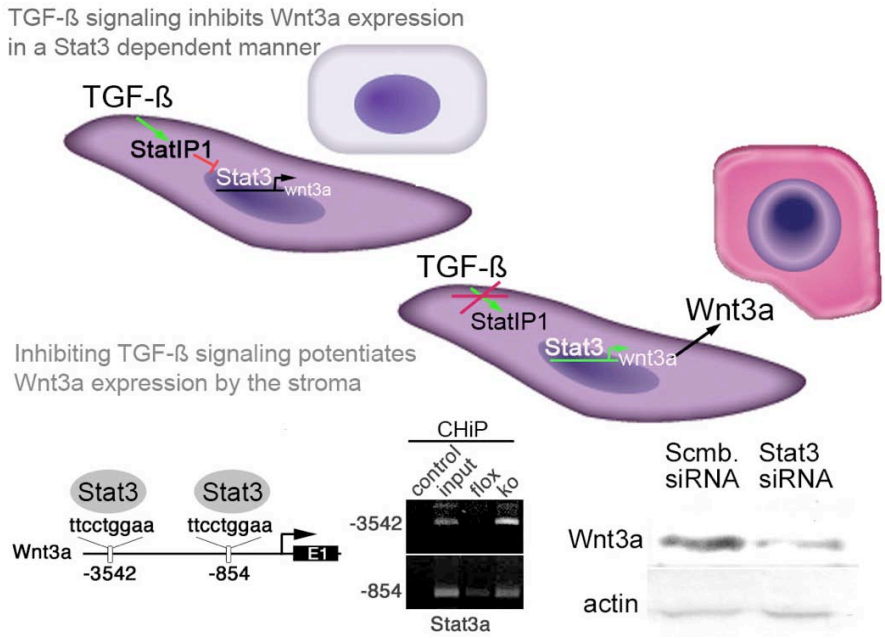


**Figure 17.** Wnt3a expression is down regulated by TGF-ß in prostate stromal cells. Paracrine Wnt3a signaling promote epithelial transformation. Wnt3a promoter analysis suggested Stat transcription factor binding consensus sites. ChIP analysis suggested greater Stat3 binding to the Wnt3a -854 and -3542 promoter elements in $Tgfbr2^{fspKO}$ stromal cells compared to $Tgfbr2^{floxE2/floxE2}$ stromal cells. Western blotting for Wnt3a following siRNA-knockdown of Stat3 in $Tgfbr2^{fspKO}$ stromal cells showed inhibition of Wnt3a expression. The scrambled (Scmb.) siRNA did not affect Wnt3a expression. (Li et al., 2008a).

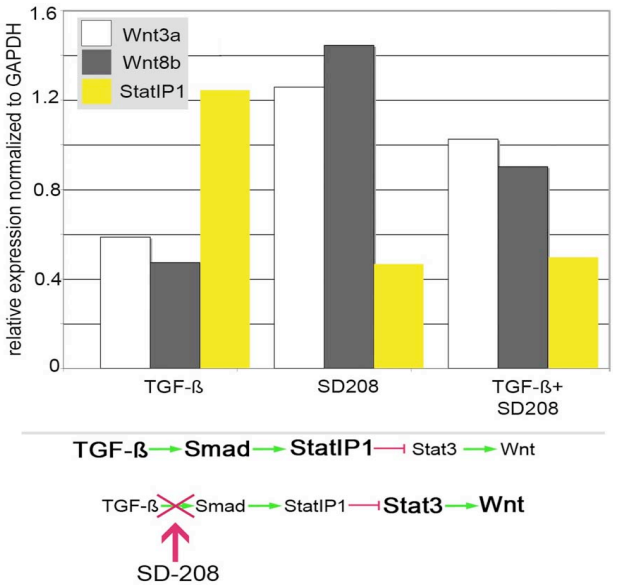


**Figure 18.** Wnt3a, Wnt8b, and StatIP1 mRNA expression is up regulated by SD208. Quantitative realtime RT-PCR revealed antagonism of TGF-ß signaling induced canonical Wnt expression, but reduced StatIP1 expression proportionately in primary osteoblasts. TGF-ß inhibits Wnt signaling in a Stat3 dependent manner.

Collectively, these data from pharmacologic and genetic mouse models of TGF-ß blockade indicate that TGF-β has direct effects to inhibit osteoblast differentiation. The effects of TGF-β to stimulate osteoclast activity appear to be direct, as evidenced by reduced

osteoclast activity in mice with targeted osteoclast deletion of TβRII. Since mice with osteoblast deletion of TβRII also have reduced osteoclast activity, there appear to be indirect effects as well. These effects of TGF-β on bone cells add an additional level of complexity to our understanding of the role of TGF-β in the pathophysiology of bone metastases (**Figure 19**) and have important implications to treat patients with bone metastases. TGF-β inhibitors could have differential effects on tumor metastases, depending on the osteolytic or osteoblastic phenotype.

We tested SD-208 on bone metastases due to the mixed

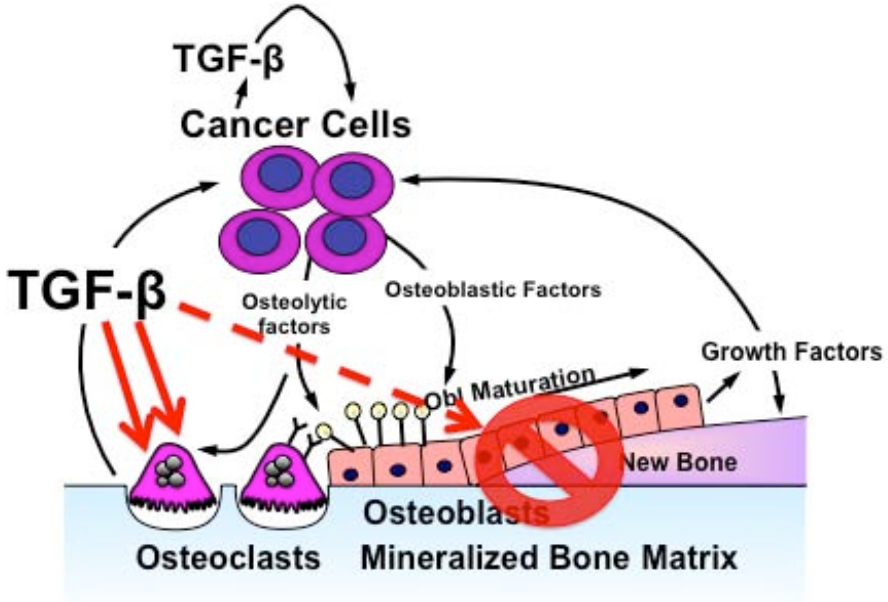


**Figure 19**: **TGF-β effects on bone in the context of metastases.** In addition to effects on cancer cells, TGF-β acts on osteoclasts to stimulate bone resorption, and osteoblasts to inhibit differentiation. These effects could further promote tumor growth in bone.

osteolytic/osteoblastic tumor C42B. No effect was observed in treated compared to control animals. Quantitative histomorphometry is underway on bones from all experiments.

**Aim 2: Identification of PMEPA1 as a major target gene of TGFβ in metastatic cancer cells and analysis of role of PMEPA1 in TGFβ signaling.**

We previously identified the PMEPA1 gene as the most highly upregulated gene in prostate cancer cells treated with TGFβ. The background on this protein is provided in the previous report. The protein sequence suggests that the protein could regulate intracellular signaling in particular via the TGFβ pathway. Data are now provided to uspport this hypothesis.

**PMEPA1 is expressed in cell lines that cause bone metastases**. Using RT-PCR, we found that PMEPA1 is expressed in different PrCa cell lines, LnCap, C4-2B and DU145, the BrCa cells MDA-MB-231 and the lung adenocarcinoma

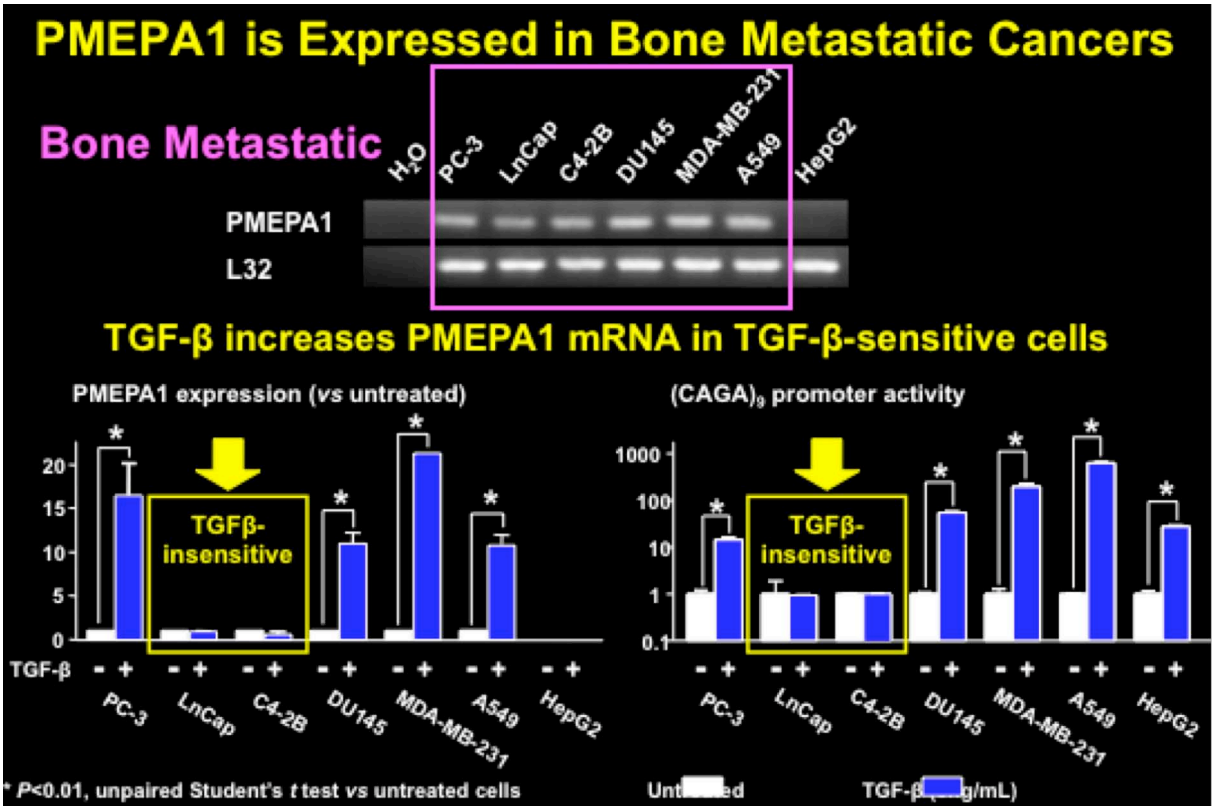


**Figure 20**: **PMEPA1 is expressed in cell lines that cause bone metastases**. RT-PCR, showed that PMEPA1 was expressed in different PrCa cell lines, LnCaP, C4-2B and DU145, BrCa MDA-MB-231 and lung adenocarcinoma A549. The hepatocarcinoma HepG2 did not express detectable PMEPA1. When cells were treated with TGF-β for 24 hours, PMEPA1 mRNA was increased in most of the cells but not in LnCaP or in its derivative C4-2B. However LnCaP and C4-2B are TGF-β insensitive.

A549. The hepatocarcinoma HepG2 did not express detectable PMEPA1. When cells were treated with TGF-β for 24 hours, PMEPA1 mRNA was increased in most of the cells but not in LnCaP or in its subclone C4-2B (**Figure 20**). However we tested (as others have previously reported in the literature) that the LnCaP and C4-2B cell lines are TGF-β insensitive.

**TGF-β increases PMEPA1 transcription and protein**. We validated the increase of PMEPA1 expression induced by TGF-β in PC-3 cells. PMEPA1 mRNA was quickly increased by TGF-β and reached a peak by 4 hours. This TGF-β induction was prevented by adding the specific TGF-β receptor inhibitor, SD-208. We used classical cycloheximide and actinomycin-D inhibitor treatments to determine if the effects were transcriptional or translational. We found that the translation inhibitor cycloheximide did not block TGF-β induction of PMEPA1, while the transcription inhibitor actinomycin D prevented the increase of PMEPA1

mRNA. The results (**Figure 21**) suggest that TGF-β regulates PMEPA1 expression through transcriptional control. Western blot (bottom panel) showed PMEPA1 protein increase at 48 hours.

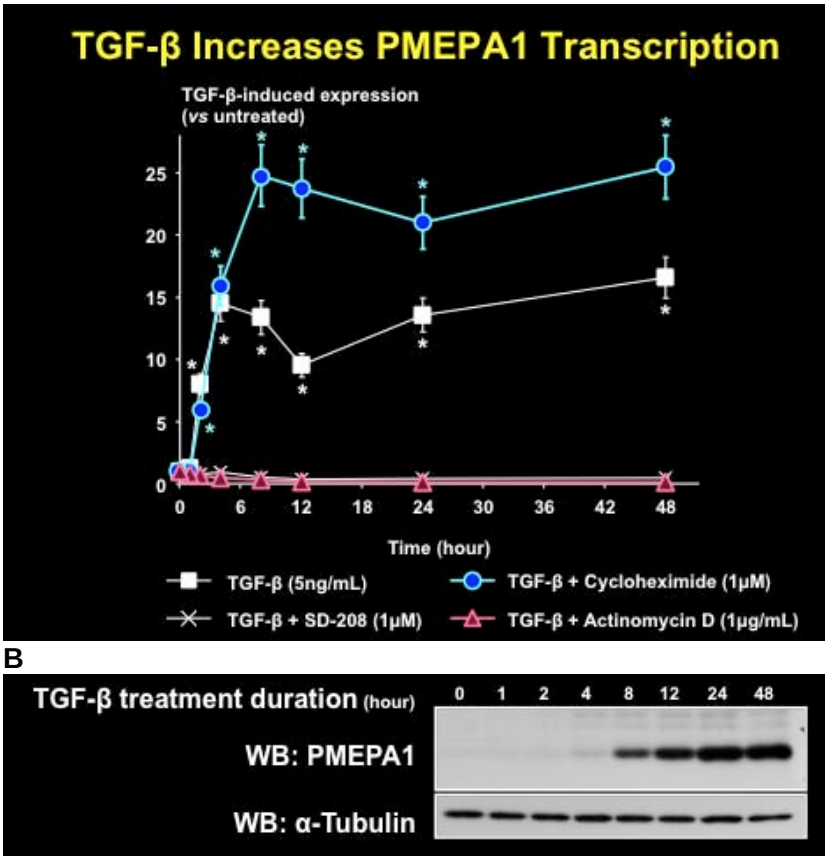


**Figure 21: TGF-β increases PMEPA1 transcription and protein**. PMEPA1 expression was induced by TGF-β in PC-3 cells. PMEPA1 mRNA quickly increased by TGF-β and reached a peak by 4 hours. TGF-β induction was prevented by adding the specific TGF-β receptor inhibitor, SD-208. Classical cycloheximide and actinomycin-D treatments used to determine if the effects were transcriptional or translational. The translation inhibitor cycloheximide did not block TGF-β induction of PMEPA1, while the transcription inhibitor actinomycin D prevented the increase of PMEPA1 mRNA. The results suggest that TGF-β regulates PMEPA1 expression via transcription. Western blot (bottom panel) showed PMEPA1 protein increase at 48hrs

**The PMEPA1 gene covers 63kb.** Alternative splicing and multiple transcription starts give rise to 4 different mRNA variants. These mRNA encodes 3 different protein isoforms. Isoforms a & b contain a transmembrane domain, while isoform c, the shortest, is cytosolic (**Figure 22**).

**TGF-β induces the cytosolic (c) isoform of PMEPA1 in PC-3 cells:** The isoforms of PMEPA1 were cloned and expressed in COS cells (left panel). Western blot showed that the PMEPA1 antibody detected all isoforms (**Figure 23**). In PC-3 cells, only the cytosolic isoform was induced by TGF-β (right panel)

**Selection of shRNA vectors which knock-down all isoforms of PMEPA1.** We validated a vector expressing a short hairpin RNA against the 3' extremity of PMEPA1 mRNA, analog to all variants. Using real-time PCR, we showed that in CHO cells transfected to express one of the PMEPA1 isoform, there was a 90% decrease of all corresponding PMEPA1 mRNA (**Figure 24**). An empty vector or a vector expressing a non-specific shRNA had no effect on PMEPA1 mRNA quantity. Similarly, using Western Blot, the shRNA against

PMEPA1 specifically decreased PMEPA1 protein quantity regardless of the isoform.

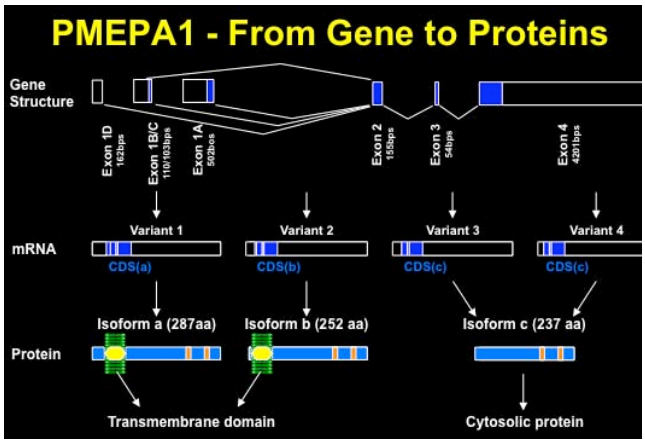


**Figure 22: The PMEPA1 gene covers 63kb.** Alternative splicing and multiple transcription starts give rise to 4 different mRNA variants. These mRNA encodes 3 different protein isoforms. Isoforms a & b contain a transmembrane domain, while isoform c, the shortest, is cytosolic.

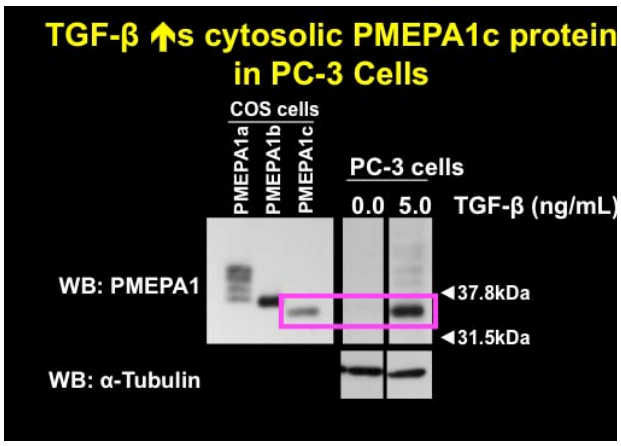


**Figure 23: TGF-β induces the cytosolic form of PMEPA1 in PC-3 cells:** The isoforms of PMEPA1 were cloned and expressed in COS cells (left panel). Western blot showed that the PMEPA1 antibody detected all isoforms. In PC-3 cells, only the cytosolic isoform was induced by TGF-β (right panel).

**PMEPA1 knockdown decreases TGF-β but not BMP signaling.** We tested TGF-β signaling in PC-3 using the (CAGA)9 promoter when the cells were transfected with a vector expressing either a non-targeting shRNA or an shRNA against PMEPA1. Knockdown of PMEPA1 in PC-3 cells, induced a significant decrease of the (CAGA)9 promoter activity induced by TGF-β. This result suggests that PMEPA1 in PC-3 cells increases TGF-β signaling (**Figure 25**). There was no effect on BMP promoter activity as assessed by BRE activity or an unrelated SV40 promoter.

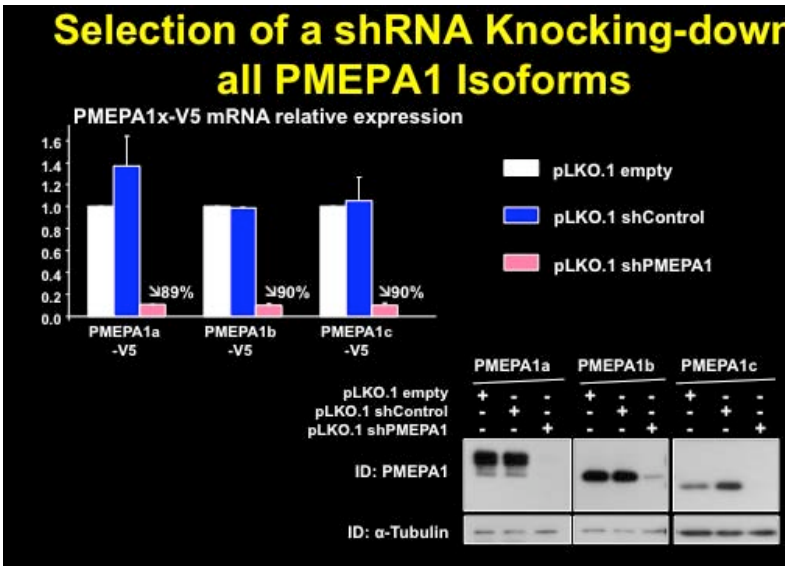


**Figure 24: Selection of shRNA vectors for knock-down all isoforms of PMEPA1.** Validation of vector expressing a short hairpin RNA against the 3' end of PMEPA1 mRNA, common to all variants. By PCR (upper panel) of CHO cells transfected to express one of the PMEPA1 isoform, there was a 90% decrease of all corresponding PMEPA1 mRNAs. Empty vector or one expressing a non-specific shRNA had no effect on PMEPA1 mRNA quantity. By western blot (lower panel) the shRNA against PMEPA1 specifically decreased PMEPA1 protein quantity regardless of the isoform.

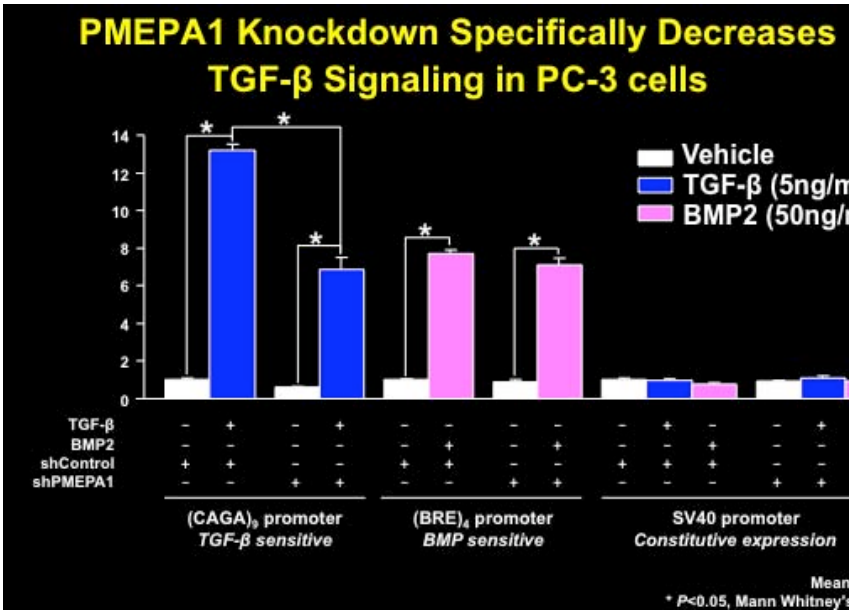


**Figure 25: PMEPA1 knockdown decreases TGF-β but not BMP signaling.** TGF-β signaling in PC-3 tested with (CAGA)9 promoter when cells were transfected with a vector expressing either a non-targeting shRNA or an shRNA against PMEPA1. Knockdown of PMEPA1 in PC-3 cells significantly decreased (CAGA)9 promoter activity induced by TGF-β. This result suggests that PMEPA1 in PC-3 cells increases TGF-β signaling. There was no effect on BMP promoter activity as assessed by BRE activity or an unrelated SV40 promoter.

**Model for PMEPA1 role in bone metastases:** We hypothesize that PMEPA1, when induced by TGF-β at the site of bone metastases, interacts with Smurf proteins, to prevent the degradation of Smads and the TβR. This results in a sustained TGF-β signaling and an increase of bone metastases development (**Figure 26**). PMEPA1 could also directly affect Smad activity when interacting with them by a mechanism that remains to be elucidated. Experiments are underway to test the function of PMEPA1 protein expression on TGFβ signaling in prostate cancer bone metastases. In vivo experiments described below were not consistent with this model and suggest that the different isoforms of PMEPA1 have different and divergent effects on TGFβ signaling in prostate cancer cells.

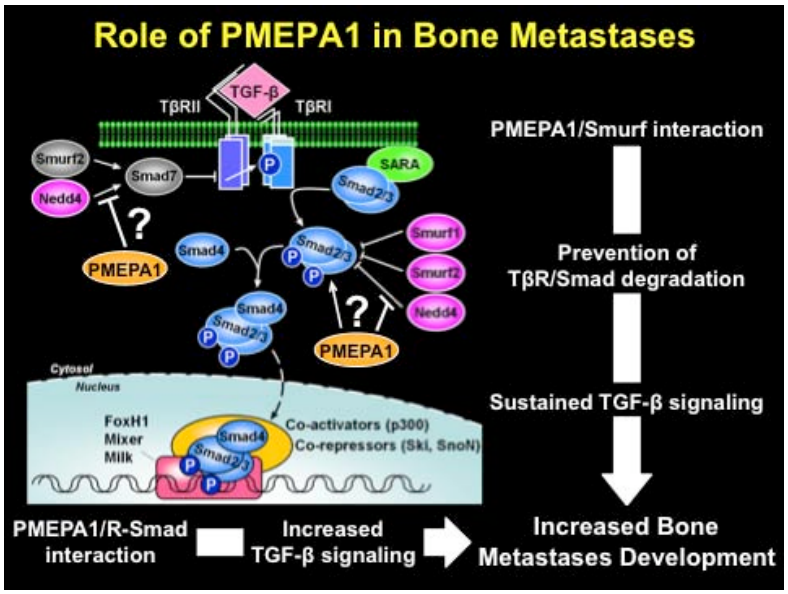


**Figure 26: Model for PMEPA1 role in bone metastases:** PMEPA1, when induced by TGF-β at the site of bone metastases, may interact with Smurf proteins to prevent the degradation of Smads and the TβRs. This results in sustained TGF-β signaling and increased bone metastases. PMEPA1 could also directly affect Smad activity when interacting with them by a mechanism that remains to be elucidated.

**S**everal stable knockdown clones of PMEPA1 or control clones were produced in PC-3 prostate cancer cells and described in figure 27. Clones were stable for greater than 75 days in the absence of the selective antibiotic. PMEPA1 was not detected at the protein level by Western blot, in these clones, compared to controls (**Figure 27**). Cell growth in vitro was not signficantly different (**Figure 28**).

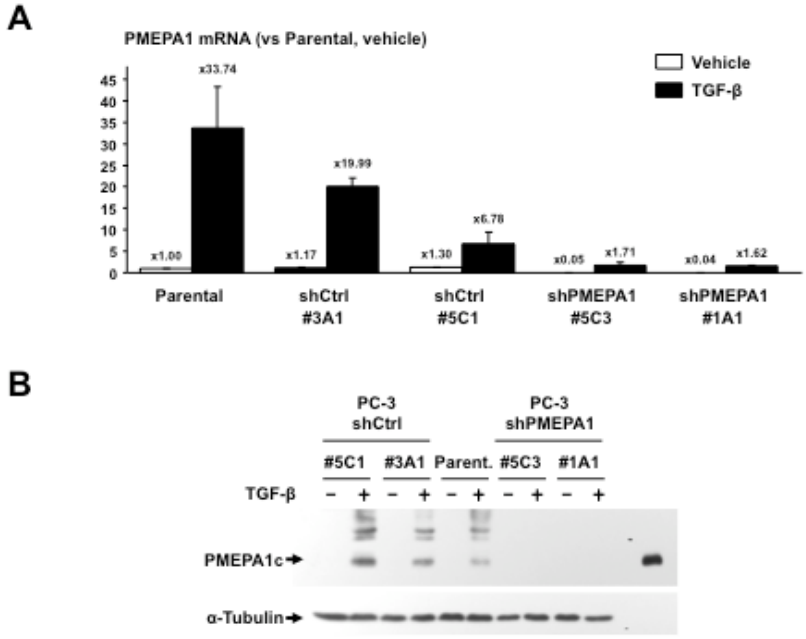


**Figure 27:** Stable knockdown of PMEPA1 expression in PC-3 prostate cancer cells. PC-3 parental cells were transfected with a pLKO.1 vector expressing a non-target shRNA (shCtrl) or an shRNA against PMEPA1 (shPMEPA1) and single cell clones were isolated after antibiotic selection (puromycin, 250pg/mL). Stability of the transfection was assessed by culturing PC-3 shCtrl clones (shCtrl #3A1 and #5C1) and PC-3 shPMEPA1 clones (shPMEPA1 #5C3 and #1A1) in absence of antibiotic during 75 days and by measuring the expression of PMEPA1 mRNA and protein in the presence or absence of TGF-β (5ng/mL, 24h). A. Total RNA was extracted and mean ± SEM expression of PMEPA1 was measured using semi-quantitative RT-PCR (n=3). B. Proteins were extracted from treated cells and PMEPA1 level was assayed by Western-blotting, α-tubulin was used as loading control.

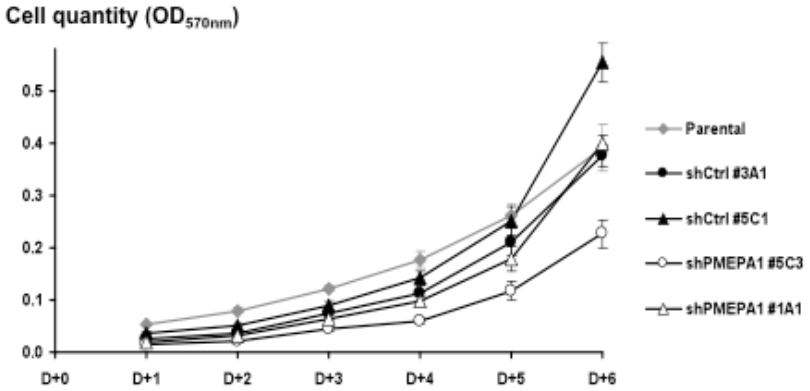


**Figure 28:** PC-3 parental cells or PC-3 cells stably transfected to express an shRNA control (shCtr #3A1 and #5C1) or against PMEPA1 (shPMEPA1 #5C3 and #1A1) were seeded in 96 well-plate (500 cells per well) and cultured in complete medium for 6 days. Cells quantity was assessed using an MTT assay and results are represend as the average ± SEM optical density at 750nm ($OD_{750nm}$) of a sextuplicate.

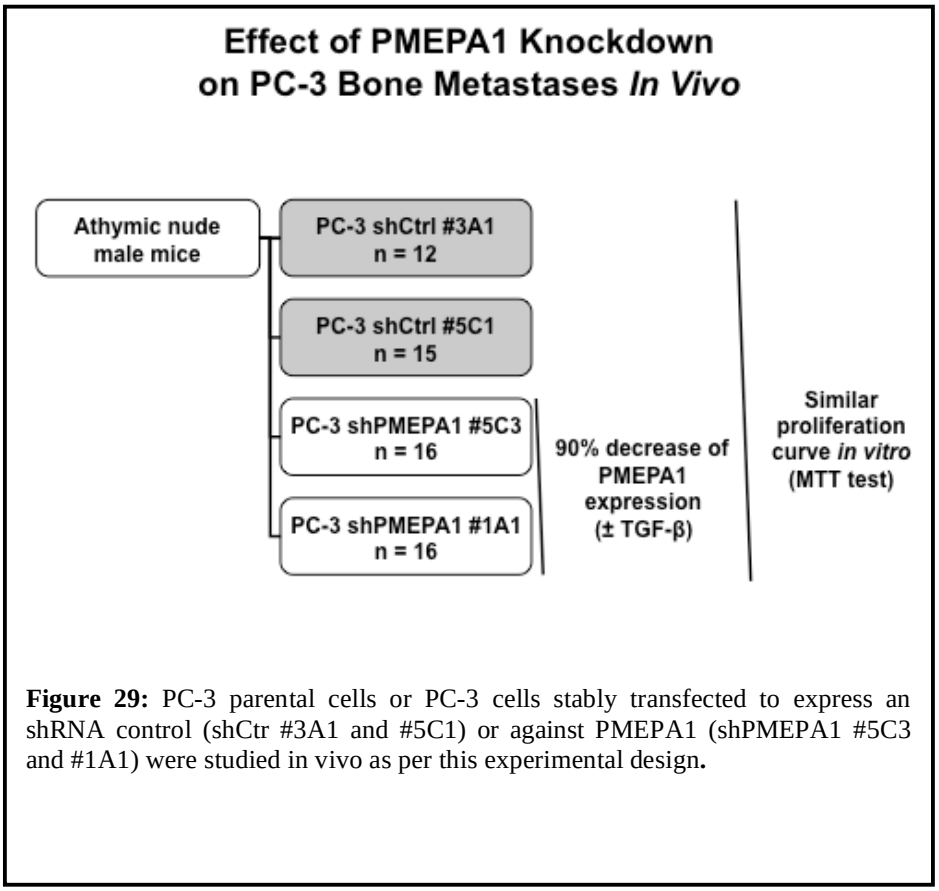


**Figure 29:** PC-3 parental cells or PC-3 cells stably transfected to express an shRNA control (shCtr #3A1 and #5C1) or against PMEPA1 (shPMEPA1 #5C3 and #1A1) were studied in vivo as per this experimental design**.**

**B**one metastases were studies using these clones in male nude mice were studied as per the experimental design illustrated in Figure 29. Unexpectedly, osteolytis was increased in mice bearing PC-3 clones in which PMEPA1 was stably knocked down (**Figure 30**). To investigate possible reasons for this increase in osteolysis, each clone was tested for the expression of osteolytic factors in the presence or absence of TGFβ. As illustrated in **Figure 31**, no differences were detected in IL-6, IL-8, IL-11, PTHrP or CTGF. Thus, further studies are needed to elucidate the complex role of PMEPMA1 as a TGFβ target gene in bone metastases. Possibilities include isoform-specific effects and although the current shRNA was designed to knockdown all isoforms, it is possible that each isoform has different effects and that knockdown of all result in a balance between all isoforms. Specific experiments to reexpress each isoform in the presence of the global knockdown are in progress.

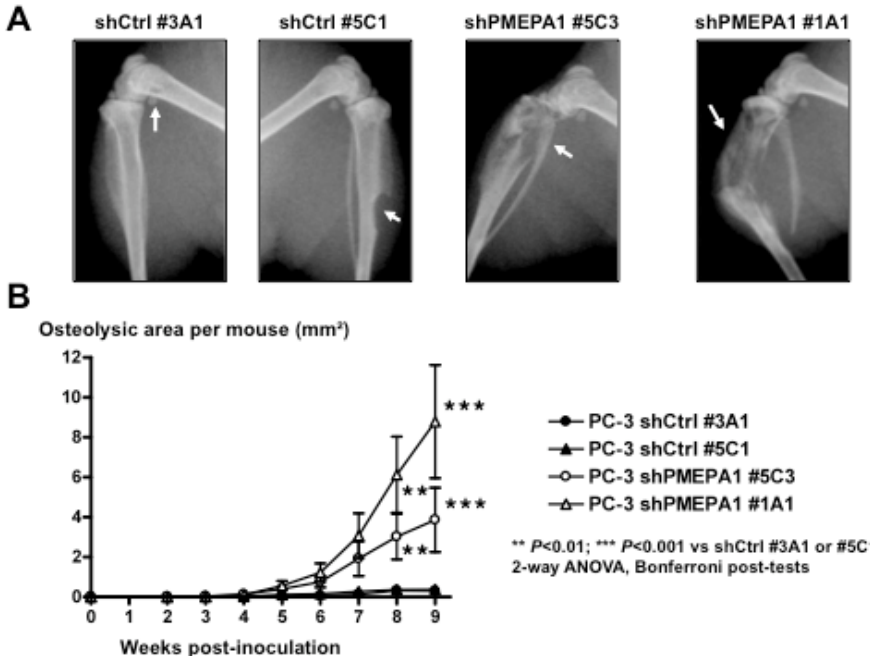


**Figure 30:** Knockdown of PMEPA1 in PC-3 prostate cancer cells increases osteolysic lesions in a mouse model of bone metastases. Four-week old, female Balb/C athymic mice received an intracardiac inoculation of PC-3 cells transfected to express an shRNA control (shCtr #3A1 and #5C1) or an shRNA against PMEPA1 (shPMEPA1 #5C3 and #1A1) in the left cardiac ventricle ($10^5$ cells in 100µL PBS, n=12 to 16 per group). The development of bone metastases was surveyed by radiographies. A. Representative radiographies of mouse hindlimbs 9 weeks after tumor cell inoculation. Arrow indicates osteolytic lesions. B. Osteolytic areas were measured on x-ray and results are expressed as the average ± SEM osteolytic area per mouse. ** P<0.01 and *** P<0.001 vs shCtrl #3A1 or #5C1 using a 2-way ANOVA followed by a Bonferroni post-test.

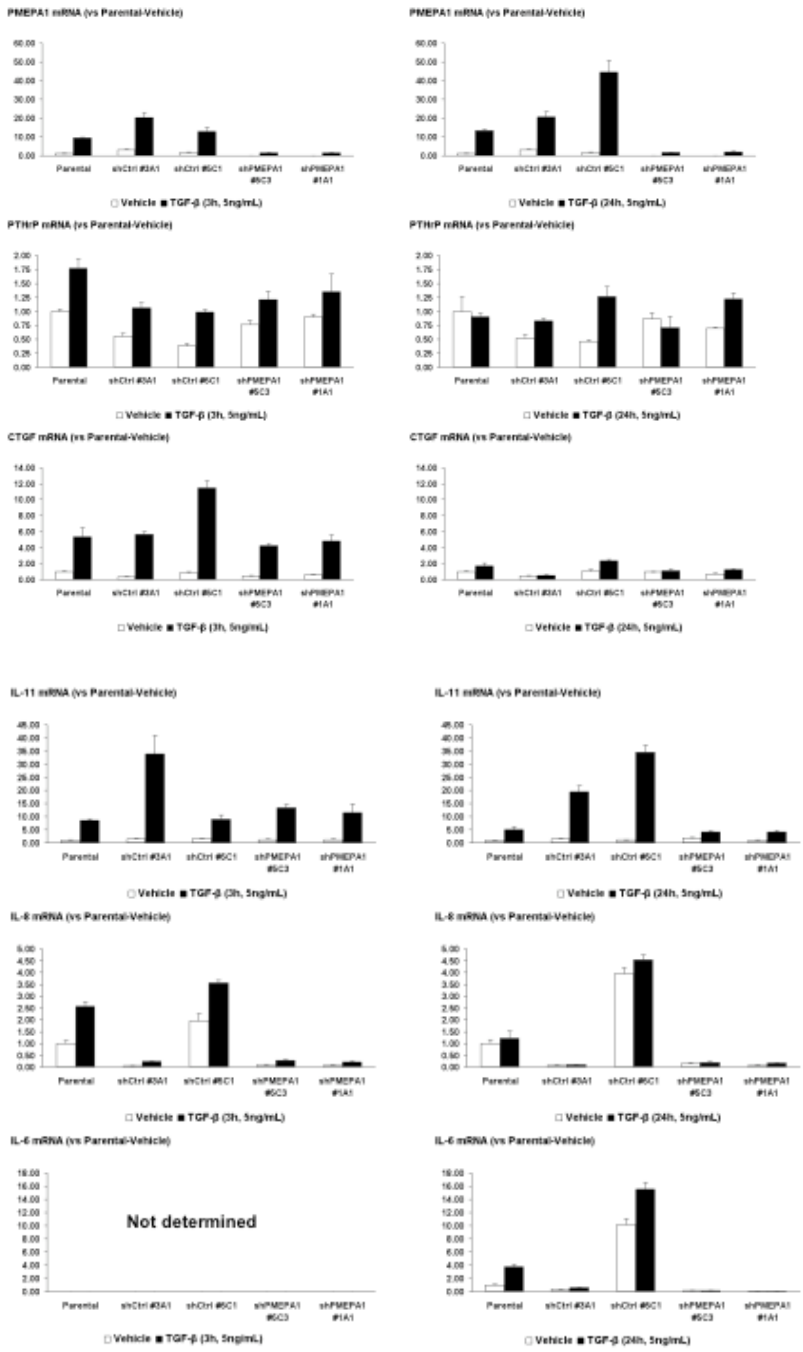


**Figure 31:** Stable knockdown of PMEPA1 in PC-3 prostate cancer cells does not affect the expression of pro-osteolytic genes. Parental PC-3 cells or PC-3 cells transfected to express an shRNA control (shCtr #3A1 and #5C1) or an shRNA against PMEPA1 (shPMEPA1 #5C3 and #1A1) were cultured in the presence or absence of TGF-β (5ng/mL) for 3 or 24 hours. Total RNA was extracted and expression of PMEPA1 and pro-osteolytic genes PTHrP, CTGF, IL-11, IL-8 and IL-8 was measured using semi-quantitative RT-PCR and the ribosomal protein L32 as housekeeping gene. Measure were done in triplicate and results represent the average ± SEM gene expression vs vehicle-treated PC-3 parental cells.

## KEY RESEARCH ACCOMPLISHMENTS

**Aim 1:**

- TGFβ RI kinase inhibitor, SD-208, effective against bone metastases due to PC3 prostate cancer model
- SD-208 ineffective against C42B prostate cancer bone metastasis model
- SD-208 ineffective, possibly deleterious against LuCaP23.1 prostate cancer bone metastasis xenograft model
- The p38 MAP kinase inhibitor SD-282 ineffective against all three prostate cancer bone metastasis models and accelerated bone metastases due to PC3 prostate cancer.
- TGFβ inhibition increased bone mass by stimulating osteoblast differentiation and inhibiting osteoclastic bone resorption. The effects on osteoblasts may be mediated by stat3 induction of Wnt 3a and 8b.

**Aim 2:**

- TGFβ regulation of PMEPA1 promoter determined at molecular level
- Role of three protein isoforms of PMEPA1 in TGFβ signaling potentiation shown in vitro, but in vivo studies suggest complex and isoform-specific effects of PMEPA1 on TGFβ signaling in vivo.

## REPORTABLE OUTCOMES

**Presentations: October 2004 – October 2008**

1. Molecular mechanisms of bone metastases. National Cancer Institute, NIH, Nov 2004.
2. TGFβ blockade in bone metastases. Biogen Advisory Board, Cambridge, MA, Dec 2004.
3. Molecular mechanisms of bone metastases. Endocrinology Grand Rounds, NIH, Bethesda, MD, Dec 2004.
4. Bone metastases: Molecular mechanisms and therapeutic interventions. Visiting Professor, Johns Hopkins Cancer Center, Baltimore, MD, Feb 2005.
5. Molecular mechanisms of osteoblastic bone metastases. Orthopedic Research Society Meeting, Washington, DC, Feb 2005.
6. Blockade of TGFβ signaling in breast cancer metastases to bone. TGFβ Keystone Meeting, Keystone, CO, Mar 2005.
7. Endothelin-1 in osteoblastic bone metastases: Mechanisms and therapeutic implications. Experimental Biology Meeting, San Diego, CA, Apr 2005.
8. Mechanisms of osteoblastic bone metastases. Fourth North American Symposium Skeletal Complications of Malignancy, NIH/NCI, Bethesda, MD, Apr 2005.
9. Mechanisms of osteolytic metastases to bone: Implications for therapy.

Visiting Professor, Fox Chase Cancer Center, Philadelphia, PA, May 2005.

10. Role of TGFβ in breast cancer metastases to bone. Seminar, Serono, Boston, MA, May 2005.
11. Molecular mechanisms of osteoblastic metastases: Implications for therapy. Prostate Cancer: Road Map to the Future, Roswell Park Institute Sponsored Symposium, Niagara Falls, NY, Jul 2005.
12. Targeting the endothelin axis in osteoblastic bone metastases: Mechanisms and implications. Prostate Cancer Foundation Scientific Retreat, Scottsdale, AZ, Oct 2005.
13. What makes bone a favorable site for metastases? AACR Tumor Microenvironment and Protease Meeting, Bonita Springs, FL, Dec 2005.
14. Bisphosphonate update 2006. 26th Annual Scripps Clinical Hematology and Oncology Meeting, San Diego, CA, Feb 2006.
15. TGFβ in bone metastases: Implications for therapy. Research Seminar, University of Lyon, Lyon France, Mar 2006.
16. TGFβ in bone metastases: Pathophysiology to treatment. Research Seminar, INSERM Unit 627, Hospital St. Louis, Paris, France, Mar 2006.
17. Gene signatures in bone metastases: Role of TGFβ. European Calcified Tissue Society Meeting, Prague, Czech Republic, May 2006.
18. TGFβ in skeletal complications of malignancy. Seminar at Schering, Berlin, Germany, May 2006.
19. Osteoporosis in the cancer patient. First international Meeting on Secondary Causes of Osteoporosis, Florence, Italy, Jul 2006.
20. PTHrP in osteoblastic bone metastases. PPP meeting, Newfoundland, Canada, Jul 2006.
21. Pathophysiology of metastases. Regional Medical Liaison meeting, UCSF, San Francisco, CA, Jul 2006.
22. Bone micrometastases. International Breast Cancer Conference, Kona, HI, Aug 2006.
23. Pathophysiology of bone metastases. International Metastases Meeting, Tokushima, Japan, Sep 2006.
24. TGFβ in bone metastases. Animal Model Working Group, American Society for Bone and Mineral Research Meeting, Philadelphia, PA, Sep 2006.
25. RANK ligand in pathological bone remodeling. American Society for Bone and Mineral Research Meeting, Philadelphia, PA, Sep 2006
26. Molecular mechanisms of bone metastases; Insight into pathophysiology. American Society for Bone and Mineral Research Meeting, Philadelphia, PA, Sep 2006
27. Molecular mechanisms of bone metastases: Role of TGFβ. Juan March Fat and Bone Meeting, Madrid, Spain, Sep 2006.
28. Molecular mechanisms of bone metastases: Osteolytic and osteoblastic. Italian Cancer Society Meeting, Bari, Italy, Oct 2006.
29. TGFβ in bone metastases: Pathophysiology to treatment. Visiting Professor, University of Minnesota, Minneapolis, MN, Dec 2006.
30. TGFβ signaling in breast cancer bone metastases: Friend or foe? Cancer

and Bone Society Meeting, San Antonio, TX, Dec 2006.

31. Molecular mechanisms of bone metastases: Insight into therapy. Endocrine Grand Rounds, University of Texas Health Science Center at San Antonio, TX, Dec 2006.
32. Skeletal complications of cancer and cancer treatment. Bone Club, San Antonio, TX, Dec 2006.
33. Skeletal health in the cancer patient. Maine State Osteoporosis Meeting, Sugarloaf, MN, Jan 2007.
34. Effects of bisphosphonates on tumor cells. Consensus on Bone Loss in Cancer Patients on Aromatase Inhibitors, Geneva, Switzerland, Feb 2007.
35. TGFβ in bone metastases: Pathophysiology to treatment. Institute for Molecular Medicine, University of Lisbon, Lisbon, Portugal, Mar 2007.
36. RANK ligand in prostate cancer metastases to bone. Medical Grand Rounds, Hospital Santa Ana, University of Lisbon, Lisbon, Portugal, Mar 2007.
37. Skeletal health in the cancer patient. Endocrine Grand Rounds, Oregon Health Sciences University, Portland, OR, Apr 2007.
38. TGFβ signaling in breast cancer bone metastases: Friend or foe? Research Seminar, Oregon Health Sciences University, Portland, OR, Apr 2007.
39. TGFβ in bone metastases: Pathophysiology to treatment. Endocrinology Grand Rounds, Mount Sinai School of Medicine, New York, NY, Apr 2007.
40. TGFβ signaling in breast cancer bone metastases: Friend or foe? Advances in Mineral Metabolism Meeting, Snowmass, CO, Apr 2007.
41. TGFβ signaling in cancer metastases to bone: Friend or foe? Cleveland Clinic, Cleveland, OH, Apr 2007.
42. Biology of bone metastases. FASEB Meeting, Washington, DC, Apr 2007.
43. Endothelins in pathologic and normal bone remodeling. Bone Club, University of Pittsburgh, Pittsburgh, PA, May 2007.
44. Endothelins in pathologic and normal bone remodeling. Research Seminar, Wyeth, Collegeville, PA, May 2007.
45. TGFβ in cancer and bone: Friend or foe? Research Seminar, University of Rochester, Rochester, NY, Jul 2007.
46. Endothelins: Cancer, bone and beyond. Research Seminar, Vanderbilt University, Nashville, TN, Aug 2007.
47. TGFβ-regulated genes in prostate cancer. Department of Defense IMPACT meeting, Atlanta, GA, Sep 2007.
48. Mechanisms and treatment of bone metastases. International Carcinoid Meeting, Norfolk, VA, Sep 2007.
49. Cancer and bone. National Academy of Continuing Medical Education Meeting, Fort Lauderdale, FL, Sep 2007
50. TGFβ signaling in cancer and bone: Friend or foe? University of Alabama, Birmingham, AL, Oct 2007.
51. TGFβ signaling in bone metastases due to breast cancer, prostate cancer and melanoma. Skeletal Complications of Malignancy Meeting, Philadelphia, PA, Oct 2007.
52. TGFβ in cancer and bone: Friend or foe? University of Miami, Miami, FL,

Oct 2007.

53. Role of TGF-beta in solid tumor metastases to bone: Implications for therapy. Endocrine Grand Rounds, Vanderbilt University, Nashville, TN, Dec 2007.
54. TGFβ in cancer and bone: Friend or foe? Yale Core Center for Musculoskeletal Disorders, Bone Biology Seminar Series, Yale University, Cambridge, MA, Jan 2008.
55. Transforming growth factor beta (TGF-β): Role in bone metastases due to breast cancer, prostate cancer and melanoma. Keystone Symposia: TGF-β Family in Homeostasis and Disease, Santa Fe, NM, Feb 2008.
56. Mechanisms of bone metastasis and novel therapeutic strategies. IBMS Davos Workshops: Bone Biology and Therapeutics, Davos, Switzerland, Mar 2008.
57. Role of T cells and bone resorption: data from mouse models. Swiss Bone and Mineral Society, Zurich, Switzerland, Mar 2008.
58. Molecular mechanisms of bone metastases: Implications for therapy. Endocrine Grand Rounds, University of Texas Southwestern Medical Center, Dallas, TX, Ma 2008.
59. TGFβ: Role in site-specificity of metastases to bone. American Association for Cancer Research Annual Meeting 2008, San Diego, CA, Apr 2008.
60. TGFβ: Cancer, bone and beyond. Hematology/Oncology Grand Rounds and Cancer Center Seminar Series, University of Virginia, Charlottesville, VA, Apr 2008.
61. TGFβ: Cancer, Bone and Beyond. Michigan Diabetes and Research Training Seminar Series, University of Michigan, Ann Arbor, MI, May 2008.
62. TGFβ: Cancer, bone and beyond. Endocrinology Grand Rounds, University of Pittsburgh, Pittsburgh, PA, May 2008.
63. The biology of bone metastases: Therapeutic implications. University-Wide Endocrine Conference, University of Pittsburgh, Pittsburgh, PA, May 2008.
64. TGFβ: Role in bone metastases. Second International Conference on Osteoimmunology: Interactions of the Immune and Skeletal Systems, Rhodes, Greece, Jun 2008.
65. TGFβ: Cancer, bone and beyond. Endocrine Society Annual Meeting, San Francisco, CA, Jun 2008.
66. Molecular mechanism of bone metastases: Insight into pathophysiology and treatment 2008. Tokyo Medical and Dental University, Tokyo, Japan, Jun 2008.
67. TGFβ: Cancer, bone and beyond. TGFβ Signaling in Cancer, Sapporo Cancer Center, Sapporo, Japan, Jun 2008.
68. Molecular mechanisms of bone metastases. International Meeting for Cancer-Induced Bone Diseases, Edinburgh, Scotland, Jun 2008.
69. TGFβ: Cancer, bone and beyond. Research Seminar, Genzyme Inc., Boston, MA, June 2008
70. Biology of Bone Metastases: Implications for Therapy. Endocrine Grand Rounds, Indiana University, Indianapolis, IN, Jul 2008.
71. How to deliver a scientific presentation: A 6 hour workshop. Metastases

Research Society and American Association for Cancer Research Joint Meeting, Vancouver, BC, Jul 2008.

72. Biology of bone metastases – Implications for therapy. Internal Medicine Grand Rounds, Eastern Virginia Medical School, Norfolk, VA, Aug 2008.
73. TGFβ: Cancer, bone and beyond. Endocrine Grand Rounds, Eastern Virginia Medical School, Norfolk, VA, Aug 2008.
74. Can we improve the bone health of breast cancer patients by specifically targeting the biology of the bone? 2008 Breast Cancer Symposium: Integrating Emerging Science into Clinical Practice, Washington, DC, Sep 2008.
75. TFGβ: Cancer, bone and beyond. Lady Davis Institute for Medical Research, McGill University, Montreal, Quebec, Canada, Sep 2008.
76. TGFβ: Cancer, bone and beyond. American Society for Bone and Mineral Research, Montreal, Canada, Sep 2008.

**Publications: October 2004 – Present (March 2009)**

**Peer Reviewed**

1. Kozlow W, **Guise TA**. Breast cancer metastasis to bone: mechanisms of osteolysis and implications for therapy. J Mammary Gland Biol Neoplasia 10(2):169-80, April 2005. PMID: 16025223.
2. Titus B, Frierson HF Jr, Conaway M, Ching K, **Guise T**, Chirgwin J, Hampton G, Theodorescu D. Endothelin axis is a target of the lung metastasis suppressor gene RhoGDI2. Cancer Res 65(16):7320-7, August 2005. PMID: 16103083.
3. Clines GA, **Guise TA**. Hypercalcaemia of malignancy and basic research on mechanisms responsible for osteolytic and osteoblastic metastasis to bone. Endocr Relat Cancer 12(3):549-83, Sep 2005. PMID: 16172192.
4. Bendre MS, Margulies AG, Walser B, Akel NS, Bhattacharrya S, Skinner RA, Swain F, Ramani V, Mohammad KS, Wessner LL, Martinez A, **Guise TA**, Chirgwin JM, Gaddy D, Suva LJ. Tumor-derived interleukin-8 stimulates osteolysis independent of the receptor activator of nuclear factor-kappaB ligand pathway. Cancer Res 65(23):11001-9, December 2005. PMID: 16322249.
5. Zudaire E, Martinez A, Garayoa M, Pio R, Kaur G, Woolhiser MR, Metcalfe DD, Hook WA, Siraganian RP, **Guise TA**, Chirgwin JM, Cuttitta F. Adrenomedullin is a cross-talk molecule that regulates tumor and mast cell function during human carcinogenesis. Am J Pathol 168(1):280-91, January 2006. PMID: 16400030.
6. Bartholin L, Wessner L, Chirgwin JM, **Guise, TA**. The human Cyr61 gene is a transcriptional target of transforming growth factor beta. Cancer Lett 246(1-2):230-6, February 2007. Epub 2006 April 17. PMID: 16616811.
7. **Guise TA**. Do markers of bone turnover predict clinical outcome in patients with bone metastases? Nat Clin Pract Endocrinol Metab 2(5):258-9, May 2006. PMID: 16932296.
8. Seth P, Wang ZG, Pister A, Zafar MB, Kim S, **Guise T**, Wakefield L. Development of oncolytic adenovirus armed with a fusion of soluble

transforming growth factor-beta receptor II and human immunoglobulin Fc for breast cancer therapy. Hum Gene Ther 17(11):1152-60, November 2006. PMID: 17032151.

9. Theriault RL, Biermann JS, Brown E, Brufsky A, Demers L, Grewal RK, **Guise T**, Jackson R, McEnery K, Podoloff D, Ravdin P, Shapiro CL, Smith M, Van Poznak CH. NCCN Task Force Report: Bone health and cancer care. J Natl Compr Canc Netw 4 Suppl 2:S1-20, May 2006. PMID: 16737674.
10. Clines GA, Mohammad KS, Bao Y, Stephens OW, Suva LJ, Shaughnessy JD Jr, Fox JW, Chirgwin JM, **Guise TA**. Dickkopf homolog 1 mediates endothelin-1-stimulated new bone formation. Mol Endocrinol 21(2):486-98, February 2007. Epub 2006 October 26. PMID: 17068196.
11. **Guise TA**, Mohammad KS, Clines G, Stebbins EG, Wong DH, Higgins LS, Vessella R, Corey E, Padalecki S, Suva L, Chirgwin JM. Basic mechanisms responsible for osteolytic and osteoblastic bone metastases. Clin Cancer Res 12(20):6213s-6s, October 2006. PMID: 17062703.
12. Lipton A, Berenson JR, Body JJ, Boyce BF, Bruland OS, Carducci MA, Cleeland CS, Clohisy DR, Coleman RE, Cook RJ, **Guise TA**, Pearse RN, Powles TJ, Rogers MJ, Roodman GD, Smith MR, Suva LJ, Vessella RL, Weilbaecher KN, King L. Advances in treating metastatic bone cancer: Summary statement for the First Cambridge Conference. Clin Cancer Res 12(20):6209s-12s, October 2006. PMID: 17062702.
13. **Guise TA**. Bone loss and fracture risk associated with cancer therapy. Oncologist 11(10):1121-1131, November/December 2006. PMID: 17110632.
14. Javelaud D, Mohammad KS, McKenna CR, Fournier P, Luciani F, Niewolna M, André J, Delmas V, Larue L, **Guise TA**, Mauviel A. Stable overexpression of Smad7 in human melanoma cells impairs bone metastasis. Cancer Res 67(5):2317-24, Mar 2007. PMID: 17332363.
15. Brown SA, **Guise TA**. Drug insight: the use of bisphosphonates for the prevention and treatment of osteoporosis in men. Nat Clin Pract Urol 4(6):310-20, June 2007. PMID: 17551535.
16. Kingsley LA, Chirgwin JM, **Guise TA**. Breaking new ground to build bone. Proc Natl Acad Sci USA 104(26):10753-4, June 2007. Epub 2007 June 20. PMID: 17581868.
17. Fournier PGJ, **Guise TA**. BMP7: A new bone metastases prevention? Am J Pathol 171(3):739-43, Sep 2007. Epub 2007 August 9. PMID: 17690188.
18. Khosla S, Burr D, Cauley J, Dempster DW, Ebeling PR, Felsenberg D, Gagel RF, Gilsanz V, **Guise T**, Koka S, McCauley LK, McGowan J, McKee MD, Mohla S, Pendrys, DG, Raisz LG, Ruggiero SL, Shafer DM, Shum L, Silverman SL, Van Poznak CH, Watts N, Woo SB, Shane E. Bisphosphonate-associated osteonecrosis of the jaw: Report of a task force of the American Society for Bone and Mineral Research. J Bone Miner Res 22(10):1479-91, October 2007. PMID: 17663640.
19. Kingsley LA, Fournier PG, Chirgwin JM, **Guise TA**. Molecular biology of bone metastasis. Mol Cancer Ther 6(10):2609-17, October 2007. PMID: 17938257.
20. Brown SA, **Guise TA**. Cancer-associated bone disease. Curr Osteoporos

Rep 5(3):120-7, Sep 2007. PMID: 17925193.
21. Chirgwin JM, **Guise TA**. Skeletal metastases: Decreasing tumor burden by targeting the bone microenvironment. J Cell Biochem 102(6):1333-42, December 2007. PMID: 17907152.
22. Brown SA, Clines GA, **Guise TA**. Local effects of malignancy on bone. Curr Opin Endocrinol Diabetes Obes 14(6):436-41, December 2007. PMID: 17982349.
23. Akhtari M, Mansuri J, Newman KA, **Guise T**, Seth P. Biology of breast cancer bone metastasis. Cancer Biol Ther 7(1):3-9, January 2007. Epub 2007 October 13. PMID: 18059174.
24. **Guise TA**, Oefelein MG, Eastham JA, Cookson MS, Higano CS, Smith MR. Estrogenic side effects of androgen deprivation therapy. Rev Urol 9(4):163-80, Fall 2007. PMID: 18231613.
25. Kozlow W, Heras-Herzig A, Brown S, **Guise TA**. Osteoporosis due to cancer treatment. Endocrine-Related Cancer In Press 2008.
26. Clines GA, **Guise TA**. Molecular mechanisms and treatment of bone metastasis. Expert Rev Mol Med 10:e7, Mar 2008. PMID:18321396.
27. Hadji P, Body JJ, Aapro MS, Brufsky A, Coleman RE, **Guise T**, Lipton A, Tubiana-Hulin M. Practical guidance for the management of aromatase inhibitor-associated bone loss. Ann Oncol Apr 2008 [Epub ahead of print]. PMID: 18448451.
28. Coleman RE, **Guise TA**, Lipton A. Roodman GD, Berenson JR, Body JJ, Boyce BF, Calvi LM, Hadji P, McCloskey EV, Saad F, Smith MR, Suva LJ, Taichman RS, Vessella RL, Weilbaecher KN. Advancing treatment for metastastic bone cancer: consensus recommendations from the Second Cambridge Conference. Clin Cancer Res 14(20):6387-95, Oct 2008.
29. Mohammad KS, Chen CG, Balooch G, Stebbins E, McKenna CR, Walton H, Niewolna M, Peng XH, Nguyen DHN, Ionova-Martin SS, Bracey JW, Hogue WR, Vong DH, Ritchie RO, Suva LJ, Derynck R, **Guise TA**, Alliston T. Pharmacologic inhibition of TGF-β type 1 receptor kinase has anabolic and anti-catabolic effects on bone. PloS ONE 2009 (In press).

**Invited Reviews**

1. Clines GA, Chirgwin JM, **Guise TA**. Skeletal complications of malignancy: Central role for the osteoclast. IN: Topics in Bone Biology, Volume 2; edited by Bronner, Rubin, Farach-Carson; Springer-Verlag; 151-174, 2005.
2. Aris RM, **Guise TA**. Cystic fibrosis and bone disease: are we missing a genetic link? Eur Respir J 25(1):9-11, January 2005. PMID: 15640316.
3. **Guise TA**, Kozlow WM, Heras-Herzig A, Padalecki SS, Yin JJ, Chirgwin JM. Molecular mechanisms of breast cancer metastases to bone. Clin Breast Cancer 5 Suppl(2):S46-53, February 2005. PMID: 15807924.
4. Clines GA, **Guise TA**. Mechanisms and treatment for bone metastases. Clin Adv Hematol Oncol 2(5):295-301, May 2004. PMID: 16163196.
5. **Guise TA**. Thromboembolism to metastasis: The platelet-lysophosphatidic acid connection. IBMS BoneKey 2005 Mar 1 doi:10.1138/20050154.

6. Chirgwin JM, **Guise TA**. Does prostate-specific antigen contribute to bone metastases? Clin Cancer Res 12(5):1395-7, Mar 2006. PMID: 16533760.
7. Heras-Herzig A, **Guise TA.** Disorders of calcium metabolism. IN: Therapy of Renal Diseases and Related Disorders, Fourth edition; WN Suki, SG Massry (eds); Kluwer Academic Publishers; Ch 5. In Press, 2006.
8. Clines GA, **Guise TA**. Mechanisms of bone destruction and bone formation by metastatic tumors. Primer on the Metabolic Bone Diseases and Disorders of Mineral Metabolism, Sixth Edition; edited by Murray J. Favus, MD et al. In Press 2006.
9. Fournier P, Chirgwin JM, **Guise TA**. New insights into the role of T cells in the vicious cycle of bone metastases. Curr Opin Rheumatol 18(4):396-404, July 2006. PMID: 16763461.
10. Siclari VA, **Guise TA**, Chirgwin JM. Molecular interactions between breast cancer cells and the bone microenvironment drive skeletal metastases. Cancer Metastasis Rev 25(4):621-33, December 2006. PMID: 17165131.
11. Bartholin L, **Guise TA**. TGFβ in breast cancer osteolysis. IN: Textbook: TGFβ in Health and Disease; S Jakalew, Ed; Ch 7. In Press 2007.
12. Brown SA, Clines GA, **Guise TA**. Local effects of malignancy on bone. Curr Opin Endocrinol Diabetes Obes 14(6):436-41, December 2007. PMID: 17982348.
13. Heras-Herzig A, Kozlow W, Brown S, **Guise TA**. Osteoporosis associated with cancer and cancer treatment. IN: Osteoporosis Third Edition, Vol II; Academic Press; Editors: Marcus R, Feldman D, Nelson DA, Rosen CJ, Boston, Ch 54:1337-1374, 2008.
14. **Guise TA**. Antitumor effects of bisphosphonates: Promising preclinical evidence. Cancer Treat Rev 34S1:S19-S24, 2008. Epub2008 May 15. PMID: 18486348.
15. Mohammad KS, Chirgwin JM, **Guise TA**. Assessing new bone formation in neonatal calvarial organ cultures. Methods Mol Biol 455:37-50, 2008. PMID: 18463809.
16. Brown SA, **Guise TA**. Cancer treatment-related bone disease. Crit Rev Eukaryot Gene Expr 19(1):47-60. 2009 Featured on cover.

**Funding: October 2004 – October 2008**

***Active Grant Awards***

1. National Institutes of Health (NCI), "TGFβ in the bone microenvironment: role in metastases" (R01-CA69158-12; Guise, PI, 20% effort). Awarded: 12/01/07-11/30/12; direct costs per year. Total costs: Interim funding from NCI for awarded 07/01/07 to 12/01/07.
2. National Institutes of Health (NIDDK), "Endothelin-1 in normal and pathological bone remodeling" (R01DK067333; Guise, PI; 20% effort). Awarded: 02/01/05-12/31/09; Annual direct costs: Total cost:

3. National Institutes of Health (NIDDK), "Prostate cancer metastasis to bone:

Role of adrenomedullin" (R01 DK065837) (Guise, PI; 20% effort). Awarded: 04/01/05-03/30/10; Direct costs per year: Total cost:

4. Prostate Cancer Foundation, "Inhibition of prostate cancer bone metastases with endothelin receptor blockade plus bisphosphonate antiresorptive: preclinical testing and molecular mechanisms." Awarded: 02/01/04-01/31/08. Total costs:
5. US Army Prostate Cancer Program Idea Award PC040341, "Preclinical evaluation of serine/threonine kinase inhibitors against prostate cancer metastases" (Guise, PI, 15% effort). Awarded: 10/01/04-09/30/08; Direct costs: Total costs: **THIS AWARD**
6. V-Foundation, "Effects of a high bone turnover state induced by estrogen deficiency on the development and progression of breast cancer and bone metastases." Awarded: 10/01/04-09/30/08; Direct and total costs:
7. Mary K. Ash Foundation, "Inhibition of breast cancer bone metastases with anti-hypoxic treatment" (Guise, PI). Awarded: 07/01/05-06/30/08; Total cost:

8. P01 (NIH, NCI), "Signaling and Progression in Prostate Cancer: Core D: Tissue Analysis Laboratory" (Theodorescu, PI; Guise Project Co-Leader, Core C 10% effort). Awarded: 06/01/04-05/30/09; Direct costs per year:

9. P01 (NIH, NCI), "Signaling and Progression in Prostate Cancer: Core B: Cell culture, animal models and imaging" (Theodorescu, PI; Guise Project Leader, Core B 10% effort). Awarded: 06/01/04-05/30/09; Direct costs per year:

**Grant Awards from Trainees of Guise Laboratory (Fournier, Clines, Kozlow, Dunn Kingsley) obtained during funding period**

PC061185 PG Fournier (PI) 12/15/06 - 12/14/08
US Department of Defense - PCRP. Prostate Cancer Training Award (Postdoctoral - Ph.D.)
*TGF-β induction of PMEPA1: Role in bone metastases due to prostate cancer*
Total costs:

KG080657 Guise, Theresa (PI) on behalf of Juarez, Patricia 10/01/08-9/30/10
Susan G. Komen for the Cure
Program: Post Doctoral Fellowship - Basic Research (Import 2008)
HALOFUGINONE INHIBITION OF TGF-BETA SIGNALING: TREATMENT FOR BONE METASTASES.
Total costs:

BC073157 Dunn, Lauren Ann Kingsley (PI) 08/01/08-07/31/11
Departent of Defense Breast Cancer Research Program Predoctoral Traineeship Award: "Inhibiting breast cancer bone metastasis by targeting the HIF-1$\alpha$ signaling pathway"
Total costs:

BC043416 Kozlow, Wende (PI) 05/01/04-0430/09
Department of Defense Breast Cancer Research Program Multidisciplinary Award: “Effect of high bone turnover due to aromatase inhibitors on breast cancer bone metastases”
Total costs:

PC PC073756 Clines, Gregory (PI)
Department of Defense 3/1/08 – 2/28/11
Prostate Cancer Research Program (direct costs, per year)
New Investigator Award
*“Regulation of prostate cancer bone metastasis by DKK1”*

K08 CA118428 Clines, Gregory (PI) 7/1/06 – 6/30/11
NIH, NCI (directs costs, per year)
*”Molecular actions of tumor-derived endothelin-1 in the bone microenvironment”*

**Pending Grants (Applied for during the last year of funding)**

1U01CA143057-01 Differential TGF-β Signaling in the bone microenvironment: impact on tumor growth. Guise, Theresa (PI), Bhowmick, Neil (Co-PI)

R01CA Effect of Radiation on Skeletal Health Bateman, Ted (PI), Guise, Theresa (Co-PI)

R01 1RC2CA148479-01 Supplement Validation of Therapeutic Targets that Modulate the Tumor Microenvironment, Guise, Theresa (PI)

NIH GO Grant Molecular target discovery and development center: validation of therapeutic targets that modulate the tumor microenvironment, Submitted through Indiana University to NIH, Guise, Theresa (Co-PI), Yoder, Mervin (Co-PI), Pollok, Karen (Co-PI)

**Recent Previous Grant Awards**

1. Department of Defense, subcontract from Emory University: “Targeting the lethal phenotype of metastatic prostate cancer” (Guise and Chirgwin, Co-PIs, 10% effort). Awarded: 02/01/03-3/31/08.
2. National Institutes of Health (NCI), “Breast cancer osteolysis: PTHrP regulation by TGFβ”. (R01-CA69158-11; Guise, PI, 20% effort). Awarded: 04/01/01-03/31/06.

**CONCLUSIONS**

A central tenet in the field of bone metastases is that the bone microenvironment supplies factors, such as TGF-β, stimulating prostate cancer cell signaling and altering their phenotype.

TGF-β signaling in cancer is however complex and can lead to the activation of numerous genes. We have identified many of these genes by microarray analysis and have validated the gene reported here. PMEPA1 was the most highly upregulated gene. We cloned the PMEPA1 promoter and gene and mapped the TGFβ response element. Silencing PMEPA1 in prostate cancer line PC-3 blocked TGFβ signaling in vitro, but increased bone metastases in vivo. These results were the opposite of what we expected and are currently pursuing other experiments to determine whether these effects are isoform-specfic or cell type-dependent.

In vivo experiments determined the effects of a TGFβ RI kinase inhibitor, SD-208, on the development and progression of prostate cancer metastases to bone due to PC-3, LuCAP and C42B. Different prostate cancers showed different effects, depending on the radiographic phenotype of the bone metastases. SD-208 improved osteolytic bone metastases due to PC-3, but had no effect and possibly worsened osteoblastic bone metastases due to LuCAP23.1, with no effect on mixed C42B lesions. The results in C42B were not surprising, since the line is unresponsive to TGFβ. However, the effect of this compound to increase osteoblastic bone metastases is a significant concern. We have initiated an agreement with Eli Lilly to study another TGFβRI kinase that is currently in clinical trials for patients with bone metastases due to all solid tumors. We will also study the effect of a TGFβ antibody in these models and have initiated an agreement with Genzyme.

The p38 MAP kinase inhibitor SD-282 showed no efficacy against any of the bone metastases models and was not studied in additional experiments originally proposed. In particular we concluded that it would be wasteful of experimental animals to carry out combination treatments with this agent, which was the substance of the originally proposed Aim 3. Furthermore, SD-282 worsened bone metastases due to PC-3 prostate cancer. Finally SD-282 was no longer available for study. Instead, we studied the effects of TGFβ blockade on bone and found that it increased bone mass, due to effects on osteoblasts and osteoclast. These effects could be mediated through osteoblast production of Wnt ligands, regulated by Stat3 and will be investigated further.

**Overall, we conclude that**:

- TGFβ signaling is a useful target for treatment of prostate cancer bone metastases, provided that the tumor cells are responsive to the factor and show components of osteolytic lesions.
- TGFβ inhibitors are not beneficial when the bone metastases phenotype is predominantly osteoblastic.
- Non-canonical (ie Smad-independent) pathways downstream of the TGFβ receptors, such as p38 MAP kinase, do not appear to be appropriate targets for pharmacological treatment of prostate cancer bone metastases.
- There is no advantage to combined treatment targeting TGFβ receptors and p38 MAP kinase.

- PMEPA1 may be an important target of TGFβ in prostate cancer cells and responsible for potentiating responsiveness of tumor cells in bone to the local actions of bone-released TGFβ. Its regulation and isoform-specific effects are complex and will be the subject of future grant proposals.
- TGFβ inhibition increases bone mass systemically thru effects to stimulate differentiation of osteoblasts and inhibiting osteoclasts. The effects on osteoblasts may be via stat3 induction of Wnt ligand production (3a and 8b).

## REFERENCES


Abasolo I, Yang L, Haleem R, Xiao W, Pio R, Cuttitta F, Montuenga LM, Kozlowski JM, Calvo A, Wang Z. Overexpression of adrenomedullin gene markedly inhibits proliferation of PC3 prostate cancer cells in vitro and in vivo. Mol Cell Endocrinol, *199*:179-187, 2003.

Adler HL, McCurdy MA, Kattan MW, Timme TL, Scardino PT, Thompson TC. Elevated levels of circulating interleukin-6 and transforming growth factor-beta1 in patients with metastatic prostatic carcinoma. J Urol*, 161*:182-187, 1999.

Akhurst RJ, Derynck R. TGF-beta signaling in cancer--a double-edged sword. Trends Cell Biol, *11*:S44-51, 2001.

Anan T, Nagata Y, Koga H, Honda Y, Yabuki N, Miyamoto C, Kuwano A, Matsuda I, Endo F, Saya H, Nakao M. Human ubiquitin-protein ligase Nedd4: expression, subcellular localization and selective interaction with ubiquitin-conjugating enzymes. Genes Cells, *3*:751-763, 1998.

Bakin RE, Gioeli D, Sikes RA, Bissonette EA, Weber MJ. Constitutive activation of the Ras/mitogen-activated protein kinase signaling pathway promotes androgen hypersensitivity in LNCaP prostate cancer cells. Cancer Res, *63*:1981-1989, 2003a.

Bakin RE, Gioeli D, Bissonette EA, Weber MJ. Attenuation of Ras signaling restores androgen sensitivity to hormone-refractory C4-2 prostate cancer cells. Cancer Res, *63*:1975-1980, 2003b.

Bartholin L, Wessner LL, Chirgwin JM, Guise TA. The human Cyr61 gene is a transcriptional target of transforming growth factor beta in cancer cells. Cancer Lett. 2006

Bello-DeOcampo D, Tindall DJ. TGF-betal/Smad signaling in prostate cancer. Curr Drug Targets, *4*:197-207. 2003.

Bendre MS, Gaddy-Kurten D, Mon-Foote T, Akel NS, Skinner RA, Nicholas RW, Suva LJ. Expression of interleukin 8 and not parathyroid hormone-related

protein by human breast cancer cells correlates with bone metastasis in vivo. Cancer Res, *62*:5571-5579, 2002.

Blackledge G. Growth Factor Receptor Tyrosine Kinase Inhibitors; Clinical Development and Potential for Prostate Cancer Therapy. J Urol, *170*:S77-S83, 2003.

Blanchere M, Saunier E, Mestayer C, Broshuis M, Mowszowicz I. Alterations of expression and regulation of transforming growth factor beta in human cancer prostate cell lines. J Steroid Biochem Mol Biol, *82*:297-304, 2002.

Boyde A, Maconnachie E, Reid SA, Delling G, Mundy GR. Scanning electron microscopy in bone pathology: Review of methods. Potential and applications. Scanning Electron Microscopy *IV*:1537-1554, 1986.

Brigstock DR. Regulation of angiogenesis and endothelial cell function by connective tissue growth factor (CTGF) and cysteine-rich 61 (CYR61). Angiogenesis, *5*:153-165, 2002.

Brunschwig EB, Wilson K, Mack D, Dawson D, Lawrence E, Willson JK, Lu S, Nosrati A, Rerko RM, Swinler S, Beard L, Lutterbaugh JD, Willis J, Platzer P, Markowitz S. PMEPA1, a transforming growth factor-beta-induced marker of terminal colonocyte differentiation whose expression is maintained in primary and metastatic colon cancer. Cancer Res, *63*:1568-1575, 2003.

Carducci MA, Padley RJ, Breul J, Vogelzang NJ, Zonnenberg BA, Daliani DD, Schulman CC, Nabulsi AA, Humerickhouse RA, Weinberg MA, Schmitt JL, Nelson JB. Effect of endothelin-A receptor blockade with atrasentan on tumor progression in men with hormone-refractory prostate cancer: a randomized, phase II, placebo-controlled trial. J Clin Oncol, *21*:679-689, 2003.

Cher ML. Mechanisms governing bone metastasis in prostate cancer. Curr Opin Urol, *11*:483-488, 2001.

Chesneau V, Becherer JD, Zheng Y, Erdjument-Bromage H, Tempst P, Blobel CP. Catalytic properties of ADAM19. J Biol Chem, *278*:22331-22340, 2003.

Chipuk JE, Cornelius SC, Pultz NJ, Jorgensen JS, Bonham MJ, Kim SJ, Danielpour D. The androgen receptor represses transforming growth factor-beta signaling through interaction with Smad3. J Biol Chem, *277*:1240-1248, 2002.

Chirgwin JM, Guise TA. Molecular mechanisms of tumor-bone interactions in osteolytic metastases. Crit Rev Eukaryot Gene Expr, *10*:159-178, 2000.

Chirgwin JM, Guise TA. Molecular mechanisms of cancer metastases to bone. Curr Opin Orthop, *14*:317-321, 2003a.

Chirgwin JM, Guise TA. Cancer metastasis to bone. Science & Medicine, **9**:140-151, 2003b.

Chung LW. Prostate carcinoma bone-stroma interaction and its biologic and therapeutic implications. Cancer, *97*(3 Suppl):772-778, 2003.

Corey E, Quinn JE, Bladou F, Brown LG, Roudier MP, Brown JM, Buhler KR, Vessella RL. Establishment and characterization of osseous prostate cancer models: intra-tibial injection of human prostate cancer cells. Prostate, *52*:20-33, 2002.

Crawford ED. Epidemiology of prostate cancer. Urology, *62*(6 Suppl 1):3-12, 2003.

Dallas SL, Rosser JL, Mundy GR, Bonewald LF. Proteolysis of latent transforming growth factor-beta (TGF-beta )-binding protein-1 by osteoclasts. A cellular mechanism for release of TGF-beta from bone matrix. J Biol Chem, *277*:21352-21360, 2002.

Derynck R, Zhang YE. Smad-dependent and Smad-independent pathways in TGF-beta family signalling. Nature, *425*:577-584, 2003.

Deftos LJ. Prostate carcinoma: production of bioactive factors. Cancer, *88*(12 Suppl):3002-3008, 2000.

Feng XH, Liang YY, Liang M, Zhai W, Lin X. Direct interaction of c-Myc with Smad2 and Smad3 to inhibit TGF-beta-mediated induction of the CDK inhibitor p15(Ink4B). Mol Cell, *9*:133-143, 2002.

Festuccia C, Angelucci A, Gravina GL, Villanova I, Teti A, Albini A, Bologna M, Abini A. Osteoblast-derived TGF-beta1 modulates matrix degrading protease expression and activity in prostate cancer cells. Int J Cancer, *85*:407-415, 2000.

Fidler IJ. The pathogenesis of cancer metastasis: the ‘seed and soil’ hypothesis revisited. Nat Rev Cancer, *3*:1-6, 2003.

Fu Z, Smith PC, Zhang L, Rubin MA, Dunn RL, Yao Z, Keller ET. Effects of raf kinase inhibitor protein expression on suppression of prostate cancer metastasis. J Natl Cancer Inst, *95*:878-889, 2003a.

Fu Y, O'Connor LM, Shepherd TG, Nachtigal MW. The p38 MAPK inhibitor, PD169316, inhibits transforming growth factor beta-induced Smad signaling in human ovarian cancer cells. Biochem Biophys Res Commun, *310*:391-397, 2003b.

Gallwitz WE, Guise TA, Mundy GR. Guanosine nucleotides inhibit different syndromes of PTHrP excess caused by human cancers in vivo. J Clin Invest, *110*:1559-1572, 2002.

Giannini G, Ambrosini MI, Di Marcotullio L, Cerignoli F, Zani M, MacKay AR, Screpanti I, Frati L, Gulino A. EGF- and cell-cycle-regulated STAG1/PMEPA1/ERG1.2 belongs to a conserved gene family and is overexpressed and amplified in breast and ovarian cancer. Mol Carcinog, *8*:188-200, 2003.

Gioeli D, Mandell JW, Petroni GR, Frierson HF Jr, Weber MJ. Activation of mitogen-activated protein kinase associated with prostate cancer progression. Cancer Res, *59*:279-284, 1999.

Gioeli D, Zecevic M, Weber MJ. Immunostaining for activated extracellular signal-regulated kinases in cells and tissues. Methods Enzymol, *332*:343-353, 2001.

Granchi S, Brocchi S, Bonaccorsi L, Baldi E, Vinci MC, Forti G, Serio M, Maggi M. Endothelin-1 production by prostate cancer cell lines is up-regulated by factors involved in cancer progression and down-regulated by androgens. Prostate, *49*:267-277, 2001.

Grotendorst GR, Okochi H, Hayashi N. A novel transforming growth factor beta response element controls the expression of the connective tissue growth factor gene. Cell Growth Differ, *7*:469-480, 1996.

Guise TA, Yin JJ, Taylor SD, Kumagai Y, Dallas M, Boyce BF, Yoneda T, Mundy GR. Evidence for a causal role of parathyroid hormone-related protein in the pathogenesis of human breast cancer-mediated osteolysis. J Clin Invest, *98*:1544-1549, 1996.

Guise TA, Mundy GR. Cancer and bone. Endocr Rev, *19*:18-55, 1998.

Guise TA, Chirgwin JM. Role of bisphosphonates in prostate cancer bone metastases. Semin Oncol, *30*:717-723, 2003a.

Guise TA, Chirgwin JM. Transforming growth factor-beta in osteolytic breast cancer bone metastases. Clin Orthop, *415*:S32-38, 2003b.

Hauschka PV, Mavrakos AE, Iafrati MD, Doleman SE, Klagsbrun M. Growth factors in bone matrix. Isolation of multiple types by affinity chromatography on heparin-Sepharose. J Biol Chem, *261*:12665-12674, 1986.

Hayes SA, Huang X, Kambhampati S, Platanias LC, Bergan RC. p38 MAP kinase modulates Smad-dependent changes in human prostate cell adhesion. Oncogene, *22*:4841-4850. 2003.

Hortobagyi GN, Theriault RL, Porter L, Blayney D, Lipton A, Sinoff C, Wheeler H, Simeone JF, Seaman J, Knight RD. Efficacy of pamidronate in reducing skeletal complications in patients with breast cancer and lytic bone metastases. Protocol 19 Aredia Breast Cancer Study Group. N Engl J Med., *335*: 1785-1791, 1996.

Hwa V, Oh Y, Rosenfeld RG. Insulin-like growth factor binding protein-3 and -5 are regulated by transforming growth factor-beta and retinoic acid in the human prostate adenocarcinoma cell line PC-3. Endocrine, *6*:235-242, 1997.

Itoh S, Thorikay M, Kowanetz M, Moustakas A, Itoh F, Heldin CH, ten Dijke P. Elucidation of Smad requirement in transforming growth factor-beta type I receptor-induced responses. J Biol Chem, *278*:3751-3761, 2003.

Janda E, Lehmann K, Killisch I, Jechlinger M, Herzig M, Downward J, Beug H, Grunert S. Ras and TGF[beta] cooperatively regulate epithelial cell plasticity and metastasis: dissection of Ras signaling pathways. J Cell Biol, *156*:299-313, 2002.

Johnson GL, Lapadat R. Mitogen-activated protein kinase pathways mediated by ERK, JNK, and p38 protein kinases. Science, *298*:1911-1912, 2002.

Kakonen SM, Selander KS, Chirgwin JM, Yin JJ, Burns S, Rankin WA, Grubbs BG, Dallas M, Cui Y, Guise TA. Transforming growth factor-beta stimulates parathyroid hormone-related protein and osteolytic metastases via Smad and mitogen-activated protein kinase signaling pathways. J Biol Chem, *277*:24571-24578, 2002.

Kang Y, Siegel PM, Shu W, Drobnjak M, Kakonen SM, Cordon-Cardo C, Guise TA, Massague J. A multigenic program mediating breast cancer metastasis to bone. Cancer Cell, *3*:537-549, 2003.

Keller ET. The role of osteoclastic activity in prostate cancer skeletal metastases. Drugs Today, *38*:91-102, 2002.

Kozawa O, Kawamura H, Hatakeyama D, Matsuno H, Uematsu T. Endothelin-1 induces vascular endothelial growth factor synthesis in osteoblasts: involvement of p38 mitogen-activated protein kinase. Cell Signa1, *2*:375-380, 2000.

Li, X., Placencio, V. R., Iturregui, J. M., Uwamariya, C., Sharif-Afshar, A. R., Koyama, T., Hayward, S. W., and Bhowmick, N. A. *Prostate tumor progression is mediated by a paracrine TGF-ß/Wnt3a signaling axis.* Oncogene. 2008. 27(56):7118-30.

Liao Y, Hung MC. Regulation of the activity of p38 mitogen-activated protein kinase by Akt in cancer and adenoviral protein E1A-mediated sensitization to apoptosis. Mol Cell Biol, *23*:6836-6848, 2003.

Lum *et al.*1999. JBC. 274:13613

Lynch CC, Hikosaka A, Acuff HB, Martin MD, Kawai N, Singh RK, Vargo-Gogola TC, Begtrup JL, Peterson TE, Fingleton B, Shirai T, Matrisian LM, Futakuchi M. MMP-7 promotes prostate cancer-induced osteolysis via the solubilization of RANKL. Cancer Cell. 2005 May;7(5):485-96.

Mackie EJ, Ramsey S. Modulation of osteoblast behaviour by tenascin. J Cell Sci, *109*:1597-1604, 1996.

Mackie EJ, Abraham LA, Taylor SL, Tucker RP, Murphy LI. Regulation of tenascin-C expression in bone cells by transforming growth factor-beta. Bone, *22*:301-307, 1998.

Maeda S, Hayashi M, Komiya S, Imamura T, Miyazono K. Endogenous TGF-beta signaling suppresses maturation of osteoblastic mesenchymal cells. EMBO J. 2004 Jan 29 [Epub ahead of print]

Merrell M, Suarez-Cuervo C, Harris KW, Vaananen HK, Selander KS. Bisphosphonate induced growth inhibition of breast cancer cells is augmented by p38 inhibition. Breast Cancer Res Treat, *81*:231-241, 2003.

Miyake H, Pollak M, Gleave ME. Castration-induced up-regulation of insulin-like growth factor binding protein-5 potentiates insulin-like growth factor-I activity and accelerates progression to androgen independence in prostate cancer models. Cancer Res, *60*:3058-3064, 2000.

Mohammad KS, Guise TA. Mechanisms of osteoblastic metastases: role of endothelin-1. Clin Orthop, *415*:S67-74, 2003.

Mohammad KS, Chen CG, Balooch G, Stebbins E, McKenna CR, Walton H, Niewolna M, Peng XH, Nguyen DHN, Ionova-Martin SS, Bracey JW, Hogue WR, Vong DH, Ritchie RO, Suva LJ, Derynck R, Guise TA, Alliston T. Pharmacologic inhibition of TGF-β type 1 receptor kinase has anabolic and anti-catabolic effects on bone. PloS ONE 2009 (In press).

Mundy GR. Metastasis to bone: causes, consequences and therapeutic opportunities. Nat Rev Cancer, *2:*584-593, 2002.

Muraoka RS, Dumont N, Ritter CA, Dugger TC, Brantley DM, Chen J, Easterly E, Roebuck LR, Ryan S, Gotwals PJ, Koteliansky V, Arteaga CL. Blockade of TGF-

beta inhibits mammary tumor cell viability, migration, and metastases. J Clin Invest, *109*:1551-1559, 2002.

Nelson JB. Endothelin Inhibition: Novel Therapy for Prostate Cancer. J Urol, *170*:S65-S68, 2003.

O'Keefe RJ, Guise TA. Molecular mechanisms of bone metastasis and therapeutic implications. Clin Orthop, *415*(Suppl):S100-104, 2003.

Park BJ, Park JI, Byun DS, Park JH, Chi SG. Oncogenic conversion of transforming growth factor-beta1 effect by oncogenic Ha-Ras-induced activation of the mitogen-activated protein kinase signaling pathway in human prostate cancer. Cancer Res, *60*:3031-3038, 2000.

Park JI, Lee MG, Cho K, Park BJ, Chae KS, Byun DS, Ryu BK, Park YK, Chi SG. Transforming growth factor-beta1 activates interleukin-6 expression in prostate cancer cells through the synergistic collaboration of the Smad2, p38-NF-kappaB, JNK, and Ras signaling pathways. Oncogene, *22*:4314-4332, 2003.

Pfitzenmaier J, Quinn JE, Odman AM, Zhang J, Keller ET, Vessella RL, Corey E. Characterization of C4-2 prostate cancer bone metastases and their response to castration. J Bone Miner Res, *18*:1882-1888, 2003.

Pirtskhalaishvili G, Nelson JB. Endothelium-derived factors as paracrine mediators of prostate cancer progression. Prostate, *44*:77-87, 2000.

Rae FK, Hooper JD, Nicol DL, Clements JA. Characterization of a novel gene, STAG1/PMEPA1, upregulated in renal cell carcinoma and other solid tumors. Mol Carcinog, *32*:44-53, 2001.

Reddi AH, Roodman D, Freeman C, Mohla S: Mechanisms of tumor metastasis to the bone: challenges and opportunities. *J Bone Miner Res*, 18:190-194, 2003

Roberts AB, Wakefield LM. The two faces of transforming growth factor beta in carcinogenesis. Proc Natl Acad Sci USA, *100*:8621-8623, 2003.

Ruggeri B, Singh J, Gingrich D, Angeles T, Albom M, Chang H, Robinson C, Hunter K, Dobrzanski P, Jones-Bolin S, Aimone L, Klein-Szanto A, Herbert JM, Bono F, Schaeffer P, Casellas P, Bourie B, Pili R, Isaacs J, Ator M, Hudkins R, Vaught J, Mallamo J, Dionne C. CEP-7055: a novel, orally active pan inhibitor of vascular endothelial growth factor receptor tyrosine kinases with potent antiangiogenic activity and antitumor efficacy in preclinical models. Cancer Res, 63:5978-5991, 2003.

Saad F, Gleason DM, Murray R, Tchekmedyian S, Venner P, Lacombe L, Chin JL, Vinholes JJ, Goas JA, Chen B. A randomized, placebo-controlled trial of

zoledronic acid in patients with hormone-refractory metastatic prostate carcinoma. J Natl Cancer Inst, *94*:1458-68, 2002.

Safadi FF, Xu J, Smock SL, Kanaan RA, Selim AH, Odgren PR, Marks SC Jr, Owen TA, Popoff SN.
Expression of connective tissue growth factor in bone: its role in osteoblast proliferation and differentiation in vitro and bone formation in vivo. J Cell Physiol, *196*:51-62, 2003.

Shah AH, Tabayoyong WB, Kundu SD, Kim SJ, Van Parijs L, Liu VC, Kwon E, Greenberg NM, Lee C. Suppression of tumor metastasis by blockade of transforming growth factor beta signaling in bone marrow cells through a retroviral-mediated gene therapy in mice. Cancer Res, *62*:7135-7138, 2002.

Schultz RM. Potential of p38 MAP kinase inhibitors in the treatment of cancer. Prog Drug Res, *60*:59-92, 2003.

Shariat SF, Shalev M, Menesses-Diaz A, Kim IY, Kattan MW, Wheeler TM, Slawin KM. Preoperative plasma levels of transforming growth factor beta(1) (TGF-beta(1)) strongly predict progression in patients undergoing radical prostatectomy. J Clin Oncol, *19*:2856-2864, 2001.

Siegel PM, Shu W, Cardiff RD, Muller WJ, Massague J. Transforming growth factor beta signaling impairs Neu-induced mammary tumorigenesis while promoting pulmonary metastasis. Proc Natl Acad Sci USA, *100*:8430-8435, 2003.

Street J, Bao M, deGuzman L, Bunting S, Peale FV Jr, Ferrara N, Steinmetz H, Hoeffel J, Cleland JL, Daugherty A, van Bruggen N, Redmond HP, Carano RA, Filvaroff EH. Vascular endothelial growth factor stimulates bone repair by promoting angiogenesis and bone turnover. Proc Natl Acad Sci U S A. 2002 Jul 23;99(15):9656-61

Tang B, Vu M, Booker T, Santner SJ, Miller FR, Anver MR, Wakefield LM. TGF-beta switches from tumor suppressor to prometastatic factor in a model of breast cancer progression. J Clin Invest, *112*:1116-1124, 2003.

Thalmann GN, Anezinis PE, Chang SM, Zhau HE, Kim EE, Hopwood VL, Pathak S, von Eschenbach AC, Chung LW. Androgen-independent cancer progression and bone metastasis in the LNCaP model of human prostate cancer. Cancer Res, *54*:2577-2581, 1995.

Thomas RJ, Guise TA, Yin JJ, Elliott J, Horwood NJ, Martin TJ, Gillespie MT. Breast cancer cells interact with osteoblasts to support osteoclast formation. Endocrinol, *140*:4451-4458, 1999.

Tokuda H, Hatakeyama D, Akamatsu S, Tanabe K, Yoshida M, Shibata T, Kozawa O. Involvement of MAP kinases in TGF-beta-stimulated vascular endothelial growth factor synthesis in osteoblasts. Arch Biochem Biophys, *415*:117-125, 2003.

Tuxhorn JA, McAlhany SJ, Yang F, Dang TD, Rowley DR. Inhibition of transforming growth factor-beta activity decreases angiogenesis in a human prostate cancer-reactive stroma xenograft model. Cancer Res, *62*:6021-6025, 2002.

Uy HL, Mundy GR, Boyce BF, Story BM, Dunstan CR, Yin JJ, Roodman GD, Guise TA. Tumor necrosis factor enhances parathyroid hormone-related protein-induced hypercalcemia and bone resorption without inhibiting bone formation in vivo. Cancer Res, *57*:3194-3199, 1997.

van der Pluijm G, Sijmons B, Vloedgraven H, Deckers M, Papapoulos S, Lowik C. Monitoring metastatic behavior of human tumor cells in mice with species-specific polymerase chain reaction: elevated expression of angiogenesis and bone resorption stimulators by breast cancer in bone metastases. J Bone Miner Res, *16*:1077-1091, 2001.

Wikstrom P, Damber J, Bergh A. Role of transforming growth factor-beta1 in prostate cancer. Microsc Res Tech, *52*:411-419, 2001.

Wu TT, Sikes RA, Cui Q, Thalmann GN, Kao C, Murphy CF, Yang H, Zhau HE, Balian G, Chung LW. Establishing human prostate cancer cell xenografts in bone: induction of osteoblastic reaction by prostate-specific antigen-producing tumors in athymic and SCID/bg mice using LNCaP and lineage-derived metastatic sublines. Int J Cancer, *77*:887-894, 1998.

Xu LL, Shanmugam N, Segawa T, Sesterhenn IA, McLeod DG, Moul JW, Srivastava S. A novel androgen-regulated gene, PMEPA1, located on chromosome 20q13 exhibits high level expression in prostate. Genomics, *66*:257-263, 2000.

Xu LL, Shi Y, Petrovics G, Sun C, Makarem M, Zhang W, Sesterhenn IA, McLeod DG, Sun L, Moul JW, Srivastava S. PMEPA1, an androgen-regulated NEDD4-binding protein, exhibits cell growth inhibitory function and decreased expression during prostate cancer progression. Cancer Res, *63*:4299-4304, 2003.

Yang YA, Dukhanina O, Tang B, Mamura M, Letterio JJ, MacGregor J, Patel SC, Khozin S, Liu ZY, Green J, Anver MR, Merlino G, Wakefield LM. Lifetime exposure to a soluble TGF-beta antagonist protects mice against metastasis without adverse side effects. J Clin Invest, *109*:1607-1615, 2002.

Yin JJ, Selander K, Chirgwin JM, Dallas M, Grubbs BG, Wieser R, Massague J, Mundy GR, Guise TA. TGF-beta signaling blockade inhibits PTHrP secretion by breast cancer cells and bone metastases development. J Clin Invest, *103*:197-206, 1999.

Yin JJ, Mohammad KS, Kakonen SM, Harris S, Wu-Wong JR, Wessale JL, Padley RJ, Garrett IR, Chirgwin JM, Guise TA. A causal role for endothelin-1 in the pathogenesis of osteoblastic bone metastases. Proc Natl Acad Sci USA, *100*:10954-10959, 2003

Yoneda T, Sasaki A, Dunstan C, Williams PJ, Bauss F, De Clerck YA, Mundy GR. Inhibition of osteolytic bone metastasis of breast cancer by combined treatment with the bisphosphonate ibandronate and tissue inhibitor of the matrix metalloproteinase-2. J Clin Invest, *99*:2509-2517, 1997.

Zheng *et al.* 2004. JBC. 279:42898

Zhou W, Park I, Pins M, Kozlowski JM, Jovanovic B, Zhang J, Lee C, Ilio K. Dual regulation of proliferation and growth arrest in prostatic stromal cells by transforming growth factor-beta1. Endocrinology, *144*:4280-4284, 2003.

## APPENDIX

### Statement of Work

Task 1 (Specific Aim 1) – months 01-06. Test TβRI kinase inhibitor at 2 doses (plus untreated controls) against PC3 cells; Completed

Task 2 (Specific Aim 1) – months 07-12. Analyze bone and tumor parameters from mice from preceding Task 1. Completed

Task 3 (Specific Aim 1) – months 07-12. Test TβRI kinase inhibitor at 2 doses (plus untreated controls) (plus untreated controls) against LuCAP23.1 cells inoculated intratibially. Completed once. Repeat experiment completed and data analysis in progress for second experiment.

Task 4 (Specific Aim 1) – months 13-18. Analyze bone and tumor parameters from mice from preceding Task 3. Data analysis in progress for second experiment

Task 5 (Specific Aim 1) – months 13-18. Test TβRI kinase inhibitor at 2 doses (plus untreated controls) against C4-2B cells inoculated intratibially; Completed once. Repeat experiment completed and data analysis in progress for second experiment.

Task 6 (Specific Aim 1) – months 19-24. Analyze bone and tumor parameters from mice from Task 5. Data analysis in progress for second experiment.

Task 7 (Specific Aim 1) – months 01-06. Test p38 MAPK inhibitor at 2 doses (plus untreated controls) against PC3. Completed

Task 8 (Specific Aim 1) – months 07-12. Analyze bone and tumor parameters from mice from preceding Task 7. Completed

Task 9 (Specific Aim 1) – months 07-12. Test p38 MAPK inhibitor at 2 doses (plus untreated controls) against LuCAP23.1 cells. Completed

Task 10 (Specific Aim 1) – months 13-18. Analyze bone and tumor parameters from mice from preceding Task 9. Data analysis in progress

Task 11 (Specific Aim 1) – months 13-18. Test p38 MAPK inhibitor at 2 doses (plus untreated controls) against C4-2B cells inoculated intratibially; Completed

Task 12 (Specific Aim 1) – months 19-24. Analyze bone and tumor parameters from mice from Task 11. Completed for bone.

Task 13 (Specific Aim 2) – months 01-12. Isolate mRNAs from PC3 and C4-2B cells grown +/- TGFβ and +/- TβRI kinase and p38 MAPK inhibitors at 1 dose each. Analyze RNAs by Affymetrix gene array and process data. Simplified experiment focusing on PC3 cells treated +/- TGFβ completed, identifying PMEPAS1 as most up-regulated mRNA.

Task 13a (Specific Aim 2) – months 13-18. Validate genes identified in previous Task 13 by RT-PCR analysis of mRNAs prepared in that Task. Completed.

Task 14 (Specific Aim 2) – months 18-24. Generate and characterize stable cell lines of PC3 and C4-2B cells overexpressing FLAG-tagged PMEPA1 protein and, as practical, one or more other candidate factors identified in the previous two Tasks 13 & 13a. Simplified version of Task completed, focusing on PMEPA1 in PC3 cells, but with knockdown, rather than overexpression.

Task 15 (Specific Aim 2) – months 25-30. Carry out animal experiments as in Tasks 1 and 5 with control and PMEPA1 overexpressing cell lines Simplified version of Task 15 to be done in year 04, focusing on PMEPA1 knockdown in PC3 cells. Experiment completed.

Task 16 (Specific Aim 2) – months 31-36. Analyze bone and tumor parameters from mice from preceding Task 15. Data analysis in progress

Task 17 (Specific Aim 3) – months 19-24. Test TβRI and p38 MAP kinase inhibitors singly and combined at optimized doses, plus an untreated control, against PC3 cells. Task abandoned due to lack of efficacy of p38 MAP kinase

inhibitor against bone metastases as well as inability to obtain p38 MAP kinase inhibitor.

Task 18 (Specific Aim 3) – months 25-30. Analyze bone and tumor parameters from mice from preceding Task 17. Task abandoned due to lack of efficacy of p38 MAP kinase inhibitor against bone metastases as well as inability to obtain p38 MAP kinase inhibitor.

Task 19 (Specific Aim 3) – months 21-26. Test TβRI & p38 MAP kinase inhibitors singly and combined at optimized dose, plus an untreated control, against LuCAP23.1. Task abandoned due to lack of efficacy of p38 MAP kinase inhibitor against bone metastases as well as inability to obtain p38 MAP kinase inhibitor.

Task 20 (Specific Aim 3) – months 27-32. Analyze bone and tumor parameters from mice from preceding Task 19. Task abandoned due to lack of efficacy of p38 MAP kinase inhibitor against bone metastases as well as inability to obtain p38 MAP kinase inhibitor.

Task 21 (Specific Aim 3) – months 25-30. Test TβRI & p38 MAP kinase inhibitors singly and combined at optimized dose, plus an untreated control, against C4-2B cells. Task abandoned due to lack of efficacy of p38 MAP kinase inhibitor against bone metastases as well as inability to obtain p38 MAP kinase inhibitor.

Task 22 (Specific Aim 3) – months 31-36. Analyze bone and tumor parameters from mice from preceding Task 21. Task abandoned due to lack of efficacy of p38 MAP kinase inhibitor against bone metastases as well as inability to obtain p38 MAP kinase inhibitor.

Task 23 (Specific Aims 1-3) – months 03-36. Analyze data, prepare manuscripts and reports. Manuscript preparation in progress.

Since Tasks were abandoned due to lack of efficacy of p38 MAP kinase inhibitor as well as the inability to obtain sufficient drug to complete aims as planned, we performed studies to characterize the effects of TGFβ blockade on normal bone and the mechanisms by which such inhibition causes increased bone mass, described in this final report.

OPEN ACCESS Freely available online

PLoS one

# Pharmacologic Inhibition of the TGF-β Type I Receptor Kinase Has Anabolic and Anti-Catabolic Effects on Bone

**Khalid S. Mohammad[1], Carol G. Chen[2,3], Guive Balooch[4], Elizabeth Stebbins[5], C. Ryan McKenna[1], Holly Davis[1], Maria Niewolna[1], Xiang Hong Peng[1], Daniel H. N. Nguyen[3], Sophi S. Ionova-Martin[5], John W. Bracey[6], William R. Hogue[6], Darren H. Wong[5,7], Robert O. Ritchie[4], Larry J. Suva[6], Rik Derynck[2,8,9], Theresa A. Guise[1], Tamara Alliston[2,3,9]***

**1** Department of Internal Medicine, Division of Endocrinology, University of Virginia, Charlottesville, Virginia, United States of America, **2** Graduate Program in Oral and Craniofacial Sciences, University of California San Francisco, San Francisco, California, United States of America, **3** Department of Orthopaedic Surgery, University of California San Francisco, San Francisco, California, United States of America, **4** Department of Materials Science and Engineering, University of California, Berkeley and Materials Science Division, Lawrence Berkeley National Laboratories, Berkeley, California, United States of America, **5** Scios, Inc, Fremont, California, United States of America, **6** Department of Orthopaedic Surgery, Center for Orthopaedic Research, Barton Research Institute, University of Arkansas for Medical Sciences, Little Rock, Arkansas, United States of America, **7** Pfizer RTC, Cambridge, Massachusetts, United States of America, **8** Department of Cell and Tissue Biology, University of California San Francisco, San Francisco, California, United States of America, **9** Institute of Regeneration Medicine, University of California San Francisco, San Francisco, California, United States of America

## Abstract

During development, growth factors and hormones cooperate to establish the unique sizes, shapes and material properties of individual bones. Among these, TGF-β has been shown to developmentally regulate bone mass and bone matrix properties. However, the mechanisms that control postnatal skeletal integrity in a dynamic biological and mechanical environment are distinct from those that regulate bone development. In addition, despite advances in understanding the roles of TGF-β signaling in osteoblasts and osteoclasts, the net effects of altered postnatal TGF-β signaling on bone remain unclear. To examine the role of TGF-β in the maintenance of the postnatal skeleton, we evaluated the effects of pharmacological inhibition of the TGF-β type I receptor (TβRI) kinase on bone mass, architecture and material properties. Inhibition of TβRI function increased bone mass and multiple aspects of bone quality, including trabecular bone architecture and macro-mechanical behavior of vertebral bone. TβRI inhibitors achieved these effects by increasing osteoblast differentiation and bone formation, while reducing osteoclast differentiation and bone resorption. Furthermore, they induced the expression of Runx2 and EphB4, which promote osteoblast differentiation, and ephrinB2, which antagonizes osteoclast differentiation. Through these anabolic and anti-catabolic effects, TβRI inhibitors coordinate changes in multiple bone parameters, including bone mass, architecture, matrix mineral concentration and material properties, that collectively increase bone fracture resistance. Therefore, TβRI inhibitors may be effective in treating conditions of skeletal fragility.

**Citation:** Mohammad KS, Chen CG, Balooch G, Stebbins E, McKenna CR, et al. (2009) Pharmacologic Inhibition of the TGF-β Type I Receptor Kinase Has Anabolic and Anti-Catabolic Effects on Bone. PLoS ONE 4(4): e5275. doi:10.1371/journal.pone.0005275

**Editor:** Jose A. L. Calbet, University of Las Palmas de Gran Canaria, Spain

**Received** October 23, 2008; **Accepted** March 13, 2009; **Published** April 16, 2009



**Funding:** The study was funded by NIH, US DOE, The Arthritis Foundation, The Sandler Family Foundation, The Carl Nelson Chair in Orthopaedic Surgery, The Stugis Foundation, and The Aurbach Endowment. The funders had no role in study design, data collection and analysis, decision to publish, or preparation of the manuscript.

**Competing Interests:** The authors have declared that no competing interests exist.

* E-mail: tamara.alliston@ucsf.edu

## Introduction

In skeletal development, each bone is formed with a distinctive size, geometry, architecture, and material properties. Among the many growth factors and hormones involved in this process [1–3], transforming growth factor-β (TGF-β) is sequestered at high levels in bone matrix and is a critical regulator of osteogenesis [4]. Bone mass is dramatically affected by developmental manipulation of TGF-β signaling in genetically modified mouse models [5–9]. In addition to bone mass, TGF-β regulates bone matrix material properties, which impact the ability of bone to resist fracture [10]. However, little is known about the role of TGF-β in the post-natal skeleton, which responds to changes in bone or the environment to retain or improve bone quality, fundamentally defined as the ability to resist bone fracture [11].

The effects of postnatal manipulation of TGF-β signaling on bone mass and quality are difficult to predict based on developmental studies. For example, osteoporosis and bone fragility are observed in mice with increased TGF-β production [6], as well as in those that are deficient in Smad3 [8,9], a key TGF-β effector. Conversely, other mouse models with reduced TGF-β signaling have increased bone mass and quality [7,10]. In addition, the roles of TGF-β on the proliferation, differentiation, and apoptosis of cells in both the osteoblast and osteoclast lineages have been extensively studied [4,12–14]. In spite of this wealth of information, the net effect of postnatal TGF-β signaling on bone remains unknown.

The recent development of specific inhibitors of the TGF-β type I receptor (TβRI) kinase that block most if not all TGF-β signaling events [15–17] now enables an investigation of this fundamental

question. ATP-competitive inhibitors of the TβRI kinase, such as SD-208, can effectively limit TGF-β-mediated lung fibrosis and tumorigenesis in vivo at doses that are too low to exert non-specific effects on other kinases [17–20]. Since such inhibitors are in clinical trials for cancer and other disorders, it is crucial to define the effects of TGF-β blockade on the skeleton.

Maintenance of the postnatal skeleton depends on the functional coordination between bone-depositing osteoblasts and bone-resorbing osteoclasts [21]. Both cell populations express and respond to TGF-β, and TGF-β has been suggested to couple osteoblast and osteoclast activity [4]. TGF-β promotes osteoprogenitor proliferation and inhibits terminal osteoblast differentiation, in part by repressing the function of osteogenic transcription factor Runx2 [22]. TGF-β also regulates osteoblast expression of osteoclast regulatory factors m-CSF, RANKL, and OPG [23–25], whereas resorbing osteoclasts release and activate matrix-bound latent TGF-β, which feeds back to modulate osteoblast and osteoclast function [26–28]. Because the effects of TGF-β on osteoblast and osteoclast function are dynamic, dose-dependent, and specific for each cell type and stage of differentiation [4,12–14], prior studies do not indicate how the cell types present in mature bone will respond to a systemic alteration in TGF-β signaling.

In the current study, we found that the TβRI kinase inhibitor, SD-208, affects osteoblast and osteoclast function to coordinately regulate several bone parameters, resulting in increased bone mass and trabecular bone volume, as well as increased mineral concentration and elastic modulus of bone matrix. This was associated with an increased resistance to vertebral fracture. These results suggest that pharmacologic inhibition of TGF-β signaling may have therapeutic utility in a variety of bone diseases characterized by poor bone quality, low bone mass and a propensity to fracture.

## Results

### Pharmacologic inhibition of the TβRI kinase increases bone mineral density

To determine the effects of pharmacologic inhibition of TGF-β signaling on bone, mice were treated for 6 weeks with either of two doses of SD-208, a small molecule that blocks ATP binding to the type I TGF-β receptor to specifically inhibit its kinase activity [17]. The 20 mg/kg SD-208 dose was chosen to achieve specific inhibition of the TβRI kinase, whereas the 60 mg/kg dose was chosen to achieve a maximal response with minimal inhibition of other pathways [19]. Using mice that express luciferase under the control of a TGF-β-responsive Smad binding element (SBE-Luc mice) [29], we confirmed the ability of SD-208 to inhibit endogenous and exogenously applied TGF-β function in bone in vivo and ex vivo (Fig. 1a, 1b). As expected, the well-established TGF-β-inducible expression of PAI-1 [30] was inhibited by SD-208 in calvarial explants, whereas the expression of reported targets of TGF-β repression, Runx2 and osteocalcin [22], was induced by SD-208 (Fig. 1c).

Longitudinal examination of the bone mineral density (BMD) by dual energy X-ray absorptiometry (DXA) showed the normal increase in BMD between 1 and 2.5 months of age. Accordingly, vehicle-treated male and female mice showed an increase of 21.8% and 29.6%, respectively, in whole body BMD after 6 weeks (Fig. 2a, 2b). Although low dose SD-208 did not affect whole body BMD, both male and female mice treated with high dose SD-208, showed significantly greater bone accrual over the same time period, with an additional 4.12% increase in male ($p<0.001$) and 5.2% increase in female ($p<0.001$) whole body BMD. The SD-208-induced increase in whole body BMD was comparable to that observed following an 8-week treatment with bisphosphonates, which can increase whole body BMD by 5% [31].

More pronounced effects were apparent in the tibia and femur, where the BMD was already significantly increased within 3 weeks of SD-208 treatment relative to vehicle-treated controls (Fig. 2c–2f). After 6 weeks, SD-208 significantly increased the BMD in male mice by 20% in the tibia ($p<0.001$), 14.8% in the femur ($p<0.001$) and 8.9% in the lumbar spine ($p<0.01$) relative to vehicle-treated mice. SD-208 increased the tibial, femoral and lumbar spine BMD in female mice by 16.3% ($p<0.001$), 11.4% ($p<0.01$) and 17.9% ($p<0.001$), respectively. Dose-dependent increases in BMD were most apparent in the femur (Fig. 2e, 2f). Thus, systemic pharmacologic inhibition of TGF-β signaling increases the BMD.

### Inhibition of the TβRI kinase increases trabecular bone

To determine if the increased BMD resulted from changes in cortical or trabecular bone, dissected femora and tibiae were analyzed using micro-computed tomography (micro-CT). Reconstructed images of trabecular bone in the distal femur showed a dose-dependent increase in trabecular bone volume following 6 weeks of SD-208 treatment in both male and female mice (Fig. 3a). This increase in trabecular bone was noted in the secondary spongiosa and did not extend to the diaphysis (Figure S1). At the high dose, SD-208 increased the femoral trabecular bone volume of male and female mice by 57.6% and 264%, respectively (Fig. 3b, Table 1). Remarkably, high-dose SD-208 increased the trabecular density of male and female femora by 192% and 581%, respectively (Fig. 3c). Increases in trabecular number and thickness were associated with a corresponding decrease in trabecular separation following treatment with SD-208 (Fig. 3d, 3e, Table 1). As shown by these and other parameters, SD-208 greatly improved trabecular bone microarchitecture in male and female femora and tibiae (Table 1). In contrast, SD-208 caused no significant differences in measured cortical bone parameters (Table 2). Therefore, the effect of 6 weeks of pharmacologic inhibition of TβRI function on BMD appears to be specific to the trabecular bone.

### Inhibition of TβRI affects both osteoblasts and osteoclasts

Increased BMD may be due to increased osteoblast activity, reduced osteoclast activity or both. Quantitative histomorphometry confirmed the SD-208 dose-dependent increase in trabecular bone that was observed by micro-CT (Fig. 4a). The significantly increased bone volume (Fig. 4b) was accompanied by a TβRI inhibitor dose-dependent increase in osteoblast number (Fig. 4c). Importantly, even the most specific low dose of SD-208 (20 mg/kg) caused significant increases in male and female bone volume and osteoblast numbers ($p<0.05$). In addition, the osteoclast numbers were reduced in the femora of SD-208 treated mice (Fig. 4d). Bones from male mice treated with the highest dose of SD-208 had twice as many osteoblasts and half as many osteoclasts as the vehicle-treated controls (Fig. 4).

These data suggest that inhibition of TGF-β signaling increases bone mass by enhancing bone formation and inhibiting bone resorption. Dynamic histomorphometry revealed that SD-208 stimulates a dose-dependent increase in the mineral apposition rate and bone formation rate in male mice (Fig. 4e, 4f). Female mice showed the same trend. Collectively, these analyses demonstrate that TβRI inhibitors increase bone mass in mature mice via anabolic and anti-catabolic mechanisms.

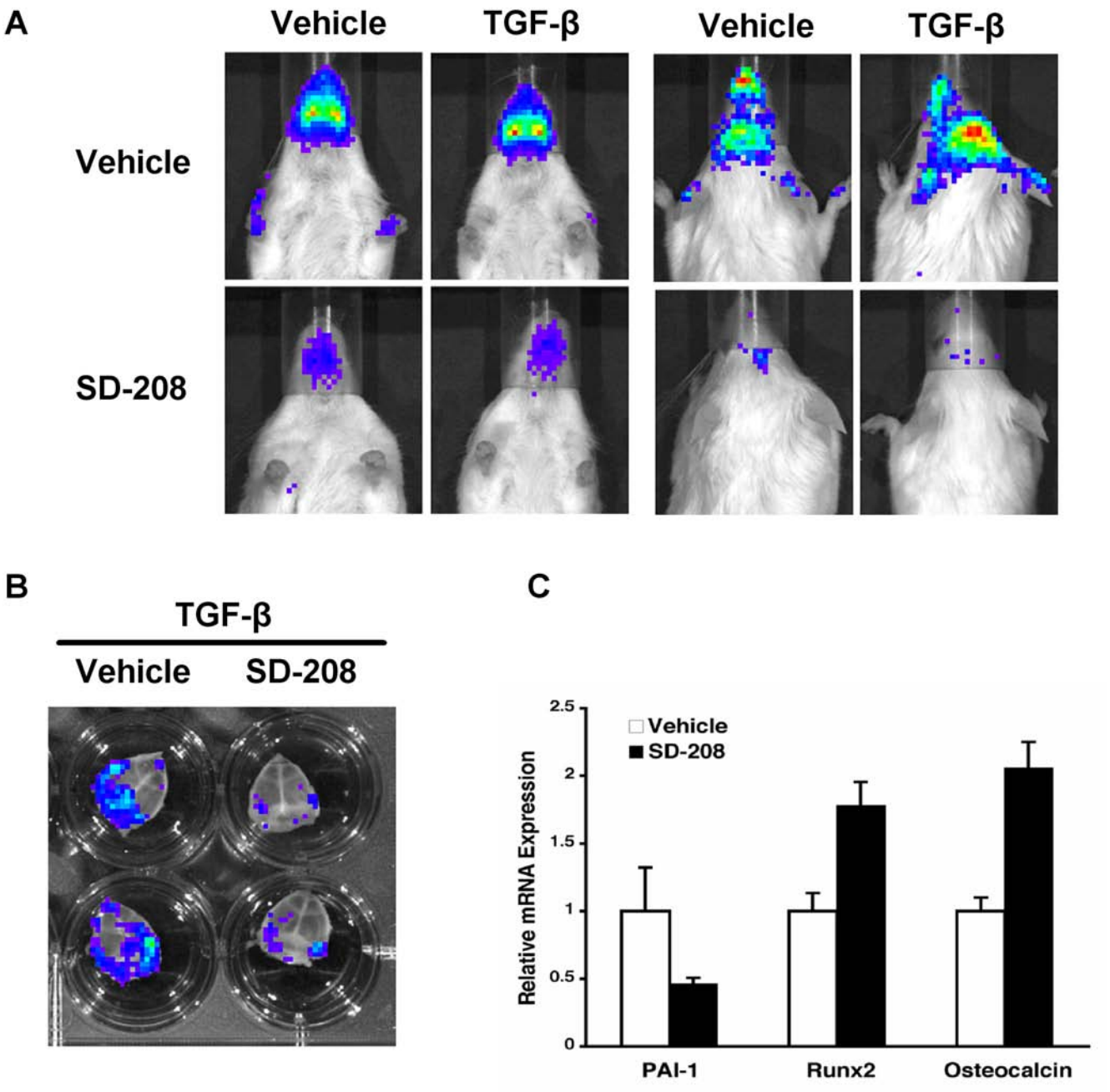


**Figure 1. SD-208 inhibition of TGF-β function in vivo.** Five hours after TGF-β administration, SBE-Luc mice showed increased bioluminescence on the dorsal and ventral surfaces of the head where relatively little superficial tissue covers skeletal elements (calvarial bone and jaws) (a). Mice pretreated with SD-208 showed less basal and TGF-β-inducible luminescence than vehicle-treated controls (a, lower panels). SD-208 also inhibited reporter activity in SBE-Luc mouse calvarial explants cultured overnight with TGF-β (b). SD-208 treatment of calvarial explants inhibits expression of the TGF-β-inducible gene, PAI-1 [30], but induces expression of Runx2 and osteocalcin, osteoblast marker genes that are targets of TGF-β repression [22].
doi:10.1371/journal.pone.0005275.g001

## TβRI inhibition promotes osteoblast differentiation and inhibits osteoclast differentiation

To determine if the changes in osteoblast and osteoclast numbers and activity resulted from changes in cell differentiation, bone marrow stromal cells that were isolated from vehicle- and SD-208-treated mice were examined ex vivo in osteoblast or osteoclast differentiation assays (Fig. 5a–5c). In vivo exposure to SD-208 enhanced the osteoblast differentiation (CFU-Ob, Fig. 5a) with no detectable effect on osteoprogenitor recruitment (CFU-F, Fig. 5b). Conversely, marrow stromal cells from mice treated with SD-208 formed fewer multinucleated cells that express the functional osteoclast marker TRAP (Fig. 5c). Thus, in vivo inhibition of TβRI with SD-208 promotes osteoblast differentiation and inhibits osteoclast differentiation.

To investigate the effect of TβRI inhibitors on the expression of osteoblast and osteoclast regulatory factors, we utilized primary calvarial osteoblasts, which retain the capacity to differentiate into mineralizing osteoblasts, and have an intact autocrine TGF-β

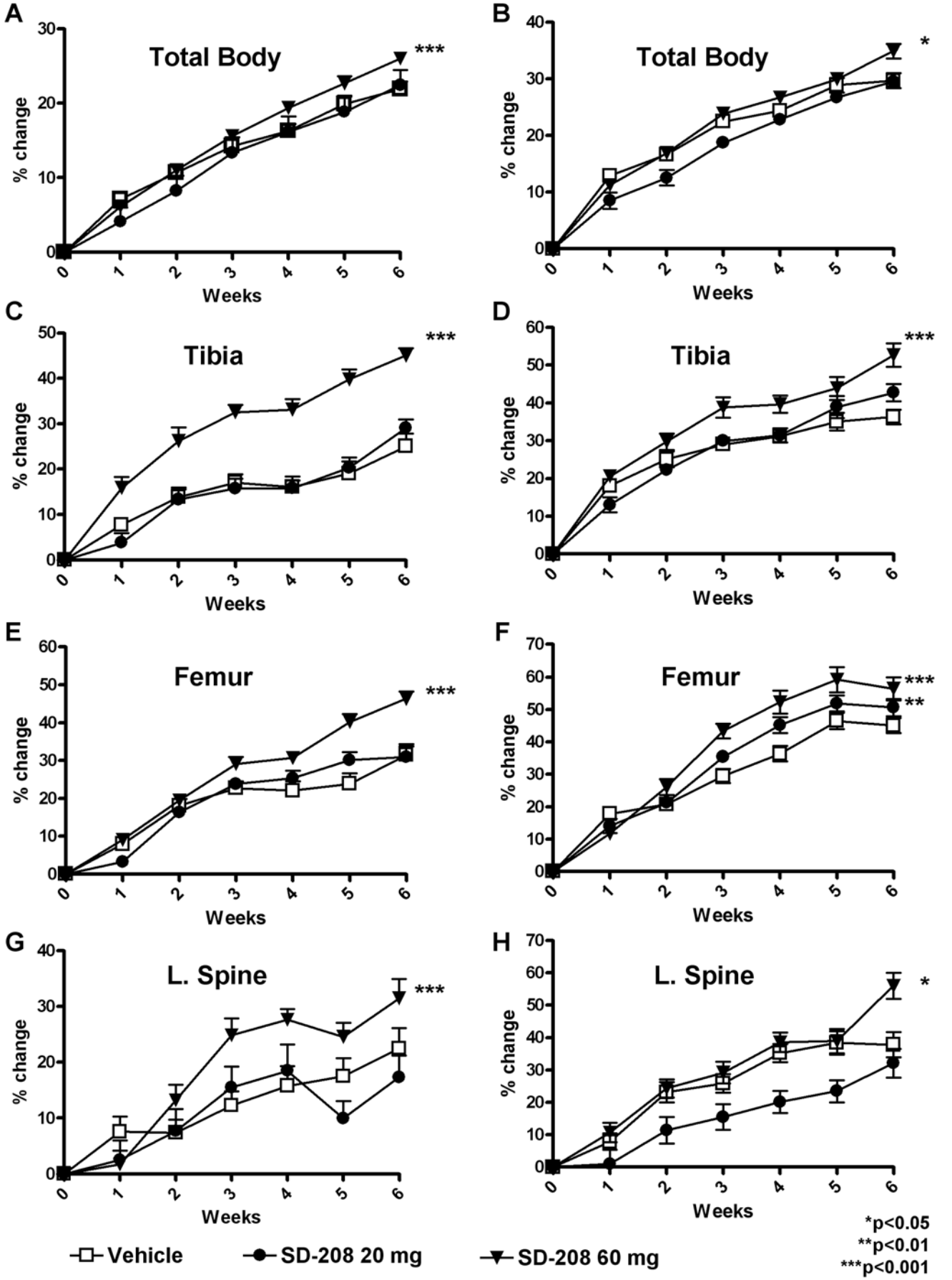
A
Total Body
% change
Weeks
***
B
Total Body
% change
Weeks
*
C
Tibia
% change
Weeks
***
D
Tibia
% change
Weeks
***
E
Femur
% change
Weeks
***
F
Femur
% change
Weeks
***
**
G
L. Spine
% change
Weeks
***
H
L. Spine
% change
Weeks
*
Vehicle
SD-208 20 mg
SD-208 60 mg
*p<0.05
**p<0.01
***p<0.001

**Figure 2. Pharmacologic TβRI inhibition increases BMD.** DXA was used to measure BMD longitudinally for male (a, c, e, g) and female mice (b, d, f, h) treated with or without the TβRI inhibitor SD-208 at 20 mg/kg or 60 mg/kg. SD-208 treatment at the 60 mg/kg dose caused an increase in total body (a, b) tibia (c, d), femur (e, f), and lumbar spine (g, h) BMD. SD-208 at the 20 mg/kg dose increased femoral BMD in female mice (f). Data represent mean±SEM ($p<0.05$, as determined by two-way analysis of variance (ANOVA).
doi:10.1371/journal.pone.0005275.g002

regulatory pathway. As in calvarial explants treated with SD-208 (Fig. 1c), another ATP-competitive TβRI kinase inhibitor, SB431542, inhibits the expression of the TGF-β-inducible gene, PAI-1 [30], in primary calvarial osteoblasts (Fig. 5d). As shown previously [22], Runx2 expression was reduced after 48 h of treatment with added TGF-β (Fig. 5d). In contrast, TβRI inhibitors induce Runx2 expression, consistent with the increased osteoblast numbers, bone formation rate, and osteoblast differentiation potential observed in SD-208-treated mice (Fig. 4c, 4f, 5a, 5d).

RANK ligand (RANKL) promotes osteoclast differentiation, function and survival [21]. After 48 h of treatment, TβRI inhibitors reduced the expression of RANKL mRNA by approximately 50% compared with the mRNA levels observed in vehicle-treated primary calvarial osteoblasts (Fig. 5e). The reduced expression of this osteoclastogenic factor is consistent with the decreased osteoclast numbers and differentiation capacity observed in SD-208-treated mice (Figs. 4d and 5c). However, RANKL function is antagonized by osteoprotegerin, the expression of which is also reduced by TβRI-I treatment. Similar results were observed after 2 h of TβRI-I treatment (data not shown). Though the inhibition of TGF-β signaling impacts both of these critical regulators of osteoclast differentiation and function, the relative RANKL/OPG ratio is unchanged. Therefore, the effect of inhibition TβRI function on other factors which regulate osteoblast and osteoclast function was investigated.

Recently, ephrin B2 and EphB4, a transmembrane ligand and receptor respectively, have been implicated as factors that couple osteoblast and osteoclast activities in bone metabolism [32]. Bidirectional signaling between ephrin B2, expressed by osteoblasts and osteoclasts, and EphB4 on osteoblasts increases osteoblast differentiation and inhibits osteoclast differentiation [32]. However, the ability of TGF-β to control ephrin signaling in bone metabolism has not been reported. Inhibition of TβRI function significantly increased the expression of both ephrin B2, the ephrin that inhibits osteoclast differentiation (Fig. 5f), and EphB4, the Eph receptor that induces osteoblast differentiation. TGF-β signaling crosstalk with the ephrin pathway may contribute to the anabolic and anti-catabolic effects of SD-208 on bone, though additional experiments are needed to establish a functional link. By affecting osteoblast and osteoclast differentiation, numbers and activity (Figs. 4c–f, 5a, 5c), the TβRI inhibitor dramatically shifts bone toward a state of metabolic anabolism.

### TβRI inhibitors increase bone matrix mineral concentration, material properties and fracture resistance

The net effect of TβRI inhibitors on bone is increased BMD, which reflects both bone mass and mineral concentration (Fig. 2). With the monochromatic light from synchrotron radiation, X-ray tomographic microscopy (XTM) permits direct quantification of the mineral concentration of bone matrix with an 8 μm resolution [33]. Analyses of femoral bone showed that SD-208 treatment resulted in a higher degree of mineralization of bone matrix (Fig. 6a). The SD-208-dependent increase in mineral concentration was evident in both the diaphysis and epiphysis (data not shown), suggesting that the mineralization of both cortical and trabecular bone were affected.

Mineral concentration is a major determinant of bone matrix material properties [34]. Using nanoindentation, material properties such as the elastic modulus and hardness of bone matrix can be determined independently of changes in bone mass or structure [35,36]. We have previously used this approach to demonstrate that TGF-β signaling in osteoblasts regulates the elastic modulus and hardness of bone matrix in genetically-modified mice [10]. Treatment of mice with SD-208 increased the elastic modulus of cortical bone relative to vehicle-treated controls. Although the measured modulus values in each group overlapped, more than half of the measurements in vehicle-treated bone were below 28 GPa, whereas less than a quarter of the values measured in SD-208-treated mice were in the same range (Fig. 6b).

Treatment with the TβRI inhibitor SD-208 affects bone on several levels, including bone mass (Figs. 2–4), bone mineral concentration and bone matrix material properties (Figs. 6a, 6b). These observations led us to perform macro-mechanical testing to evaluate the ability of SD-208-treated bones to resist fracture. Compression testing of vertebrae showed that inhibition of the TβRI kinase increased the load-to-failure relative to vehicle-treated controls (Fig. 6c, Table 3). When the femora were tested using notched or unnotched three-point bending, SD-208-dependent differences in peak load, stiffness, or fracture toughness were not observed (Table 4). The increased load-to-failure of SD-208-treated vertebral bone, but not femoral bone, is entirely consistent with the increase in trabecular but not cortical bone volume after 6 weeks of SD-208 treatment. Together these data demonstrate that TGF-β inhibitors drive functionally significant and coordinated increases in trabecular bone mass, mineral concentration and bone matrix material properties.

## Discussion

Here we explored the role of TGF-β signaling in postnatal bone by systemic administration of a TβRI inhibitor to mature mice. Pharmacologic inhibition of TGF-β signaling resulted in dose-dependent increases in BMD, trabecular microarchitecture, bone matrix elastic modulus and mineral concentration. These coordinated changes in bone mass and parameters of bone quality improved the ability of vertebral bone to resist fracture. By targeting key regulatory pathways in osteoblasts and osteoclasts, TβRI inhibitors increased the number of osteoblasts and the bone formation rate, while reducing osteoclast numbers. Therefore, TβRI inhibition elicits both anabolic and anti-catabolic activities to improve bone quality.

The TβRI inhibitor-dependent increase in tibial BMD exceeded the physiologic increase in BMD over this time period or those induced by comparable regimens utilizing clinically available bisphosphonates or PTH [31,37]. TβRI inhibitors may have more profound effects since they both stimulate bone formation and inhibit bone resorption, rather than the uncoupled effects of PTH to stimulate osteoblast activity or bisphosphonates to inhibit osteoclast activity. The effects of the TβRI inhibitor on adult bone are consistent with the developmental bone phenotypes of mice with partial inhibition of TGF-β/Smad signaling, as observed in Smad3+/− mice or DNTβRII mice that express a dominant negative TGF-β type II receptor in osteoblasts [7,10]. In contrast, more complete inhibition of TGF-β signaling in

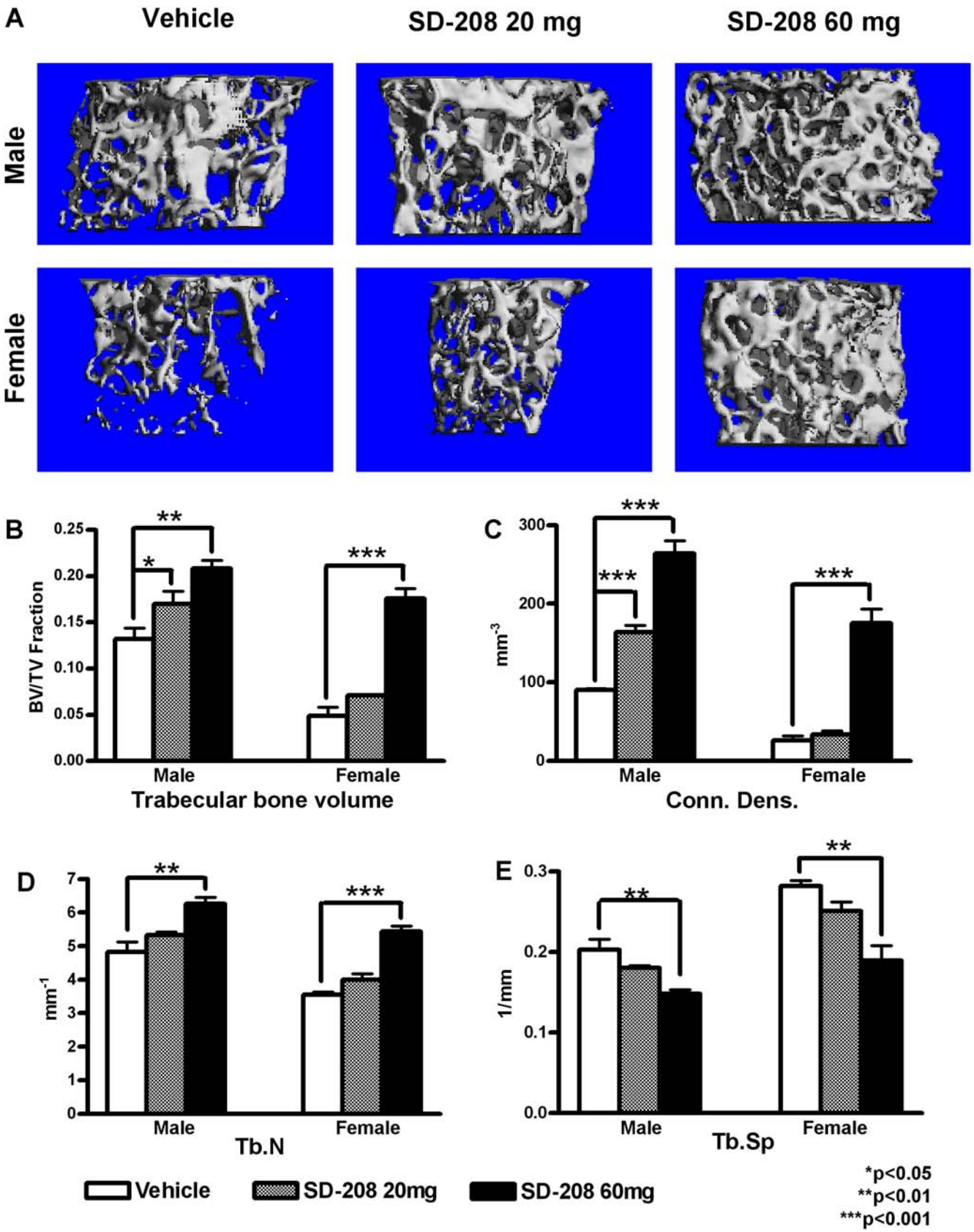


**Figure 3. Pharmacologic TβRI inhibition increases trabecular bone volume.** Micro-CT images show increased femoral trabecular bone volume following SD-208 treatment in male and female mice, relative to vehicle-treated controls (a). Quantitative analyses show that SD-208 increased trabecular bone volume (BV/TV, fraction) (b), connectivity density (c), and trabecular number (d), but decreased trabecular spacing (e) in male and female femora. Data represent mean±SEM ($p<0.05$, as determined by one-way ANOVA Newman-Keuls multiple comparison test).
doi:10.1371/journal.pone.0005275.g003

**Table 1.** Trabecular bone structural parameters are affected by TβRI inhibition.

| | Male | | | | | Female | | | | |
|---|---|---|---|---|---|---|---|---|---|---|
| | Tibia | | | Femur | | Tibia | | | Femur | |
| | Vehicle | 20 mg SD-208 | 60 mg SD-208 | Vehicle | 20 mg SD-208 | 60 mg SD-208 | Vehicle | 20 mg SD-208 | 60 mg SD-208 | Vehicle | 20 mg SD-208 | 60 mg SD-208 |
| **TBV** | 0.11±0.006 | 0.182±0.018** | 0.20±0.009** | 0.132±0.017 | 0.169±0.013* | 0.208±0.008** | 0.09±0.009 | 0.113±0.007 | 0.161±0.014** | 0.048±0.009 | 0.071±0.0009 | 0.175±0.011*** |
| **DT.Tb.Th** | 0.048±0.0006 | 0.049±0.002 | 0.047±0.0004 | 0.049±0.0012 | 0.049±0.003 | 0.046±0.0003 | 0.045±0.002 | 0.048±0.0009 | 0.046±0.0005 | 0.039±0.002 | 0.045±0.001* | 0.048±0.0005* |
| **DT.Tb.N** | 4.44±0.19 | 5.53±0.10*** | 6.19±0.15*** | 4.82±0.29 | 5.32±0.09 | 6.27±0.18** | 3.34±0.15 | 3.69±0.15 | 5.22±0.39** | 3.54±0.08 | 3.99±0.17 | 5.43±0.16*** |
| **DT.Tb.Sp** | 0.20±0.01 | 0.16±0.004 | 0.15±0.003* | 0.20±0.01 | 0.18±0.002 | 0.14±0.004** | 0.30±0.014 | 0.26±0.012 | 0.11±0.016*** | 0.28±0.006 | 0.25±0.011 | 0.18±0.018** |
| **Conn.Dens.** | 60.52±4.13 | 129.6±12.06** | 197.3±15.16*** | 90.32±1.61 | 163.1±8.68*** | 264.3±16.09*** | 47.13±5.21 | 50.55±6.01 | 138.2±25.01** | 25.7±6.13 | 33.48±4.95 | 175.2±17.97*** |
| **TRI SMI** | 2.36±0.06 | 1.98±0.13 | 1.97±0.082 | 2.39±0.11 | 2.07±0.04* | 1.78±0.009*** | 2.33±0.07 | 2.15±0.12 | 2.34±0.044 | 3.28±0.14 | 3.21±0.048 | 2.09±0.106*** |
| **TRI DA** | 2.13±0.06 | 2.11±0.07 | 1.92±0.06 | 1.33±0.009 | 1.42±0.04 | 1.33±0.03 | 2.34±0.066 | 2.6±0.023** | 2.01±0.089*** | 1.4±0.106 | 1.4±0.006 | 1.42±0.006 |

Micro-computed tomography was used to assess several quantitative parameters of trabecular bone structure. The mean values and standard deviations are presented here. Significant differences between vehicle and SD-208 treated groups are indicated (*p<0.05, **p<0.01, ***p<0.001).

doi:10.1371/journal.pone.0005275.t001

Smad3−/− and TGF-β1−/− mice is associated with low bone mass and poor bone quality, which may result, in part, from the significant systemic effects of Smad3 and TGF-β1 deletion [5,8,9].

Some effects of TβRI inhibition on bone resulted from the reduction in osteoclast numbers and differentiation potential in SD-208-treated mice (Figs. 4d, 5c). This in vivo response is striking because TGF-β has been shown to inhibit and promote osteoclast differentiation in vitro, depending on the timing, dose and experimental cell population [12]. TGF-β can act by binding directly to its receptors on osteoclasts and their progenitors, or by acting on osteoblasts to regulate the expression of osteoclast regulatory factors, such as RANKL and OPG [6,7,23–25,38–40]. Though the current study does not explore the extent to which SD-208 affects osteoclasts directly or indirectly through osteoblast-dependent mechanisms, SD-208 can directly inhibit osteoclast function in a purified osteoclast precursor population (Guise, personal communication). In addition, TβRI inhibitors regulated osteoblast expression of osteoclast regulatory factors such as RANKL, OPG, ephrin B2 and EphB4 (Fig. 5). Likely, a combination of direct and indirect mechanisms is responsible for the anti-catabolic and anabolic effects of TβRI inhibitors in vivo.

Treatment of mice with TβRI inhibitors resulted in increased osteoblast numbers and differentiation, and increased bone formation. Consistent with these data, reduced TGF-β signaling in Smad3+/− mice or DNTβRII mice also relieves the suppression of osteoblast differentiation by TGF-β, which is exerted by Smad3 and histone deacetylases [22,41], thereby contributing to increased BMD [7,10]. The increased osteogenic differentiation in response to TβRI inhibitors may also reflect a decrease in repression of BMP signaling by the inhibitory Smad6 [42]. Although changes in Smad6 expression were not observed in our experimental conditions, the BMP antagonist, Noggin, reversed some effects of TβRI inhibitors on gene expression (data not shown), affirming the previous observation that increased BMP signaling contributes to the osteogenic activity of TβRI inhibitors [42]. Therefore, despite the ability of TGF-β to promote or inhibit specific stages of osteoblast differentiation [13], the net effect of TβRI inhibitors on osteoblasts in vivo is to increase bone formation.

Ultimately, the ability of bone to resist fracture is the most clinically desirable outcome [11]. TβRI inhibition increased the peak load that vertebral bone can sustain prior to fracture, in part due to the potent anabolic effect of TβRI inhibitors on trabecular bone. Although a 6-week treatment with TβRI inhibitors was insufficient to increase cortical bone mass or geometry, it significantly increased the mineralization and material properties of cortical bone matrix, when measured using high-resolution XTM and nanoindentation. These data suggest that optimization of the dose or duration of therapy may result in detectable changes in cortical bone mass and macromechanical behavior. Furthermore, our data indicate that TGF-β signaling helps define bone matrix material properties postnatally as it does in development [10], although the effect was more modest than that observed in genetically modified mice. Although the elastic modulus of bone matrix often correlates with mineral content [1], Smad3 also regulates material properties independently of mineralization, as has recently been shown in skin [43]. The mechanisms by which TGF-β regulates the material properties of extracelullar matrices remain unknown.

In conclusion, pharmacologic inhibition of TGF-β signaling in postnatal bone increases bone quality. Coupling of osteoblast and osteoclast activity may be critical for the ability of TGF-β to coordinately control bone mass, architecture, and the material properties of bone. Therefore, therapies that produce a reliable

**Table 2.** Cortical bone structural parameters are not affected by TβRI inhibition.

| | Male | | | Female | | |
|---|---|---|---|---|---|---|
| | **Vehicle** | **SD-208 20 mg** | **SD-208 60 mg** | **Vehicle** | **SD-208 20 mg** | **SD-208 60 mg** |
| **Cort. CSA** | 0.183±0.019 | 0.182±0.016 | 0.172±0.007 | 0.155±0.007 | 0.156±0.006 | 0.152±0.003 |
| **Cort. Th.** | 0.201±0.005 | 0.178±0.006 | 0.186±0.005 | 0.186±0.011 | 0.195±0.005 | 0.188±0.004 |
| **Total CSA** | 0.329±0.038 | 0.346±0.035 | 0.405±0.025 | 0.281±0.017 | 0.285±0.015 | 0.281±0.007 |
| **Perios. Perim.** | 1.057±0.098 | 1.202±0.081 | 0.986±0.057 | 0.964±0.047 | 0.977±0.045 | 0.958±0.017 |
| **Diam. Mid Shaft** | 0.592±0.017 | 0.546±0.017 | 0.577±0.004 | 0.554±0.012 | 0.555±0.005 | 0.560±0.010 |
| **Med. Area** | 0.182±0.040 | 0.218±0.098 | 0.214±0.019 | 0.105±0.009 | 0.109±0.008 | 0.110±0.005 |
| **Endosteal Perim** | 0.761±0.078 | 0.891±0.233 | 0.729±0.055 | 0.571±0.049 | 0.596±0.038 | 0.614±0.020 |
| **Mid Diam** | 0.447±0.054 | 0.427±0.077 | 0.551±0.013 | 0.352±0.008 | 0.351±0.003 | 0.343±0.011 |

Micro-computed tomography was used to assess several quantitative parameters of cortical bone structure. The mean values and standard deviations are presented here.

doi:10.1371/journal.pone.0005275.t002

reduction in TGF-β signaling may have significant clinical benefit in the treatment of diseases characterized by low bone mass and bone fragility. However, TβRI-inhibition may be counter-indicated for the treatment of existing bone fractures, where TGF-β plays a role in fracture repair. Additional studies evaluating the efficacy and potential sex-specificity of the mature skeletal response to TβRI inhibitors, particularly in ovariectomized animals, would be needed to determine their potential therapeutic value for post-menopausal osteoporosis. Careful consideration of safety is essential, given the critical role of TGF-β in normal physiological processes including the control of cell proliferation, differentiation, and apoptosis in many tissues.

## Materials and Methods

### Ethics Statement

In all studies, mice were handled and euthanized in accordance with approved institutional, national and international guidelines.

### TβRI inhibitor treatment

Four-week old male and female C57BL/6 mice were treated for 6 weeks with vehicle (1% methylcellulose) or SD-208 (20 mg/kg once daily or 60 mg/kg twice daily) by gavage. As described, SD-208 is a specific inhibitor of the TGF-β type I receptor, developed by Scios, Inc. [17]. Based on the mouse monitoring parameters of our treatment protocol, no adverse effects of SD-208 on mouse health were detected during the study. At 10 and 3 days prior to euthanasia, an intraperitoneal injection of calcein (Sigma C-0875, 0.02 mg/g) was administered to all mice. Forelimbs, hindlimbs, and spines were collected. For studies using SBE-luciferase mice [29], mice were treated with vehicle or 60 mg/kg SD-208 as above for 3 days, prior to an intraperitoneal injection of TGF-β1 (10 μg/kg). Five hours later, mice were administered luciferin (150 mg/kg) intraperitoneally, anaesthetized with isoflourane, and imaged 10 minutes later using a bioluminescence imaging system (Xenogen).

### Bone mineral density (BMD) measurement

BMD was measured using a PIXImus mouse densitometer (GE Lunar II, Faxitron Corp., Wheeling, IL) (N = 15/group). Total body measurement was performed excluding the calvarium, mandible and teeth. Regions of interest were defined as the distal femur and proximal tibia just beneath the growth plate (12×12 pixels) and the lower lumbar spine (20×50 pixels). Values were expressed as percentage change in BMD over the pretreatment scan.

### Histomorphometry

For demineralized bone histomorphometry, tissues were fixed for 48 h in 10% formalin, demineralized in 10% EDTA for 2 weeks, and embedded in paraffin to generate 3.5 μm longitudinal sections. Trabecular bone volume of the secondary spongiosa (BV/TV%) and osteoblast number (N.Ob/high power field) were measured on hematoxylin and eosin stained sections of the distal femur, proximal tibia, and lumbar vertebrae (N≥12 mice/group). Tartrate resistant acid phosphatase (TRAP) stained sections were used to quantify osteoclast number (N.Oc/BS/mm). Dynamic bone histomorphometry was performed on 7 μm thick sections of mineralized lumbar vertebrae embedded in methylmethacrylate using standard procedures. The mineral apposition rate (MAR, μm/day) and bone formation rate (BFR/BS, $\mu m^3/\mu m^2$/day) were measured on vertebral trabecular bone using fluorescence microscopy to visualize calcein labels as described [44].

### Micro-computed tomography (micro-CT)

Formalin fixed tibiae and femora were imaged with micro-CT using a microCT-40 (Scanco Medical AG, Bassersdorf, Switzerland) using a voxel size of 12 μm in all dimensions (N≥12 mice/group). The region of interest comprised 240 transverse CT slices representing the entire medullary volume with a border lying approximately 100 μm from the cortex [45]. Morphometric variables were computed using direct, three-dimensional techniques that do not rely on assumptions about the underlying structure. Fractional bone volume (BV/TV, Fraction) and architectural properties of trabecular reconstructions, apparent trabecular thickness (Tb.Th., μm), trabecular number (Tb.N., $mm^{-1}$), trabecular spacing (Tb.Sp., 1/mm), and connectivity density (Conn.D., $mm^{-3}$) were calculated as described [46].

### Cortical bone assessment by micro-CT

The CT images of the mid-diaphysis of the tibia were segmented into bone and marrow regions by applying a visually chosen, fixed threshold for all samples, after smoothing the image with a three-dimensional Gaussian low-pass filter. The outer

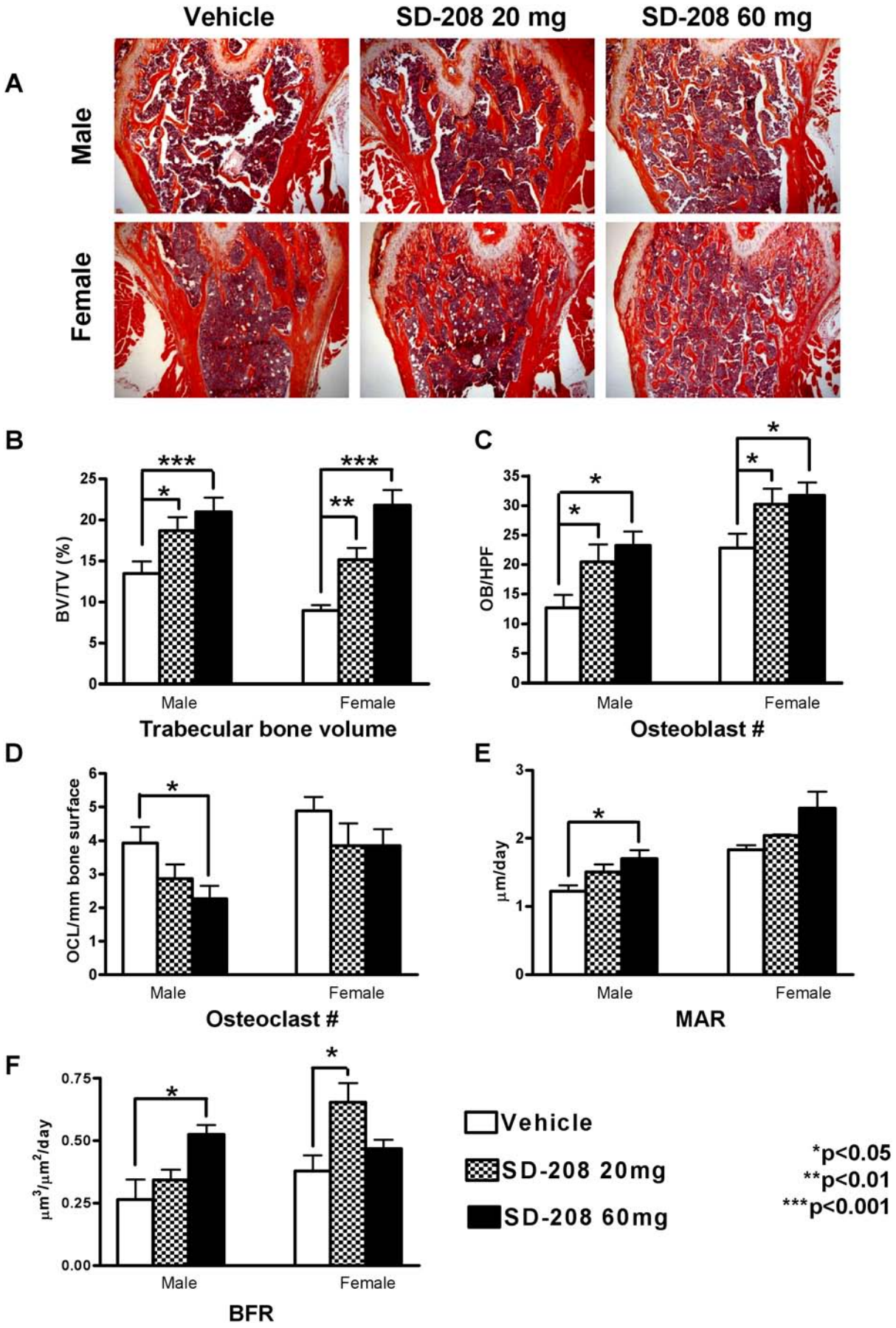
A
Vehicle
SD-208 20 mg
SD-208 60 mg
Male
Female
B
BV/TV (%)
Male
Female
Trabecular bone volume
C
OB/HPF
Osteoblast #
D
OCL/mm bone surface
Osteoclast #
E
μm/day
MAR
F
μm³/μm²/day
BFR
Vehicle
SD-208 20mg
SD-208 60mg
*p<0.05
**p<0.01
***p<0.001

**Figure 4. Pharmacologic TβRI inhibition increases osteoblast numbers but reduces osteoclast numbers.** Representative H&E stained sections of femoral bone show the SD-208-dependent increase in trabecular bone in male and female mice (a). Histomorphometry shows that SD-208 increases trabecular bone volume in the femur (b) and tibia (data not shown), as well as osteoblast number (c) in a dose-dependent manner for male and female mice. Osteoclast numbers are reduced by SD-208 (60 mg/kg) in male mice (d). Dynamic histomorphometry of male mouse lumbar vertebrae shows that SD-208 treatment (60 mg/kg) increased mineral apposition rate (MAR) (e) and bone formation rate (BFR) (f). Data represent mean±SEM (*p<0.05, **p<0.01, ***p<0.001, as determined by one-way ANOVA Newman-Keuls multiple comparison test).
doi:10.1371/journal.pone.0005275.g004

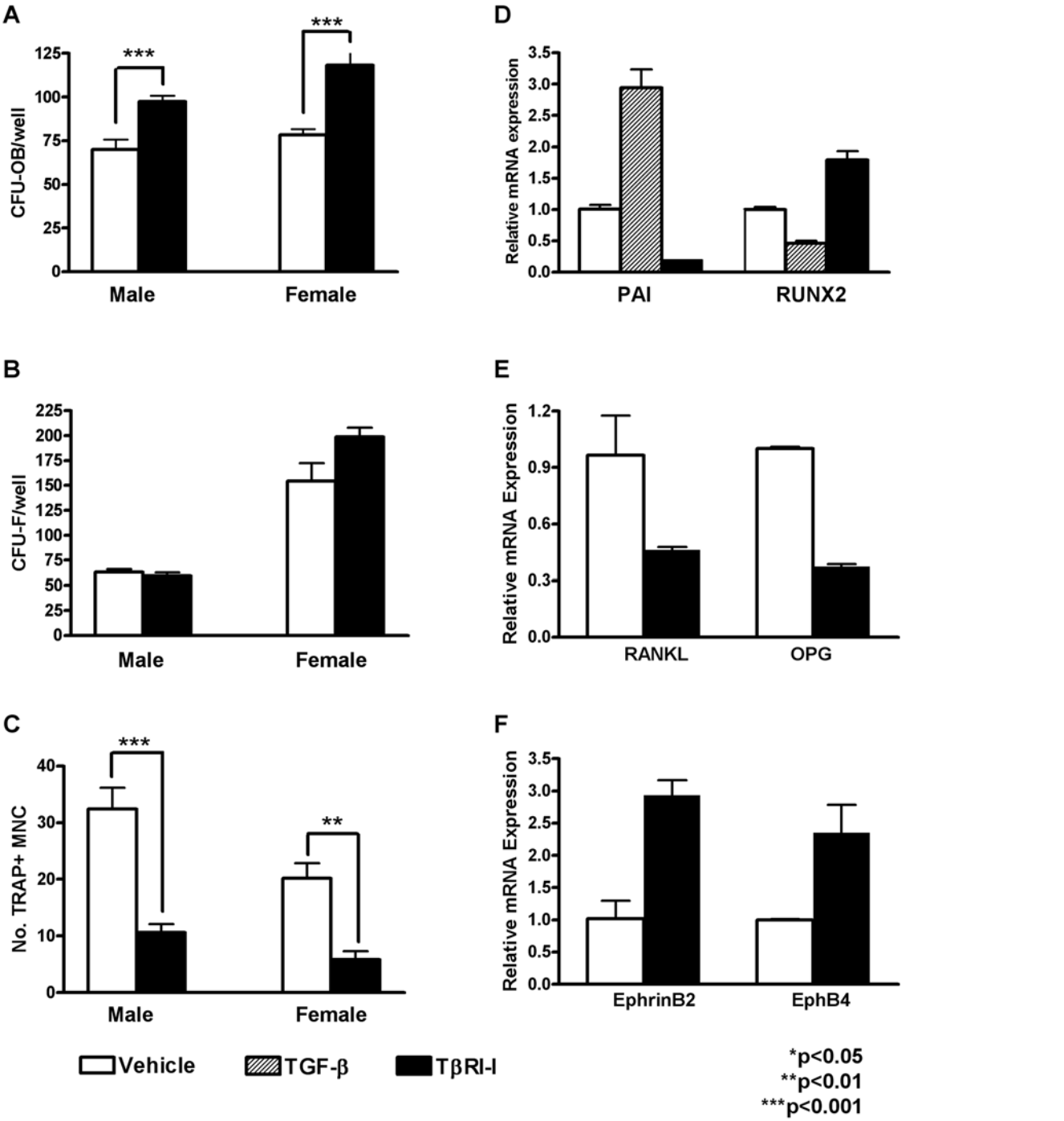


**Figure 5. TβRI inhibition promotes osteoblast differentiation and bone deposition but inhibits osteoclast differentiation.** Bone marrow isolated from male and female mice treated with SD-208 (60 mg/kg) has increased numbers of osteoblast colony forming units (CFU-OB) (a) with no change in the number of colony forming units (CFU-F) (b). The number of TRAP-positive multinucleated cells (TRAP+ MNC) is lower in cultures from SD-208 treated mice than from vehicle-treated controls (c). Primary calvarial osteoblasts treated with TβRI-inhibitor SB431542 (10μM) or vehicle for 48 h show altered mRNA expression of PAI-1 (d) and several osteoblast and osteoclast regulatory factors including Runx2 (d), RANKL and OPG (e), and ephrinB2 and EphB4 (f). Data represent mean±SEM (*p<0.05, **p<0.01, ***p<0.001, as determined by unpaired *t*-test).
doi:10.1371/journal.pone.0005275.g005

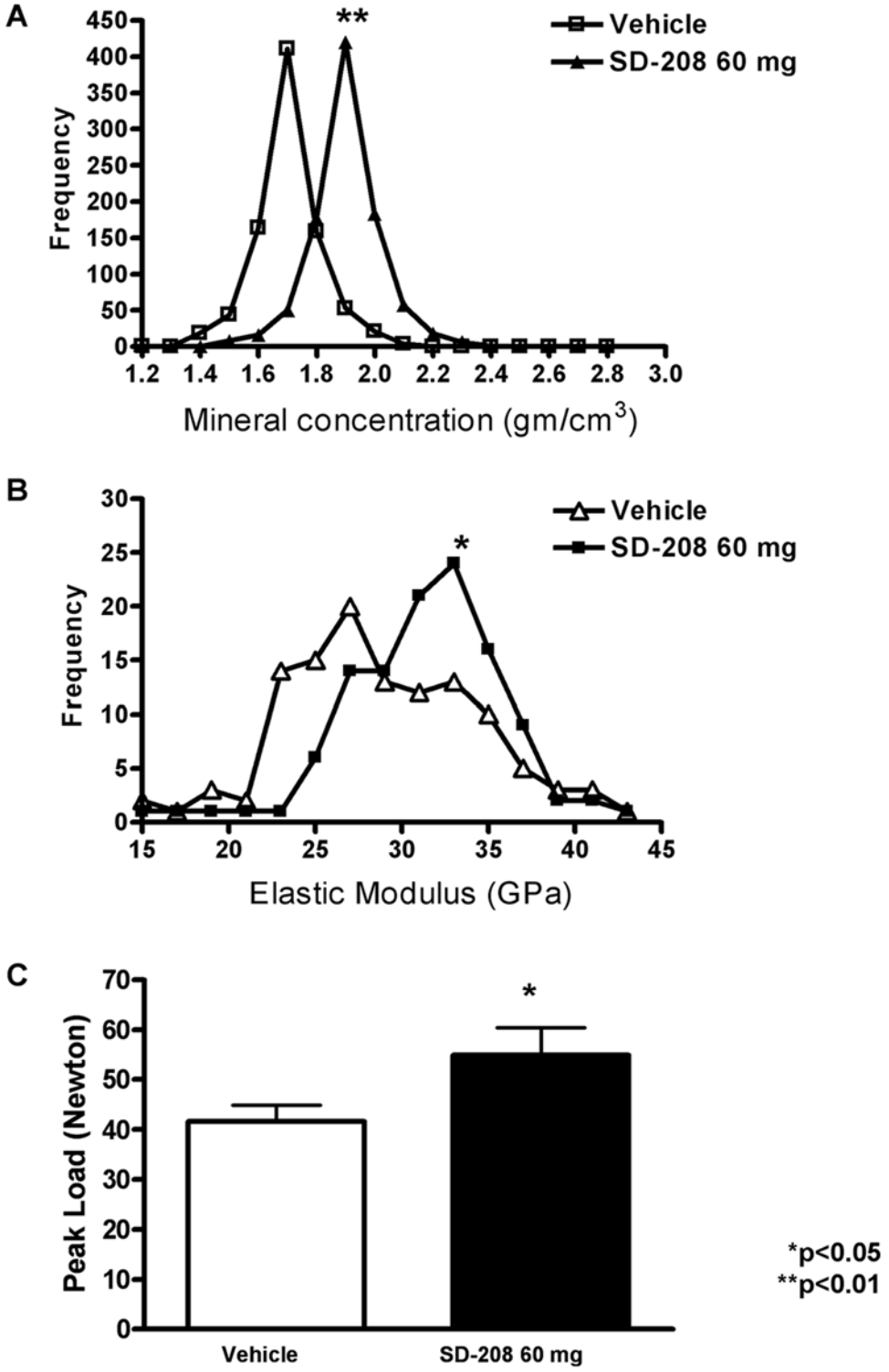


**Figure 6. TβRI inhibitors increase bone mechanical and material properties.** Analysis of each pixel from XTM scans of femora show that SD-208 (60 mg/kg) increases bone matrix mineral concentration with a mean of 1.90 g/cm$^3$+/−0.066, relative to a mean mineral concentration of 1.54 g/cm$^3$+/−0.069 for vehicle-treated controls ($p<0.05$, as determined by unpaired *t*-test) (a). Analysis of elastic modulus values from nanoindents applied to tibial cortical bone showed a similar shift ($p<0.05$) (b). Unconfined compression testing of vertebrae from male mice treated with vehicle or SD-208 (60 mg/kg) shows an increased peak load-to-failure following TβRI inhibition ($p<0.05$) (e).
doi:10.1371/journal.pone.0005275.g006

contour of the bone was found automatically with the built-in Scanco iterative contouring tool. Total area (TA) was calculated by counting all voxels within the contoured bone area, (BA) by counting all voxels that were segmented as bone, and marrow area (MA) was calculated as TA-BA. This calculation was performed on all 30 slices (1 slice = 12.5 μm), using the average for the final calculation. The outer and inner perimeter of the cortical midshaft was determined by a three-dimensional triangulation of the bone

**Table 3.** Macromechanical testing of vertebrae.

| | Male Vertebrae | |
|---|---|---|
| | **Vehicle** | **SD-208 60 mg** |
| **Peak Load** | 41.55±3.34 | 54.95±5.45* |
| **Stiffness** | 98.61±11.52 | 111.1±18.70 |

Mean values±SEM for macromechanical tests of vertebral peak load and stiffness are shown. The significance of differences between vehicle and SD-208 (60 mg/kg) treated groups is indicated with p values (*p<0.05).
doi:10.1371/journal.pone.0005275.t003

**Table 4.** Macromechanical testing of femora.

| | Male Femora | |
|---|---|---|
| | **Vehicle** | **SD-208 60 mg** |
| **Peak Load** | 16.09±0.90 | 15.55±0.52 |
| **Stiffness** | 40.32±5.59 | 47.10±1.40 |
| **Fracture Toughness** | 4.367±0.783 | 4.755±0.509 |

Mean values±SEM for macromechanical tests of femoral peak load, stiffness and fracture toughness are shown.
doi:10.1371/journal.pone.0005275.t004

surface (BS) of the 30 slices, and cortical parameters were calculated as described [47].

## Marrow stromal cell differentiation assays

Bone marrow stromal cells were flushed from 6 femora and tibiae per treatment group, collected by centrifugation (1500 rpm, 10 minutes), resuspended (αMEM, 10% FCS), and incubated for 2 h at 37°C. For osteoblast assays, cells were cultured in αMEM, 15% FBS, 50 μg/ml ascorbic acid, and 10 mM β-glycerophosphate. The number of alkaline phosphatase-positive osteoblast progenitor forming colonies (CFU-F) and Alizarin Red-positive osteoblast forming colonies (CFU-OB) was quantified microscopically after 9 or 28 days of culture, respectively, as described [48,49]. For osteoclast progenitor assays, non-adherent cells were cultured for 6 days in 10% αMEM, 1% FBS and $10^{-8}$ M $1\alpha,25(OH)_2$ vitamin $D_3$. Cultures were fixed and stained for microscopic quantification of multinucleated (MNC) TRAP+ cells.

## Tissue culture, RNA isolation, and quantitative reverse transcription PCR

Calvarial explants were isolated from 10 day old SBE-Luc mice and cultured overnight in DMEM supplemented with 10% fetal bovine serum and 5 ng/ml TGF-β1 in the presence of either 150 nM SD-208 or an equivalent volume of vehicle (1% methylcellulose). Following culture, explants were moved to media containing luciferin (150 mg/ml) for immediate visualization of luciferase reporter activity with a bioluminescent imaging system (Xenogen). Explants were then crushed in liquid nitrogen using a mortar and pestle prior to additional tissue disruption in Trizol with a Omni-GLH homogenizer (Omni Scientific). Following Trizol extraction, RNA was further purified using RNeasy columns (Qiagen).

Primary calvarial osteoblasts were isolated from 3 to 5-day old mice and cultured in osteogenic conditions as described [22]. Cells were treated with a commercially available TGF-β receptor type I inhibitory compound suspended in DMSO (SB431542, Sigma) for 48 h. All other cells received an equivalent quantity of DMSO in the presence or absence of TGF-β (5 ng/ml). Total RNA was purified using RNAeasy columns (Qiagen) and reverse transcribed for the analysis of gene expression. Transcripts were amplified using primers sets for PAI-1 5′-AACCAATTTACTGAAAA-ACTGCACAA-3′ (forward) and 5′-TCCGGTGGAGACATAA-CAGATG-3′ (reverse), Runx2 5′-CCCAGCCACCTTTACC-TACA-3′ (forward) and 5′-CAGCGTCAACACCATCATTC-3′ (reverse), OPG 5′-AGAGCAAACCTTCCAGCTGC-3′ (forward) and 5′-CTGCTCTGTGGTGAGGTTCG-3′ (reverse), RANKL 5′-CACCATCAGCTGAAGATAGT-3′ (forward) and 5′-CCAA-GATCTCTAACATGACG-3′ (reverse), EphrinB2 5′-TCGAA-CTCCAAATTTCTACCC-3′ (forward) and 5′-TGCTTGGTCT TTATCAACCA-3′ (reverse), EphB4 5′-CAAAGTATGCAGA GCCTGTG-3′ (forward) and 5′-CCGGTAATACCCAATTC-GAC-3′ (reverse). Results were detected based on amplicon binding of Sybr Green using quantitative RT-PCR and are representative of at least three independent experiments.

## X-ray tomography (XTM)

XTM studies were used to assess the degree of mineralization of the bone; procedures were based on the work of Kinney *et* al. [33]. Whole male mouse femora were scanned to determine the degree of bone mineralization (N = 3/group). Imaging was performed at the Advanced Light Source (ALS) on Beamline (8-3-2) at the Lawrence Berkeley National Laboratory by obtaining two-dimensional radiographs as the specimens were rotated through 180° in 0.5° increments. The radiographs were reconstructed into 2,500 slices by Fourier-filtered back projection with a 4.5 μm resolution. The attenuation coefficient ($mm^{-1}$) of each pixel relates directly to bone mineral concentration. The degree of bone mineralization (DBM) was obtained from Eq. (1):

$$DBM = \frac{\mu_i - \mu_o}{\mu_m - \mu_o} * C \quad (1)$$

where $\mu_i$ is measured attenuation coefficient at pixel $i$, $\mu_o$ is the attenuation coefficient of organic, $\mu_m$ is attenuation coefficient of mineral, and $C$ represents the density of hydroxyapatite.

## Nanoindentation

Dissected male mouse tibiae were embedded in a two-component epoxy resin (Stycast 1266) prior to sectioning with a precision low-speed saw to generate mid-tibial cortical bone surfaces for nanoindentation. A nanoindenter (Triboindenter, Hysitron, Minneapolis, MN) with a Berkovich tip was used to evaluate polished samples (0.25 μm) under dry conditions as described [10]. Indents were applied using a trapezoidal loading profile with a loading rate of 200 μN/second, peak load of 600 μN, and a hold period of 10 seconds. From the resulting load-deformation curves, local elastic modulus and hardness were calculated as described [50]. Three sets of 20 nanoindentation points were performed in a line with a 5 μm separation. Statistical analyses show the mean and standard error of the median elastic modulus values for each of 3 individual animals per group.

## Macroscopic mechanical testing

Whole bone strength and load to failure were determined by mechanical testing of vertebrae and intact tibiae for at least 12 mice per treatment group as previously described [45]. Thawed bones were hydrated in saline for 1 h before testing at room temperature using a MTS 858 Bionex Test Systems load frame (MTS Systems Corp, Eden Prairie, MN). Vertebral bodies (L4)

were prepared with flat and parallel cranial and caudal ends by removing the soft cartilage to expose the bone, prior to compression testing at a rate of 3 mm/minute. Tibiae were tested in a three-point bending configuration with their anterior side down on two horizontal supports spaced 7 mm apart; the central loading point was displaced downward at 0.1 mm/second on the posterior surface of the diaphysis at the midpoint of the bone length. For all tests, load-displacement data were recorded at 100 Hz (TestWorks 4.0, MTS). Curves were analyzed to determine measures of whole-bone strength, primarily peak load and stiffness [47]. Load-to-failure was recorded as the load after a 2% drop from peak load.

Fracture toughness testing was performed on at least 10 isolated femora per condition. Thawed samples were notched using a razor blade followed by a micronotching technique. Notches were evaluated to ensure that they were through-wall but notched less than 1/3 of the bone diameter. Samples were tested in 37°C HBSS in a three-point bending configuration with a custom-made rig for the ELF 3200 mechanical testing machine (ELF3200, Bose, EnduraTEC, Minnetonka, MN), in general accordance with ASTM Standard E-399 and E-1820 [51,52] and as previously described [53]. Scanning electron microscopy was used to image fracture surfaces to measure the crack area and point of failure. The fracture toughness, $K_c$, was calculated using a stress-intensity solution for circumferential through-wall flaw in cylinders [43,54]. Macro-mechanical testing was performed on male and female femora, with no SD-208-dependent differences observed in either group.

## Supporting Information

**Figure S1** The diaphysis is not filled by trabecular bone following SD-208 treatment. Although increased trabecular bone in femora from SD-208-treated mice (60 mg/kg) is evident in reconstructed micro-CT images, the trabecualr bone does not extend past the distal third of the femur. The scale bar is 1 mm.The diaphysis is not filled by trabecular bone following SD-208 treatment. Although increased trabecular bone in femora from SD-208-treated mice (60 mg/kg) is evident in reconstructed micro-CT images, the trabecualr bone does not extend past the distal third of the femur. The scale bar is 1 mm.
Found at: doi:10.1371/journal.pone.0005275.s001 (1.00 MB TIF)

## Acknowledgments

Thank you to E. Chin, S. Provot, and M. Nakamura for their contributions. XTM was performed at the Advanced Light Source at Lawrence Berkeley National Laboratory, supported by the Office of Science, U.S. Department of Energy (DE-AC02-05CH11231).

## Author Contributions

Conceived and designed the experiments: KM RD. Performed the experiments: KM SIM. Analyzed the data: KM. Contributed reagents/materials/analysis tools: KM. Wrote the paper: KM. Wrote the manuscript with critical input from all authors: TA. Planned and performed most of the experiments with assistance from CRM, HD, MN, XHP: KSM. Planned and performed nanoindentation analyses: CC. Performed XTM: GB. Participated in study design: ES. Administered drugs and did DXA measurements: HD RM. Performed CFU-F & CFU-OB: MN. Did the histology: XHP. Planned and performed gene expression studies: DN TA. Performed microCT: WH JB. Participated in study design: DW. Planned fracture toughness tests and X-ray tomography, which were performed by SSI-M and GB respectively: RR. Planned micro-tomography and macromechanical tests, which were performed by JWB and WRH: LS. Designed and coordinated the study and supervised all experiments: TAG TA.

## References

1. Currey JD (1999) The design of mineralised hard tissues for their mechanical functions. J Exp Biol 202: 3285–3294.
2. Krishnan V, Bryant HU, Macdougald OA (2006) Regulation of bone mass by Wnt signaling. J Clin Invest 116: 1202–1209.
3. Wan M, Cao X (2005) BMP signaling in skeletal development. Biochem Biophys Res Commun 328: 651–657.
4. Alliston T, Piek E, Derynck R (2008) TGF-beta family in skeletal development and disease. In: Derynck R, Miyazono K, eds. The TGF-β Family. Woodbury, NY: Cold Spring Harbor Press. pp 667–723.
5. Geiser AG, et al. (1998) Decreased bone mass and bone elasticity in mice lacking the transforming growth factor-beta1 gene. Bone 23: 87–93.
6. Erlebacher A, Derynck R (1996) Increased expression of TGF-beta 2 in osteoblasts results in an osteoporosis-like phenotype. J Cell Biol 132: 195–210.
7. Filvaroff E, et al. (1999) Inhibition of TGF-beta receptor signaling in osteoblasts leads to decreased bone remodeling and increased trabecular bone mass. Development 126: 4267–4279.
8. Borton AJ, et al. (2001) The loss of Smad3 results in a lower rate of bone formation and osteopenia through dysregulation of osteoblast differentiation and apoptosis. J Bone Miner Res 16: 1754–1764.
9. Yang X, et al. (2001) TGF-beta/Smad3 signals repress chondrocyte hypertrophic differentiation and are required for maintaining articular cartilage. J Cell Biol 153: 35–46.
10. Balooch G, et al. (2005) TGF-beta regulates the mechanical properties and composition of bone matrix. Proc Natl Acad Sci U S A 102: 18813–18818.
11. Hernandez CJ, Keaveny TM (2006) A biomechanical perspective on bone quality. Bone 39: 1173–1181.
12. Fox SW, Lovibond AC (2005) Current insights into the role of transforming growth factor-beta in bone resorption. Mol Cell Endocrinol 243: 19–26.
13. Derynck R, Schneider RA, Piek E, Alliston T (2008) TGF-beta family signaling in mesenchymal development. In: Derynck R, Miyazono K, eds. The TGF-β Family. Woodbury, NY: Cold Spring Harbor Press. pp 613–665.
14. Janssens K, ten Dijke P, Janssens S, Van Hul W (2005) Transforming growth factor-beta1 to the bone. Endocr Rev 26: 743–774.
15. Yingling JM, Blanchard KL, Sawyer JS (2004) Development of TGF-beta signalling inhibitors for cancer therapy. Nat Rev 3: 1011–1022.
16. Laping NJ, et al. (2002) Inhibition of transforming growth factor-beta1-induced extracellular matrix with a novel inhibitor of the TGF-beta type I receptor kinase activity: SB-431542. Mol Pharmacol 62: 58–64.
17. Uhl M, et al. (2004) SD-208, a novel transforming growth factor beta receptor I kinase inhibitor, inhibits growth and invasiveness and enhances immunogenicity of murine and human glioma cells in vitro and in vivo. Canc Res 64: 7954–7961.
18. Bonniaud P, et al. (2005) Progressive transforming growth factor beta1-induced lung fibrosis is blocked by an orally active ALK5 kinase inhibitor. Am J Respir Crit Care Med 171: 889–98.
19. Kapoun AM, et al. (2006) Transforming growth factor-beta receptor type 1 (TGF-beta RI) kinase activity but not p38 activation is required for TGF-beta RI-induced myofibroblast differentiation and profibrotic gene expression. Mol Pharmacol 70: 518–31.
20. Gaspar NJ, et al. (2007) Inhibition of transforming growth factor beta signaling reduces pancreatic adenocarcinoma growth and invasiveness. Mol Pharmacol 72: 152–61.
21. Takahashi N, Udagawa N, Takami M, Suda T (2002) In: Bilezikian JP, Raisz LG, Rodan GA, eds. Principles of Bone Biology. San Diego: Academic Press. pp 109–126.
22. Alliston T, et al. (2001) TGF-beta-induced repression of CBFA1 by Smad3 decreases cbfa1 and osteocalcin expression and inhibits osteoblast differentiation. EMBO J 20: 2254–2272.
23. Thirunavukkarasu K, et al. (2001) Stimulation of osteoprotegerin (OPG) gene expression by transforming growth factor-beta: Mapping of the OPG promoter region that mediates TGF-beta effects. J Biol Chem 12: 12.
24. Murakami T, et al. (1998) Transforming growth factor-beta1 increases mRNA levels of osteoclastogenesis inhibitory factor in osteoblastic/stromal cells and inhibits the survival of murine osteoclast-like cells. Biochem Biophys Res Comm 252: 747–752.
25. Karst M, Gorny G, Galvin RJ, Oursler MJ (2004) Roles of stromal cell RANKL, OPG, and M-CSF expression in biphasic TGF-beta regulation of osteoclast differentiation. J Cell Phys 200: 99–106.
26. Dallas SL, Rosser JL, Mundy GR, Bonewald LF (2002) Proteolysis of latent transforming growth factor-beta-binding protein-1 by osteoclasts. A cellular mechanism for release of TGF-beta from bone matrix. J Biol Chem 277: 21352–21360.
27. Oursler MJ (1994) Osteoclast synthesis and secretion and activation of latent transforming growth factor beta. J Bone Miner Res 9: 443–452.
28. Oreffo RO, Mundy GR, Seyedin SM, Bonewald LF (1989) Activation of the bone-derived latent TGF-beta complex by isolated osteoclasts. Biochem Biophys Res Comm 158: 817–823.

29. Lin AH, et al. (2005) Global analysis of Smad2/3-dependent TGF-beta signaling in living mice reveals prominent tissue-specific responses to injury. J Immunol 175: 547–54.
30. Carcamo J, et al. (1994) Type I receptors specify growth-inhibitory and transcriptional responses to transforming growth factor beta and activin. Mol Cell Biol 14: 3810–21.
31. Stabnov L, et al. (2002) Effect of insulin-like growth factor-1 plus alendronate on bone density during puberty in IGF-1-deficient MIDI mice. Bone 30: 909–916.
32. Zhao C, et al. (2006) Bidirectional ephrinB2-EphB4 signaling controls bone homeostasis. Cell Metab 4: 111–121.
33. Kinney J, GW Marshall J, Marshall S (1994) Three-dimensional mapping of mineral densities in carious dentin: theory and method. Scan Microsc 8: 197–204.
34. Currey JD (1969) The relationship between the stiffness and the mineral content of bone. J Biomech 2: 477–480.
35. Rho JY, Tsui TY, Pharr GM (1997) Elastic properties of human cortical and trabecular lamellar bone measured by nanoindentation. Biomater 18: 1325–1330.
36. Zysset PK, et al. (1999) Elastic modulus and hardness of cortical and trabecular bone lamellae measured by nanoindentation in the human femur. J Biomech 32: 1005–1012.
37. Iida-Klein A, et al. (2006) Effects of cyclic versus daily hPTH(1-34) regimens on bone strength in association with BMD, biochemical markers, and bone structure in mice. J Bone Miner Res 21: 274–282.
38. Kaneda T, et al. (2000) Endogenous production of TGF-beta is essential for osteoclastogenesis induced by a combination of receptor activator of NF-kappa B ligand and macrophage-colony-stimulating factor. J Immunol 165: 4254–4263.
39. Erlebacher A, Filvaroff EH, Ye JQ, Derynck R (1998) Osteoblastic responses to TGF-beta during bone remodeling. Mol Biol Cell 9: 1903–1918.
40. Karsdal MA, et al. (2003) Transforming growth factor-beta controls human osteoclastogenesis through the p38 MAPK and regulation of RANK expression. J Biol Chem 278: 44975–44987.
41. Kang JS, Alliston T, Delston R, Derynck R (2005) Repression of Runx2 function by TGF-beta through recruitment of class II histone deacetylases by Smad3. EMBO J 24: 2543–2555.
42. Maeda S, et al. (2004) Endogenous TGF-beta signaling suppresses maturation of osteoblastic mesenchymal cells. EMBO J 23: 552–563.
43. Arany PR, et al. (2006) Smad3 deficiency alters key structural elements of the extracellular matrix and mechanotransduction of wound closure. Proc Natl Acad Sci U S A 103: 9250–9255.
44. Parfitt AM, et al. (1987) Bone histomorphometry: standardization of nomenclature, symbols, and units. Report of the ASBMR Histomorphometry Nomenclature Committee. J Bone Miner Res 2: 595–610.
45. Perrien DS, et al. (2007) Inhibin A is an endocrine stimulator of bone mass and strength. Endocrinol 148: 1654–1665.
46. Hildebrand T, et al. (1999) Direct three-dimensional morphometric analysis of human cancellous bone: microstructural data from spine, femur, iliac crest, and calcaneus. J Bone Miner Res 14: 1167–1174.
47. Suva LJ, et al. (2008) Platelet dysfunction and a high bone mass phenotype in a murine model of platelet-type von Willebrand disease. Am J Pathol 172: 430–439.
48. Giuliani N, et al. (1998) Bisphosphonates stimulate formation of osteoblast precursors and mineralized nodules in murine and human bone marrow cultures in vitro and promote early osteoblastogenesis in young and aged mice in vivo. Bone 22: 455–461.
49. Gaddy-Kurten D, et al. (2002) Inhibin suppresses and activin stimulates osteoblastogenesis and osteoclastogenesis in murine bone marrow cultures. Endocrinol 143: 74–83.
50. Oliver WC, Pharr GM (2004) Measurement of hardness and elastic modulus by instrumented indentation: Advances in understanding and refinements to methodology. J Mater Res 19: 3–20.
51. E399 (1990) Standard test method for plane-strain fracture toughness of metallic materials. Philadelphia: American Society for Testing and Materials.
52. E1820 (2006) Standard test method for measurement of fracture toughness. West Conshohocken, PA: American Society for Testing and Materials.
53. Ritchie RO, et al. (2008) Measurement of the toughness of bone: A tutorial with special reference to small animal studies. Bone, Epub.
54. Zahoor A (1989) Circumferential throughwall cracks. In: Electric Power Research Institute, editors. Ductile Fracture Handbook. Palo Alto, CA: Electric Power Research Institute.